THE MECHANICAL EFFECTS OF SHORT-CIRCUIT CURRENTS IN OPEN AIR SUBSTATIONS

Working Group 02 (Effects of high currents)

of

Study committee 23 (Substations)

Prepared in coordination with :

Technical Committee N°73 (Short-circuit currents)

of the International Commission , Geneva

1987

cigré

THE MECHANICAL EFFECTS OF SHORT-CIRCUIT CURRENTS IN OPEN AIR SUBSTATIONS

Working Group 02 (Effects of high currents)
of
Study Committee 23 (Substations)

Prepared in coordination with :
Technical Committee N°73 (Short-circuit currents)
of the International Electricity Commission, Geneva

1987

The CIGRE Study Committee 23 "Substations" set up the Working Group 23.02 "Effects of high currents" in Brussels in 1971. The most important objective of WG 23.02 was to evaluate and develop calculation methods for the mechanical effects of short circuit currents in HV open air substations and similar installations.

Technical Committee 73 "Short-circuit currents" of IEC was set up in 1972 at Stockholm with the aim to standardize the procedures for the calculation of short-circuit currents and their effects.

During the years both Committees have worked in close contact with each other. This has led to co-operation and a co-ordination of their activities, which has been actively stimulated by the former Chairmen Hans Georg Muller and Frank W. Davenport of CIGRE SC 23 and Gerhard Hosemann of IEC/TC 73.

When, in 1985, CIGRE Study Committee 23 decided that WG 23.02 should prepare a comprehensive and up to date publication of the results of its work, IEC/TC 73 had finished its preparatory work for the IEC Publications 865 and 909. In this situation WG 23.02 could fulfil its task with allowance for these IEC Publications and IEC/TC 73 could participate in the work and judge the results.

This CIGRE-brochure "Mechanical effects of short-circuit currents in open air substations" is the product of this work. Thanks to the co-operation and co-ordination this brochure can also be considered as an application guide to the IEC publications 865 "Calculation of the effects of short-circuit currents" and 909 "Short-circuit current calculation in three-phase ac systems" so that the publication of a separate IEC application guide concerning open air substations to IEC Publication 865 can be avoided.

We would like to express here our high appreciation for the excellent work of the many scientists and engineers who have participated in this project and for their leader Zbigniew Nartowski, convener of CIGRE Working Group 23.02.

The chairmen of CIGRE SC 23 and IEC/TC 73 hope that the good co-operation of their committees in this field will be followed by more similarly co-ordinated activities in the future.

September 1987
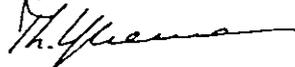
Theo Ykema
Chairman of
CIGRE SC 23

Dietrich Oeding
Chairman of
IEC/TC 73

ABSTRACT The mechanical effects of short-circuit currents in open air conventional HV and EHV substations are the subjects of this brochure. In particular the electromagnetic forces and the resulting stresses appearing in bus systems of both types of conductors, rigid (tubular) and flexible (stranded), are considered.

General descriptions of the phenomena are presented first, followed by descriptions of the testing and measurement methods. Calculation methods of varying complexity and accuracy (simple, medium and advanced) are described and a parameter sensitivity analysis is presented. Finally, guidelines for design are given which take into consideration both mechanical stresses and conductor displacements caused by short-circuit current.

RESUME Cette brochure traite des effets mécaniques des courants de court-circuit dans les postes ouverts HT et THT. Elle prend en considération les forces électromagnétiques appliquées aux deux types de connexions usuels (tubes rigides et câbles flexibles) ainsi que les contraintes mécaniques qui en résultent.

Après une description générale des phénomènes, on expose les méthodes d'essais et de mesures. Puis différentes méthodes de calcul de complexité et de precision croissantes (simples, moyennes et avancées), ainsi qu'une étude paramétrique, sont présentées.

Enfin, on donne des directives de conception prenant en compte à la fois les contraintes mécaniques et les déplacements des conducteurs dus aux courants de court-circuit.

For further information contact:

H. Adami
N.V. KEMA
P.O. Box 9035
6800 ET Arnhem
The Netherlands

THE MECHANICAL EFFECTS OF SHORT-CIRCUIT
CURRENTS IN OPEN AIR SUBSTATIONS

PREFACE The short-circuit current levels in HV and EHV networks have been increasing considerably in recent decades and further increases may be expected in the future. High levels of short-circuit current in substations result in high mechanical stresses and in some cases, displacements, on bus systems, connections to apparatus, substation equipment and bus supports.

The mechanical effects of short-circuit currents in HV and EHV open air substations were the subjects of study by Working Group 02 "Effects of High Currents" of CIGRE Study Committee 23 "Substations". In particular the electromagnetic forces appearing in conductors of both types rigid (tubular) and flexible (strained) and their resulting loading of bus support systems have been considered.

In order to improve qualitative and quantitative knowledge of short-circuit phenomena, many tests have been carried out using modern experimental technology. As well, a variety of calculation methods have been developed and verified. These range from practical calculation methods suitable for everyday design to the most advanced finite element techniques. First, rigid conductors, which presented a relatively simple case, were studied. Next, short-circuit current effects in substations with flexible conductors were examined. This case is very complex.

The Working Group has published a number of papers on the mechanical effects of short-circuit current in substations during the past several years [1-13]. With this Brochure, the Working Group presents a summary of its activities and contributions to knowledge of this subject.

The subject of the brochure is the mechanical effects of short-circuit currents in HV and EHV open air, conventional substations. The aim of this document is to give design engineers practical information about short-circuit phenomena and calculation methods and to give guidelines for design. The brochure should serve as a guide for the design engineer, specialized in the prob-lems of substation design. It contains little theoretical information. The information included in the brochure is as complete as possible. However, the reader should note that many of the problems presented herein have not been completely solved and require further work before definite guidance for substation designers can be provided.

3

CONTENTS

5 GUIDELINES FOR DESIGN

1 INTRODUCTION

1.1 Short-circuit Currents

The calculation of short-circuit currents in systems with nominal voltages up to 245 kV is described in detail in IEC Publication 909 [40], "Short-circuit calculation in three-phase AC systems. Section I: Systems with short-circuit currents having no AC component decay; Section II: Systems with short-circuit currents having an AC component decay". The procedure described can also be applied, more or less, to systems with higher voltages whose nominal values U_n are not standardized in IEC Publication 38 [36]. For this purpose, instead of U_n, a value should be used that corresponds to the mean value of the voltage with respect to time and location, provided that the differences between the voltage magnitudes in the system do not differ from one another by more than 10%.

If the voltage differences are perceptibly larger, the simplified calculation procedure according to [40 clause 6] with an equivalent voltage source at the short-circuit location should be replaced by a more elaborate procedure. This must be based on the necessary load flow calculations in order to determine the voltage and load current state prior to the short-circuit. The voltage and current changes caused by the short-circuit are then superimposed. In order to calculate these changes, a node admittance matrix is set up and sparse-matrix methods with preordered elimination are applied [71].

Nonetheless, calculation of the initial symmetrical short-circuit current I_k'' is not an elementary problem of linear algebra. The magnitude of I_k'' depends on the following influences, listed in order of importance:

1. Operation of power stations and equipment in the system.
2. Equipment impedances.
3. Voltage state of the system prior to short-circuit depending on
   - excitation of the generators
   - transformer tap-changer position,
   - type and number of loads connected in the system, including line capacitances.

Data on categories 1 and 2 are indispensable for every short-circuit current calculation. In category 2, matters are complicated by the following

- equipment tolerances
- temperature dependence of the resistances,
- nonlinear characteristics of many items e.g.
  - generator initial reactance depends on inductance,
  - transformer short-circuit voltage depends on the tap-changer position.

The resistances of arcs may be disregarded for all system voltages.

The variables in the third category generally exert a lesser effect on the result than categories 1 and 2, but in practice they vary so widely that they cannot be predetermined for the instant of a short-circuit. The principle generally used in similar situations, i.e. rating equipment deterministically for the worst case, does not

apply here because the worst case of a short-circuit expected under 3 is usually unknown and highly improbable [71].

For this reason IEC Publication 909 [40] contains a clear deterministic procedure, the so-called simplified method which provides for an equivalent voltage source at the short-circuit location. But clause 2 expressly states that, instead of the simplified standard procedure, other methods may be applied that are better adjusted to the conditions of the particular installation, provided that they give at least the same accuracy as the standard procedure.

As shown in Figs. 1.1a and b, short-circuit currents consist of an aperiodic decaying component and a periodic oscillating component. If their amplitudes remain constant during the short-circuit, as in Fig. 1.1a, this is generally known as a far-from-generator short-circuit. If their amplitude decays as in Fig. 1.1b, this is known as a near-to generator short-circuit.
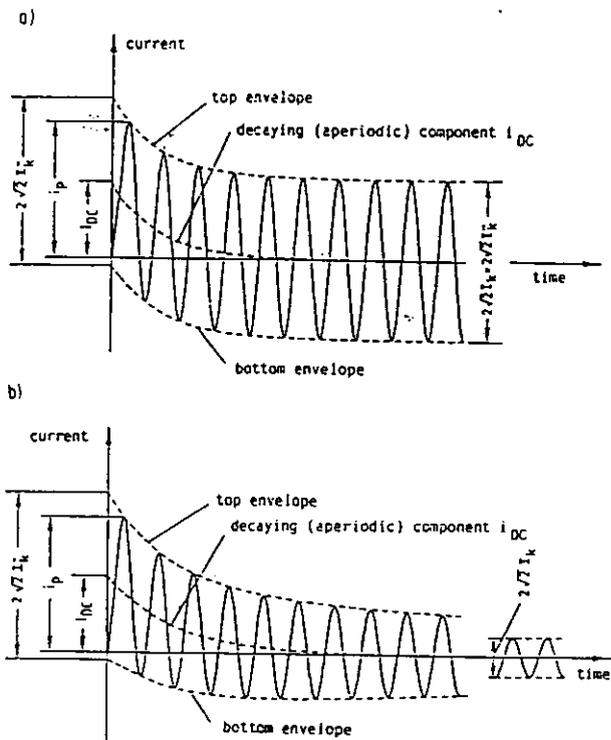
Fig. 1.1   Short-circuit current, schematic diagram [40]
a   far-from-generator
b   near-to-generator
I_k'' initial symmetrical short-circuit current
i_p peak short-circuit current
i_{DC} DC (aperiodic) component of short-circuit current
I_{DC} initial value of the aperiodic component i_{DC}

8

A short-circuit current having no AC component decay is defined by

$$i(t) = \sqrt{2}\, I_k''\, [\sin\,(\omega t + \varphi_u - \gamma_z) + \sin\,(\gamma_z - \varphi_u)\, e^{-t/\tau}] \qquad (1.1)$$

where φ_u is the voltage phase angle related to the instant at which the fault appears and γ_z is the impedance angle. I_k'' can be calculated as described in [40, section 1].

A short-circuit current having an AC component decay is defined by

$$i(t) = \sqrt{2}\,[I_k(t)\cdot\sin\,(\omega t + \varphi_u - \gamma_z) + I_k''\cdot\sin\,(\gamma_z - \varphi_u)\cdot e^{-t/\tau}] \qquad (1.2)$$

where $I_k(t)$ is the time-variable symmetrical short-circuit current (rms). It is calculated according to [40, Fig. 16] with decrement factors μ for $t = 0.02;\ 0.05;\ 0.10$ and 0.25 s, based on the usual generator data.

The decrement factor depends on the location of the short-circuit relative to the generator concerned. Therefore, in IEC Publication 865 [39], the mechanical loading by short-circuit currents is calculated without decrement factors, i.e. with $I_k(t) = I_k''$ constant.

Fig. 1.2 provides an overview of the main types of short-circuit. A diagram of their quantities is given in [40, Fig. 11]. The equation

$$I_{k2}'' = \sqrt{3}/2\ I_{k3}'' \qquad (1.3)$$

always applies to the initial symmetrical short-circuit current in the case of a balanced three-phase short-circuit and a line-to-line short-circuit without an earth connection.
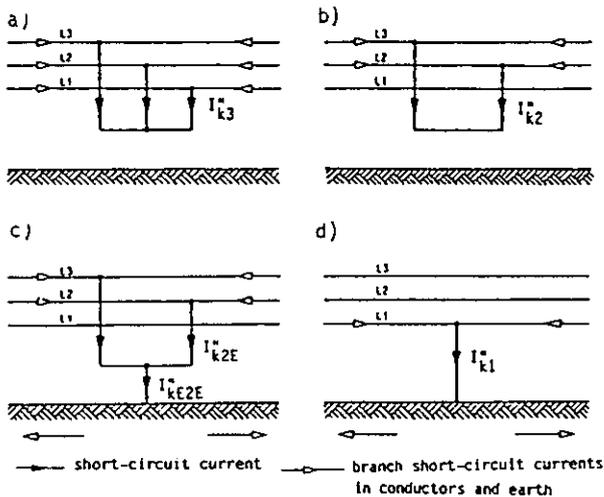
The peak value i_p of the short-circuit current is reached in the worst case after about one half cycle from the occurrence of the short-circuit at zero voltage. If the short-circuit current flows through a series circuit R+jX consisting of resistance R and reactance $X = \omega L$, then

$$i_p = \kappa\sqrt{2}\, I_k'' \qquad (1.4)$$

and

$$\kappa = 1.02 + 0.98\ e^{-3R/X} \qquad (1.5)$$

The peak value i_p in meshed networks is, in principle, difficult to calculate. Hence, it is not worth calculating in these cases because a simplified procedure according to [40, subclause 9.1.3.2] is sufficiently accurate.

A report by CIGRE Working Group 23.04 [28] states that the following maximum initial symmetrical short-circuit currents I_k'' can be expected:

voltage level	I_k'' (rms)
123 ... 170 kV	25 ..... 80 kA
245 ... 300 kV	31.5 ... 70 kA
362 ... 525 kV	25 .... 100 kA

1.2 Short-Circuit Current Forces

Short-circuit currents induce forces in, and deflections of, the current carrying elements (section 1.3). In Fig. 1.3, a conductor carrying current $i_1(t)$ in a magnetic field created by another conductor carrying current $i_2(t)$ undergoes an electromagnetic force defined by

$$d^2\vec{F}_1 = \frac{\mu_0}{4\pi}\, i_1(t) i_2(t)\, \frac{d\vec{s}_1 \times (d\vec{s}_2 \times \vec{a}_{21})}{a_{21}^3} \qquad (1.6)$$

Note that we do not have the reciprocity associated with considering only conductor elements, and that ferromagnetic areas must be represented by their equivalent boundary currents.
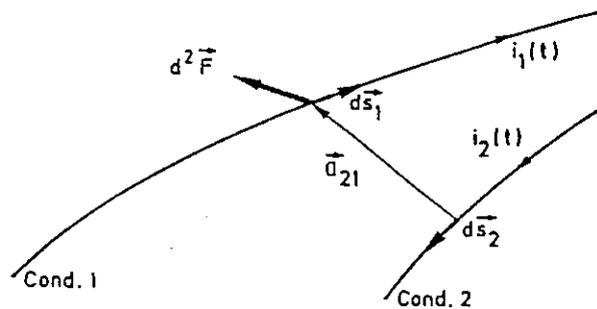
Fig. 1.3   Electromagnetic force d^2F acting on ds_1 in the magnetic field of ds_2

— short-circuit current   —o— branch short-circuit currents in conductors and earth

Fig. 1.2   Characterization of short-circuits and their currents [40]. The direction of current arrows has been chosen arbitrarily.
   a)   balanced three-phase short-circuit
   b)   line-to-line short-circuit without earth connection
   c)   line-to-line short-circuit with earth connection
   d)   line-to-earth short-circuit

If, for example, n conductors lie parallel in one plane, the force per unit length is given by the simple algebraic equation

$$F_1 = \frac{\mu_0}{2\pi}\, i_1(t)\cdot \sum_n \frac{i_n(t)}{a_n} \qquad (1.7)$$

9

and where 2 parallel conductors are located a distance 'a' apart

$$F_1 = \frac{\mu_0}{2\pi} i_1(t) \cdot i_2(t) \cdot \frac{1}{a} \qquad (1.8)$$

In other cases, Appendix 2 or equation (1.6) has to be applied, e.g. for the calculation of edge forces and complex effects requiring a numerical solution.

Currents flowing in the same direction produce attractive forces, while opposing currents produce repelling forces.

Equations (1.6 to 1.8) contain the products of time-variable currents. If each current consists only of a DC component and an AC component of frequency f, harmonics of order 0, f and 2 f can be expected in the force spectrum. A more detailed example can be seen in Fig. 3.2.

In the case of installations with rigid conductors, the distances a_n are almost constant; with flexible conductors $a_n(t)$ changes significantly with time and such conductors may be considered as only approximately parallel. For configurations with three rigid conductors lying parallel in one horizontal plane, Fig. 1.4a,b shows the force characteristic on the outer conductors and the center conductor during a three-phase short-circuit. Fig. 1.4c shows the force characteristic during a two-phase short-circuit. The angle of short-circuit initiation selected for φ_u is that which leads to the highest instantaneous force value.

In the case of the three-phase short-circuit in Fig. 1.4a,b it is clear that

- although the highest force peak occurs on the center conductor, the steady-state mean is zero

- although the peak values are slightly lower on the outer conductors than on the center conductor, the steady-state force is not equal to zero

- the force characteristics during a two-phase short-circuit, illustrated in Fig. 1.4c, are similar to those occurring on the outer conductor during a three-phase short-circuit illustrated in Fig. 1.4b.

Rigid conductors in installations with voltages of 123 kV and higher have natural frequencies which are considerably lower than 50 Hz. Therefore, the stress follows the force peaks with a delay. The three-phase short-circuit leads to the highest peak forces and sets the pattern for such installations.

For flexible conductors, the line-to-line short-circuit between center and outer conductor is decisive because it results in the smallest phase clearances.

In general, single phase line-to-earth short-circuit currents cause minor stresses and therefore may be disregarded, except for bundled conductor configurations.
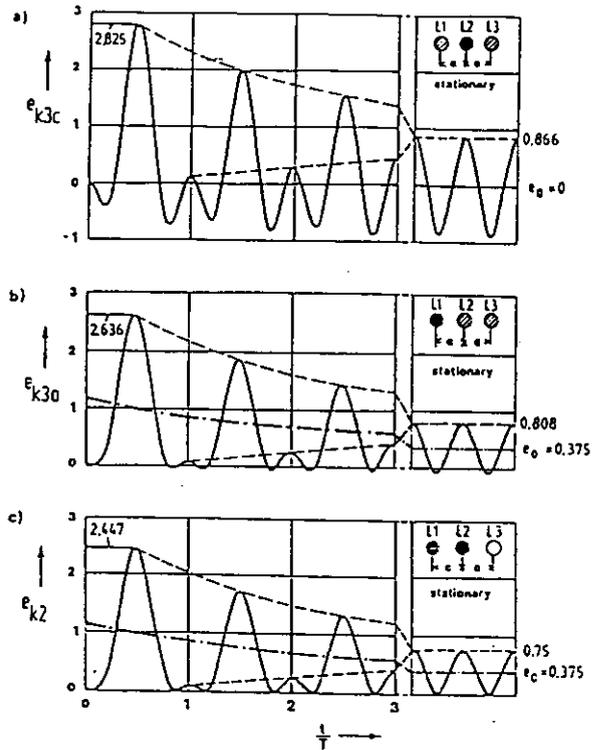
Fig. 1.4 Relative force $e_x(t)$ per unit length, worst case, for different phases and short-circuits, when R/X = 0.07 [5].

$$F'(t) = \frac{\mu_0}{2\pi a} \left(\sqrt{2} \, i_{k3}^{"}\right)^2 \cdot e_x(t)$$

a) balanced three-phase short-circuit, center conductor L2

b) balanced three-phase short-circuit, outer conductors L1 or L3

c) line-to-line short-circuit
——— complete time functions
—·— time functions neglecting oscillating components according to equ. (1.10)

1.3 Mechanical Short-Circuit Effects

1.3.1 General Phenomena

These effects are the manifestations of the response of the bus system to the exciting short-circuit current forces described in section 1.2. When rating substations in HV systems, the following mechanical quantities and procedures are decisive for short-circuits.

In installations with rigid conductors:

- Bending stresses in the conductors can produce undesirable deformations.

- Forces acting on the connections of the conductors with the insulators impose stress on the fittings and hardware.

- Bending moments, usually on the base of the insulators and substructures, can lead to breakage.

In installations with flexible conductors:

- Tensile forces in the conductors, including their terminations and associated hardware, can lead to damage.

- Forces in the insulators and their substructures can cause yielding or insulator breakage.

- A swing-out of elastically and thermally expanded conductors during a short-circuit can be the cause of secondary short-circuits.

For rigid conductors the systems of equations for calculating the stresses are linear. Different stress components may be superimposed; hence mechanical resonance of conductors at higher harmonic orders must also be considered. For flexible conductors, the systems of equations required to represent the mechanical response of practical bus systems are obviously non-linear; superposition is not possible. Table 1.1 outlines the most important short-circuit force phenomena.

Short-circuits cause rigid conductors to vibrate and flexible conductors to swing or rotate. The quotient

$$\frac{f_c}{f} = \frac{\text{lowest significant mechanical frequency of conductor}}{\text{nominal electrical frequency 50 or 60 Hz}}$$

is an important parameter for all types of motion. Where $f_c / f \gg 1$, the stress is proportional to the exciting force. Where $f_c / f \ll 1$, the stresses are lower, except for special harmonic resonances in the case of rigid conductors, and can, in many cases, be further reduced by rapid short-circuit current interruption [32]. The effects of the short-circuit duration T_k are also determined by switchgear and protection design and must be considered together (section 3.5).

Insulators and substructures exert a minor influence on rigid and flexible conductor, provided that the natural frequency of the former is $f_s > f_c$. In the case of rigid conductors, if the bending moment is measured along the insulator, a slightly curved characteristic is obtained because of inertia [20]. Experience shows that serious damage to busbars, dimensioned in this way, can be avoided.

Table 1.1
Short-Circuit Force Phenomena in HV Installations
with Parallel Conductors Arranged in One Plane

| Effect | Installations with | |
	rigid conductors	flexible conductors
$f_c \ll f$ applies for	high voltage	all voltages
Stressing of supports and conductors	by bending moments	by tensile conductor forces
Deflection	small	large
Conductor bending deformation	small	none
Critical short-circuit	three-phase	line-to-line; three phase short-circuit causes similar force
Conductor subjected to highest stress	outer conductor (high voltage)	-
Voltage phase angle φ_u after voltage zero in the observed conductor, leading to highest peak forces	center conductor L2: $\varphi_u = \pm 45°$ outer conductor L1: $\varphi_u = +165°$ outer conductor L3: $\varphi_u = -165°$	at zero voltage
Effect of three-phase rapid reclosure	significant	swing amplification unlikely; potentially significant for bundle pinch
Physical model for simplified calculation	bending beam [5], section 3.4.1	pendulum [68,104] section 4.3.2
f_c of conductor refers to	fundamental components of bending oscillations	swing-out period of pendulum, infinite short-circuit duration assumed

1.3.2 Installations with Rigid Conductors

In outdoor switchgear installations the conductors are usually arranged in one plane [11]. In the case of HV and EHV installations with rigid conductors, the heaviest stresses associated with three-phase short-circuits can be expected on the outer conductors (Eq. 3.1). These stresses occur at approximately the moment of maximum conductor deflection.

The lowest significant mechanical frequency f_c of rigid conductors is typically 2 to 10 Hz in HV installations and is calculated as defined in [39, eq. 16]. Figure 8 of Reference [39] is also a useful diagram. In order to deal with installations of all voltage ratings, the force calculations related to rigid conductors, listed in section 3 according to [39], are based on peak short-circuit current i_p for a three-phase short-circuit. The factors V_F, V_σ and V_r describe the dynamic properties of the system excited by the short-circuit current forces under worst case conditions. When using advanced methods for stress calculations, forces may be divided into their spectra according to Chapter 3. For mechanical resonances, the harmonic components f and 2f of the exciting force spectrum must also be considered.

1.3.3 Installations with Flexible Conductors

The equivalent frequency f_c of installations with flexible conductors during short-circuit can be approximated by comparison with a mathematical pendulum

$$f_c = \frac{1}{2\pi}\sqrt{\frac{\text{Resultant force/unit length caused by gravity and current}}{\text{Mass of conductor/unit length x conductor sag}}}$$

The equivalent swing-out frequency is lower before and after the short-circuit. The magnitude (in Hz) may be estimated by $f_c \approx 0.56/\sqrt{\text{sag in meters}}$ (section 4.2.2). In installations with flexible conductors, $f_c / f \ll 1$ is also valid for small spans, and therefore, the stress calculations are based on the effective value of the current I_{eff}. In the case of brief short-circuit durations in particular, this value may be significantly higher than the value of the initial symmetrical short-circuit current I''_k

$$I_{eff} = \sqrt{1 + m}\ I''_k \tag{1.9}$$

Factor m is shown in Fig. 4.2.2 according to [39, Fig 7a] and represents the influence of the DC component on the rms value of the short-circuit current.

When using advanced methods for stress calculations, the nonlinearities require step-by-step methods. The step size may be extended without significant loss of accuracy by omitting the periodic components of the exciting force spectrum. By means of the monotonous decreasing exciting current

$$i_{mon2}(t) = I''_{k2}\ \sqrt{a_2 + b_2\ e^{-2t/\tau}} \tag{1.10a}$$

$$i_{mon3}(t) = I''_{k3}\ \sqrt{a_3 + b_3\ e^{-2t/\tau}} \tag{1.10b}$$

an equivalent current force acting on the outer conductors may be defined. In the case of line-to-line short-circuits, $a_2 = 1$, $b_2 = 2$; in the case of three-phase short-circuits, $a_3 = 1.5$, $b_3 = 3.232$ with conductor distance 2a according to [5]. The ratio

$$r = \frac{\text{current force per unit length}}{\text{mass per unit length} \cdot g_n}$$

is another important parameter for flexible conductors [78]. If r is greater than about 2 and $f_c \cdot T_k$ is greater than about 0.25, flexible conductors will rotate about their point of suspension or fall back to their initial position after the short-circuit has ended. If both conditions are not fulfilled, the conductors will swing with a quasi-circular motion and tumble. The maximum stress during the short-circuit can be expected at $f_c \cdot t \approx 0.1 .. 0.25$. If $f_c \cdot T_k$ is shorter than this value, the maximum stress in t_t and t_f become lower.

In installations with flexible conductors, the stresses occurring in line-to-line short-circuits and balanced three-phase short-circuits are approximately equal. However, for line-to-line short-circuits, conductor swing-out typically results in limiting minimum clearances, (i.e. when adjacent conductors carrying short-circuit current move towards one another after the short-circuit). In the case of a balanced three-phase short-circuit, the center conductor moves only slightly because its inertia and the alternating bidirectional forces which act on it.

Tensile force maxima are shown in Fig. 1.5: for bundled conductors in t_{pi} soon after short-circuit inception [12], in t_t during the short-circuit after about $f_c \cdot t \approx 0.25$ and in t_f after the short-circuit when the conductor returns near to its initial position. Times t_{pi}, t_t and t_f in Fig. 1.5 usually lie so far apart that they allow the associated maximum stresses to be calculated separately. This makes it possible to apply simplified methods; the unlikely case that bundled conductors would be in the positions of t_t or t_f at precisely the instant of three-phase rapid reclosure can be disregarded.
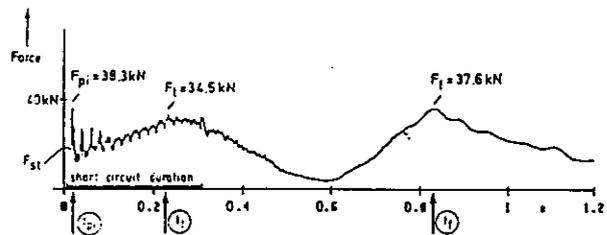
a)

Fig. 1.5a Measured tensile force of a flexible conductor bundle during and after a line-to-line short-circuit
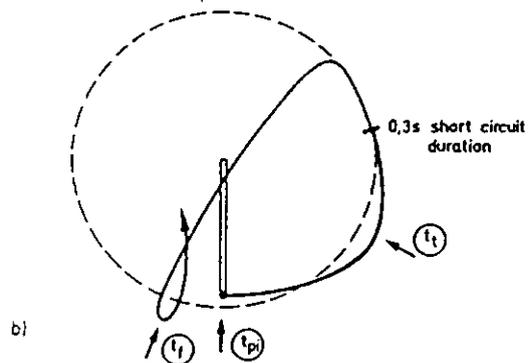
b)

Fig. 1.5b Movement of a flexible conductor during and after a line-to-line short-circuit (schematic)

12

1.4   Substation Characteristics

The flow of short-circuit current within substations, is particularly important for bus system design. In general, there are two possible locations of faults which influence the distribution of short-circuit current flow in substations: inside the substation and outside the substation.

A fault inside a substation, on a busbar, results in the highest short-circuit current. The fault current level on many of the bus sections will frequently be lower than the total fault current; however in some specific fault situations (for example, at the ends of the busbars) the full addition of all fault currents supplying the fault from connected lines, transformers, etc. will occur.

In the case of a fault outside the substation (for example, in the line or bay connecting a current source) the short-circuit current flowing through any substation part (excepting the faulted bay) is reduced. This is the most common case as a result of the frequency of faults in overhead lines.

Usually the design engineer considers the short-circuit current value on the busbars and assumes the nearest higher standard level value as the base for the short-circuit withstand design of the substation. In substations uprating, the exact calculated short-circuit current value, and the results of the short-circuit current path analysis, may be taken into consideration.

The mechanical effects of short-circuit currents (other effects are not considered in this brochure) may cause substation failure (in particular insulator breakage). Such failures appear very rarely but are very dangerous for the stability and reliability of the power system. Therefore, designers must ensure substation security against short-circuit effects. To do so, they must have a good understanding of the phenomena and have available calculation methods which make it possible to design the short-circuit capability of substations.

In this brochure, conventional open-air substations are taken into consideration. This type of substation accounts for the majority of existing substations, and will continue to be the design of choice for a considerable number of new substations.

In analyzing the mechanical effects of short-circuit currents in substations, we must consider in particular the following components.

-    conductors with their accessories
-    insulators
-    supporting structures.

The other components of substations, such as apparatus, are not considered here because utilities specify a short-circuit withstand and the inherent resistance of the apparatus is guaranteed by the manufacturer.

The short-circuit mechanical effects within the substation depend, in particular, on the types of conductors used for the busbars of the substation and the connections in the bays, namely: rigid conductors (tubes) or flexible ones (cables). The mechanical effects of short-circuit currents in such bus systems, already presented in section 1.3, are quite different in both cases.

As is usual for the analysis of complex phenomena, some typical elementary representative arrangements must be chosen. They do not represent all possible substation configurations but usually suffice for practical design purposes. The typical elementary arrangement used in substations with rigid conductors is presented in Fig. 1.6. It is part of a three phase busbar. A substation is usually designed with similar modules. The number of spans varies, and sometimes spans of uneven lengths are used. In some cases it is also necessary to calculate the forces in bus corners, A-frames and right-angle bends. Problems dealing with the rigid conductors are discussed in Chapters 3 and 5.
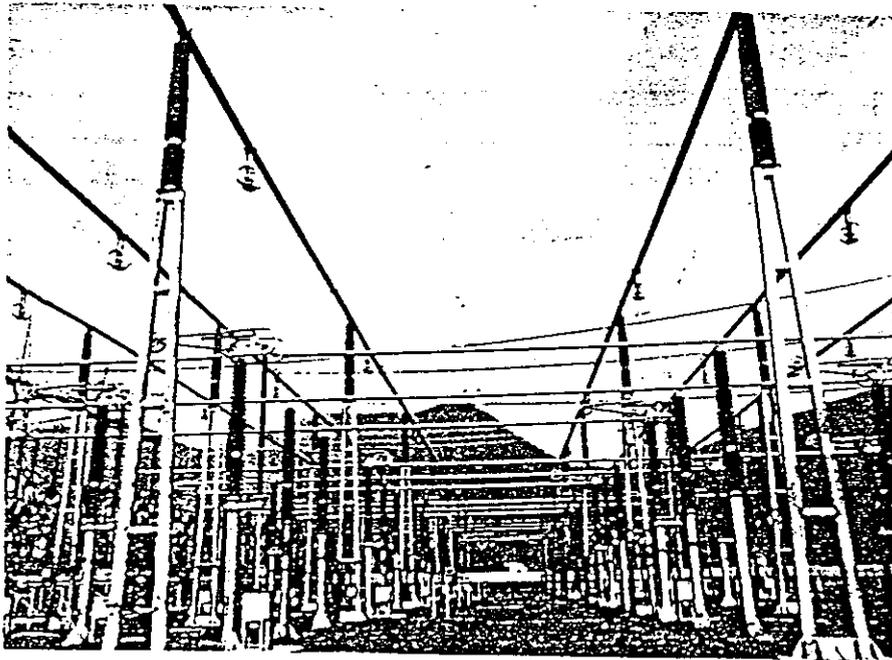
Fig. 1.6   Typical arrangement used in substations with rigid conductors

The design of substations with flexible conductors, as shown for example in Fig. 1.7, is much more complicated. The most common arrangements, three-phases in flat and parallel configuration, are presented in Fig. 1.8. We distinguish here four arrangement cases, which are discussed in Chapters 4 and 5 of this brochure.

- Case A: horizontal strain bus connected by insulator chains to steel structures (usually portals)

- Case B: vertical dropper between strained bus and apparatus

- Case C: horizontal connection between components

- Case D: jumpers connecting two strained conductor sections.
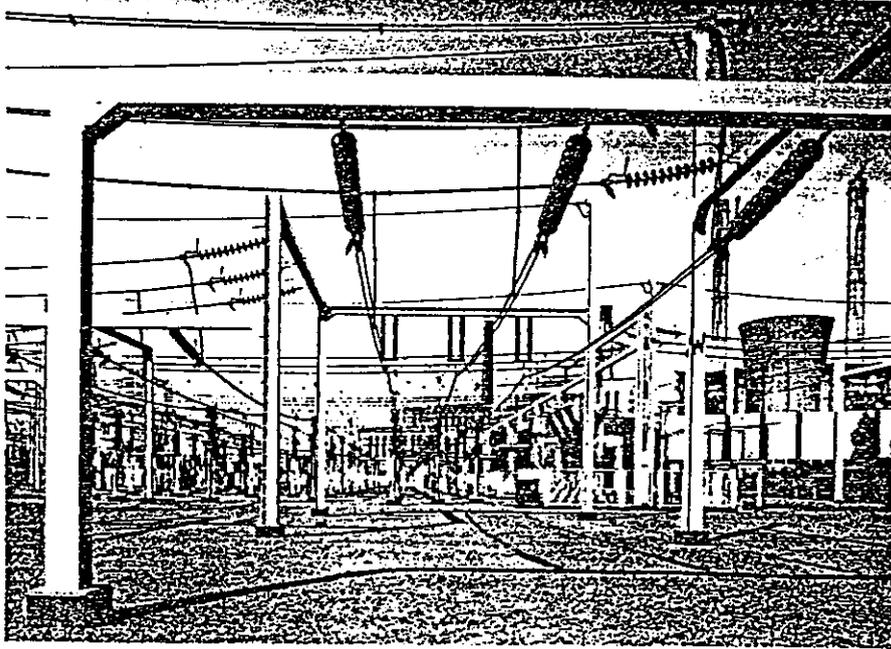
Fig. 1.7   Typical arrangement used in substations with flexible conductors
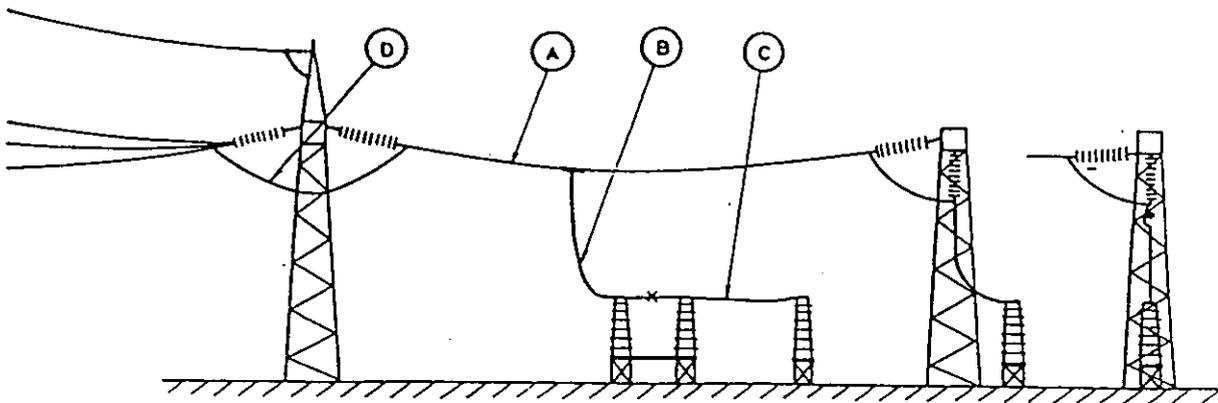
Fig. 1.8   Flexible bus configurations defined by WG 23.02 for calculation and tests

- case A: horizontal strain bus connected by insulator strings to steel structures
- case B: vertical dropper between strain bus and apparatus
- case C: horizontal connection between components
- case D: jumpers connecting two strained conductor sections

14

Typical dimensions of substations are presented in Table 1.2.

Table 1.2
Typical Dimensions of Open Air Outdoor Substations

	Rated Voltage (kV)		
	123	245	420
Substations with rigid conductors			
Bay width - (m)	7-10	14-16	20-22
Distance between phases - a(m)	2-2.5	4	5.5-6.5
Busbars span length l (m)	7-20	10-22	10-22
Substations with flexible conductors			
Bay width - (m)	7-10	14-16	20-22
Distance between phases - a(m)	2-2.5	4	5.5-6.5
Busbars span length l (m)	7-40	15-45	20-85
Bundled conductors			
Number of sub-conductors n_s	1-2	1-4	1-4
Distance between subconductors - a_s (m)	2d-0.15	2d-0.2	2d-0.45
Distance between spacers - l_s (m)	2-5	2-8	2-30

The transition span between the terminating tower of an overhead line and the line entrance portal of the substation is another specific case, not analyzed in this brochure. The flexible conductors used in the above listed cases may be simple cable or bundles, composed of two or more cables. Bundled conductor arrangements are sometimes used to meet ampacity and radio noise (caused by corona) requirements.

The mechanical effects of short-circuit current in the above arrangements depend not only on short-circuit current conditions, but also to a great degree on the geometrical dimensions of the substations and various mechanical parameters which characterize the substation components. These are briefly described below in reference to conductors (rigid and flexible), insulators (post insulators and insulator chains) and supporting structures.

Rigid conductors (tubes) are usually made from aluminum alloy of great mechanical strength and relatively low electrical resistivity. Rigid bus conductors have typical outer diameters in the range 50-300 mm with wall thickness of 4-12 mm. The maximum tube length is typically 20 m. It is possible to weld the tubes together to obtain very long (some tens of meters) uniform conductors; but such a solution is not usually

practical for the substation maintenance. The tubes are fixed to post insulators and apparatus by clamps, which are of rigid, hinged or sliding type. Because of their high stiffness and low mass, rigid bus typically vibrates easily [6,55].

The vibration mechanical frequency f_c depends on span length, tube dimensions and the type of fixation. The lowest significant mechanical frequency of rigid tubular conductors is given for example in Fig. 3.6.

Steel reinforced, aluminum conductors (ACSR) and aluminum alloy conductors (AAC) are usually used for flexible conductors (cables). Conductor cross-section A ranges from 200 to 1600 mm², diameter d from 16 to 52 mm, and mass per unit length m' from 0.5 to 4 kg/m. The span length l, for case A is usually from 10 to 60 m; however, Case C ranges to about 15 m. The jumper length is typically from about 3.5 m for 123 kV substations to about 15 m for the 420 kV substations. In case A, the full span length l between supports must be distinguished from the conductor span length l_c between the end points of insulator chains. As well, the short-circuit current carrying span length, l_F, may be only a part of the conductor length l_c.

Bundled conductors are composed of two to four or more conductors placed with the distance between subconductors a_s, where $2d \le a_s \le 0.45$ m. This distance is maintained by spacers placed at intervals along the bundle, and the distance between spacers l_s, ranges from 2 to 30 m.

Strained conductors (case A) are usually designed with an initial static tension of relatively low value (in relation to overhead lines) in the order of 10-20 N/mm². This is only a small percentage (less than 10%) of the nominal rupture conductor strength. The total sag b (the sum of the cable sag b_c and the insulator string sag component b_i) under this tension amounts to about 3% of the span length. For the maximum permissible temperature of conductors (for example 80°C), the sag is about 30% greater than the initial sag. In some countries, springs are used in series with the conductors are used to maintain constant sag, independent from conductor temperature.

Slack conductors, case C, have still lower tension, in the order 1-2 kN; the sag in this case amounts to about 8% of the span length. The rigid and flexible conductors in case C are fixed on post insulators. The main mechanical parameters of post insulators are given in Table 1.3. Some parameters, such as natural vibration frequencies and damping, are rarely provided by manufacturers. However, the most important parameter in the design is the choice of insulator cantilever strength.

Strained flexible conductors (case A) are connected to the steel supporting structures (usually portals) with insulator strings or chains. These consist of cap and pin porcelain or glass insulators or long rod porcelain insulators. Insulator chains may be single or doubled in either parallel or V arrangements. The V configuration effectively reduces the horizontal deflection of the fixation point of the strained conductors under short-circuit conditions. The most important mechanical parameters of insulator chains are given in Table 1.3. Note that the rupture strengths of insulator chains are similar to those of conductors.

Table 1.3
Post Insulators and Insulator Chains
Typical Data

		Rated Voltage (kV)		
		123	245	420
Post Insulators				
Height	(m)	1-1.7	2.1-2.5	3.15-4.5
Mass	(kg)	35-200	120-400	250-650
Minimum failing load: cantilever strength				
	(kN)	4-16	8-16	8-16
Spring rate	(N/mm)	600-2500	400-700	100-200
First natural frequency	(Hz)	20-40	7-10	4-5
Damping - log decr	(%)	0-10	0-10	0-10
Insulator chains				
Length	(m)	2	3	5
Mass	(kg)	100-150	120-180	200-300
Rupture strength	(kN)	70-120	120-240	240-530

Steel supporting structures are typically of two types: portals for strained conductors and columns supporting post insulators or apparatus. These structures, usually made from latticed or solid webbed steel, are described in section 5.3.2.

These structures are usually made from steel, latticed or solid webbed, and erected on concrete foundations (see section 5.3.2). The mechanical behaviour of such structures is characterized by their spring constant and their mechanical frequency.

Calculation methods for rigid conductors are presented in Chapter 3 and for flexible conductors in Chapter 4. Design guidelines for both cases are given in Chapter 5.

2 TESTING AND MEASUREMENTS

2.1 Introduction

As described in Chapter 1, high levels of short-circuit current result in high mechanical stresses, displacements, etc. on flexible, strained or rigid conductor systems, connections to and between apparatus and supports. These short-circuit effects are important, and in many cases predominate design requirements. The design engineer must ensure that the substation design covers the requirements that originate from short-circuit conditions.

The calculation of dynamic stresses and behaviour (e.g. displacement) of rigid and flexible busbars and connections according to the methods which are described in Chapters 3 and 4 can be applied at the design stage of substations. Most of these calculation methods have been developed in countries participating in CIGRE Working Group 23.02. The results of calculations in some cases have been compared with the results of measurements as given in [4,5,7]. Experience with calculation methods and recommendations derived from calculations, especially on rigid conductors, have been given in [5].

In the case of flexible conductors, the mechanical effects of short-circuit currents are more complicated. Typical arrangements are given in Fig. 1.8 and a number of calculation methods in Chapter 4. The more accurate the calculation method, the smaller the factor of safety needed to allow for uncertainty in calculation results. If a substation design is based only on loads and stresses resulting from simple calculation methods, safety factors on the maximum stresses will usually result in unnecessary over-dimensioning of the substation and consequently to higher cost.

To supplement calculations, full scale tests on full scale sections of the substation being designed can be performed. In this way, designers can verify the required short-circuit withstand capability of the substation. Moreover, in such tests the maximum stresses on bus components can be measured, which can contribute to optimal dimensioning and reliable design. A review of the various possible short-circuit testing arrangements and measuring methods is given in this chapter.

2.2 Tests and Experiments

Design requirements regarding short-circuit strength typically leave the choice of testing or calculation unspecified. However, in the case of testing it is important to distinguish between the two general types of tests, namely proof tests and experimental tests, depending on the objective pursued.

2.2.1 Proof Tests

Proof tests are typically full scale tests on a substation, or part thereof, usually performed in a testing laboratory to demonstrate the ability of the structure to withstand a specific set of loads. No special measurements are required to achieve this purpose.

2.2.2 Experimental Tests

Experimental tests usually involve full scale tests on a substation, or part thereof, generally performed in a testing laboratory. Such tests are required for the development, proof of validity and application of calculation methods. They are necessarily combined with extensive measurements to achieve their objective.

Open air substations, though common, are usually of unique design. This type of substation is not sufficiently numerous that the expenditure for generalized type and proof tests, as in the case of component apparatus, can be justified. If the decision between calculation or tests was simply a question of the costs of applying the method, full scale tests (e.g. [25,30,31]) would not be needed. However, the choice between calculation and/or testing in each case is governed by the overall economic considerations, taking into account:

- the costs of the tests and/or calculations
- the number of identical and/or similar installations
- the significance of design errors relative to the costs of the complete installation(s), taking into account unjustified safety margins due to prognostic uncertainties and the immediate and long-term consequences of failure(s)

While the use of calculation only, without supporting tests, is cheaper in the short term, full scale tests lead to a higher degree of design reliability and possibly lower long term costs because:

(a) The true individual structural and thermal characteristics of the components forming the assembly are automatically fully represented in the test setup. The actual original elements can be used in the tests, thus eliminating the inconsistency between design models and the "real" installation.

(b) The true individual structural and thermal withstand limits of the components are also automatically represented in the test setup (apart from statistical fluctuations in these limits). This is, in fact, a paramount advantage compared to the theoretical approach, in which these limits are, in some cases, rather uncertain or theoretical, or may depend on specified conditions of application.

The advantages of testing to confirm, develop and validate calculation methods are obvious. The objectives for testing are obviously fulfilled in the case of the full scale test; however, reduced scale laboratory testing is sometimes carried out. General uncertainty remains with laboratory model-tests (as with calculations) deriving from the unavoidable deviations between the model and the full scale installation. These deviations result primarily from the variations in the characteristics, properties and limits of the actual elements and parts tested, relative to those of the full scale design.

The obvious advantage of calculations is that the influence of parameter variations can be studied with substantially less effort and cost. The ultimate proof test or calculation validation is, of course, on site testing. This is difficult to carry out in practice; however, at least one example is given in the literature [14].

2.2.3 Calculation and Experimental Tests

All calculation methods introduced for the short-circuit design of bus systems, whether they are simple, medium complexity, or advanced structural analysis methods (FEM) require the results of:

(a) tests to assess the dynamic and static structural, thermal characteristics and withstand limits of the components

and, most important:

(b) full scale tests on typical substation arrangements combined with extensive measurements

- to prove the validity and limits of calculation methods through a variety of single cases covering the field of application;

- to solve a problem which is peculiar to sophisticated calculation methods (FEM), in that the correct development of the modelling requires the experience of calculations in comparison with measured values from full scale testing.

For these purposes, a complete and very detailed set of data describing the geometrical/structure-mechanical parameters of the complete installation tested and of its individual components is absolutely essential.

2.3 Types of Short-Circuit Tests

In general, the following short-circuit tests are relevant and can be performed for a range of current magnitudes and durations.

2.3.1 Phase-to-phase and Three-phase Short-Circuit

Both phase-to-phase and three-phase short-circuits can occur in substations. As indicated in Fig. 1.4 (Chapter 1), equation (3.4) and (3.5), the maximum magnetic forces on the outer phases generated by three phase short-circuits have the same time pattern as those generated by phase-to-phase short-circuits, but they have higher amplitudes. Therefore, three-phase short-circuit faults can be simulated by two phase short-circuit testing. The equivalent value of line-to-line short-circuit current to achieve the same force (equation 3.4) is:

$$I_{K2} = \sqrt{0.808} \cdot I_{K3} = 0.9 \cdot I_{K3}.$$

The factor for peak short-circuit current κ is the same as for the three phase short-circuit.

The maximum magnetic force on the middle phase (Fig. 1.4) is not the same as for the outer phases. Therefore, if the forces acting on the centre phase are of concern, a three-phase short-circuit test should be carried out to test the middle phase. Such tests, especially on flexible conductors, provide information on the interaction of the phases and the dynamic displacements of the system.

A view of electrical testing circuit is given in Fig. 2.1.
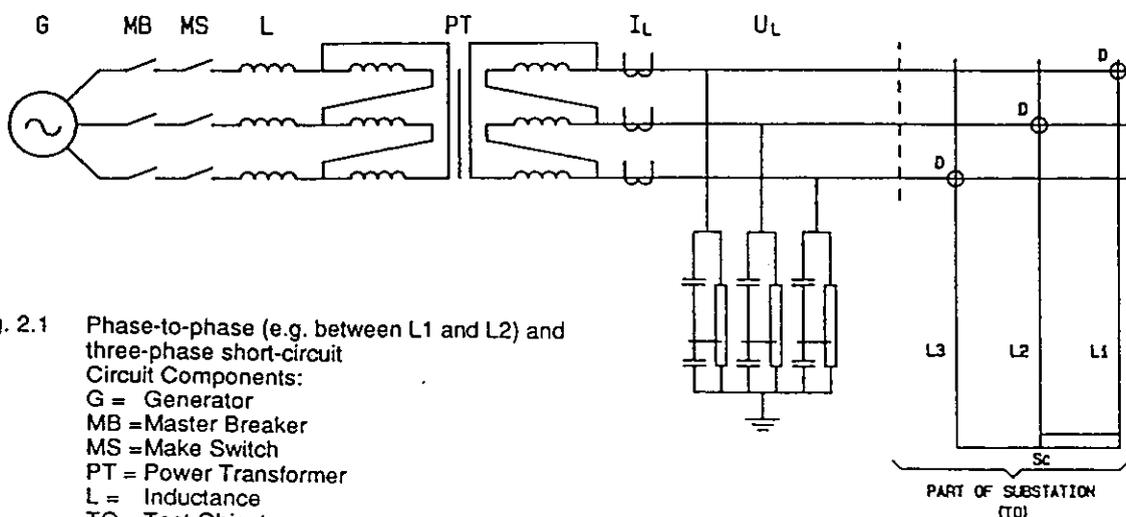
Fig. 2.1   Phase-to-phase (e.g. between L1 and L2) and
three-phase short-circuit
Circuit Components:
G = Generator
MB =Master Breaker
MS =Make Switch
PT = Power Transformer
L = Inductance
TO = Test Object
AB = Auxiliary Breaker
D = Disconnector
Measurements (Low frequency Oscillograph):
U_L = Voltage Measurement
I_L = Current Measurement

2.3.2 Autoreclosure Tests

Unsuccessful autoreclosure leads to a second short-circuit current which may result in a more severe test because the reclosure may occur before the dynamics of the initial fault have damped out. The electrical testing circuit for such tests and a typical testing oscillogram are given in Fig. 2.2 [4,18,58].

The duration of the first and the second short-circuit, as well as the time between the two can vary. The worst case (maximum stress) can occur when the first short-circuit duration = 1/4 period of mechanical frequency and time between the first and second short-circuit = 1 period of mechanical frequency followed by a second short-circuit duration = 1/4 period of mechanical frequency.

2.3.3 Short-Circuit Followed by a Load Current Condition

This real possibility, in terms of substation operations, can also be tested. This type of test is particularly relevant for bundled conductor flexible bus having large span length with or without spacers, dampers etc. to observe the dynamic behaviour and effects on the conductors after fault clearing.

2.3.4 Phase-to-phase Fault Followed by Three-Phase Short-Circuit

In some cases, three-phase short-circuits do not occur spontaneously, but start as a two phase short-circuit which changes to a three phase short-circuit. This type of fault can also be simulated in the testing laboratory.

2.3.5 Short-Circuit Initiation and Duration

The initiation of individual short-circuits, their duration and effects are discussed in sections 1.3 and 3.5. The worst case for short-circuit duration, in case of autoreclosure, is given above.
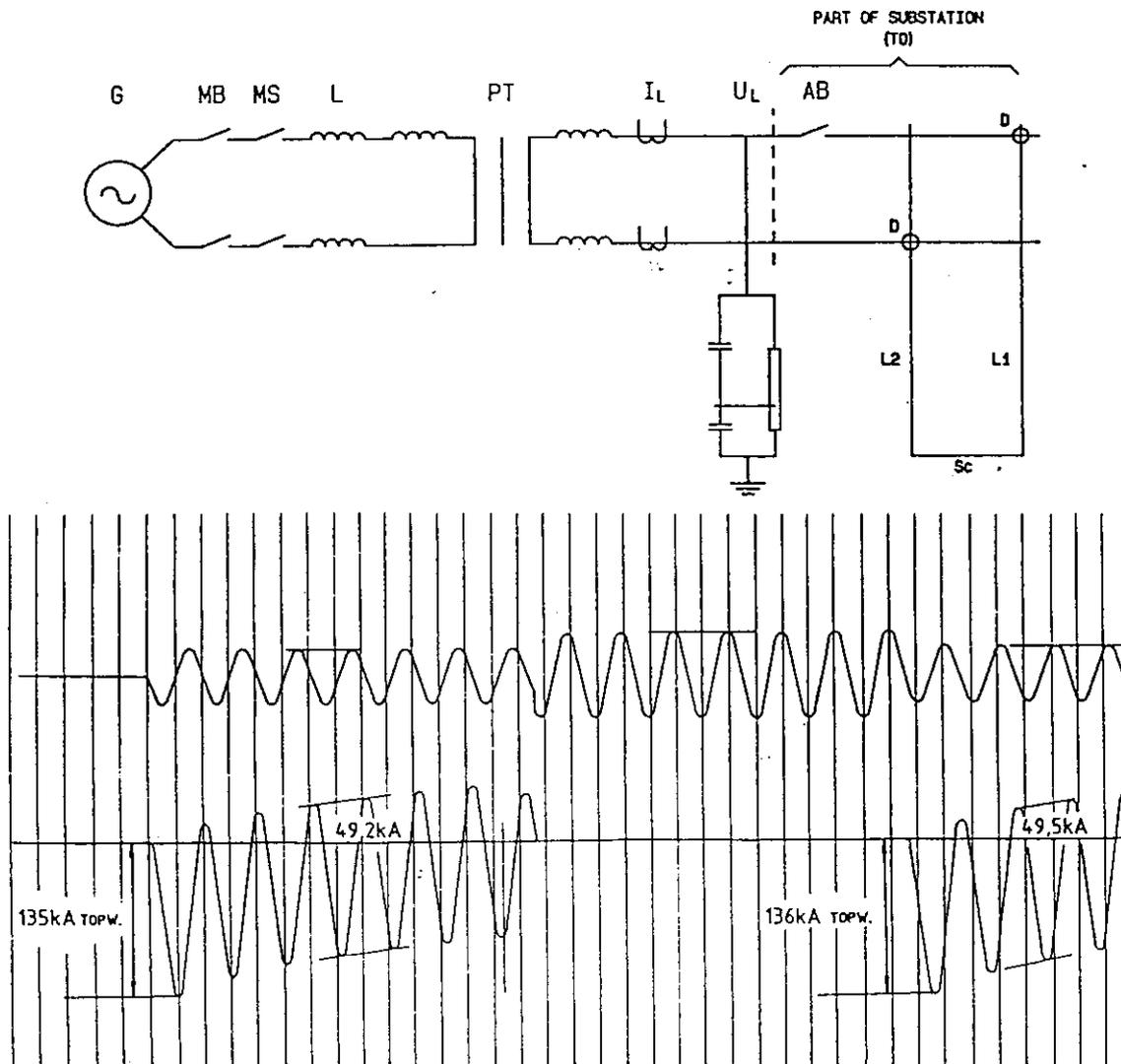
Fig. 2.2   Phase-to-phase short-circuit with autoreclosing duty cycle

2.4 Testing Arrangements

An open air substation is a complex electro-mechanical system which includes bus systems with flexible or rigid conductors, jumper connections between components and between lower and upper bus systems, insulators and structures including the apparatus such as disconnectors, circuit breakers, earthing switches and instrument transformers. (Fig. 1.8). To determine the real dynamic behaviour and effects of loads and stresses due to the short-circuits, full scale testing with very good simulation of parts of the particular substations, including its apparatus, is the most practical and reliable method which can be recommended [24,25,30,31,81,83].

Figure 2.3 illustrates an example of a real test setup. Mechanical, electrical, thermal and power arc testing of components can be carried out within such a test setup. In addition, mechanical and electrical testing of a particular piece of apparatus according to IEC or other requirements is also possible. Figure 2.4 illustrates the testing of disconnectors according to IEC-129 [38], taking into account the dimensions of the particular design.

Testing, especially full scale tests of simulated real parts of substations, has become attractive with the development of laboratory facilities having the capability to perform such realistic scale tests. Recent papers [24,25,30,31,59,81,83] review the results of full scale tests and compare them with calculations of the short-circuit current stresses on conductors, structures and apparatus. The authors report on the extensive tests performed on original parts of substations, measurements of the dynamic stresses.

In addition to extensive tests, References [25] and [31], compare the results of various tests and measurements with those from the calculations according to the advanced methods. Their conclusion is that the most accurate computer calculations can be carried out by expensive and time consuming advanced calculation methods. However, they also note that tests are not cheap, and that without appropriate tests, design principles for economically viable substations cannot be established.
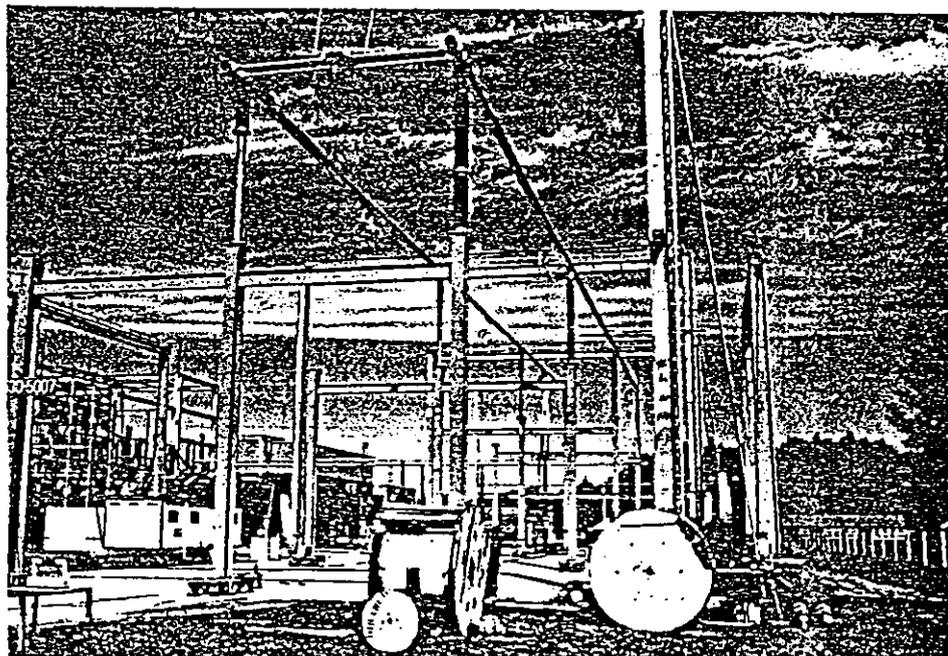
Fig. 2.3 · View of a section of substation full scale test arrangement

20

a. SKETCH OF TEST ARRANGEMENT

b. PHOTOGRAPH OF TEST-ARRANGEMENT
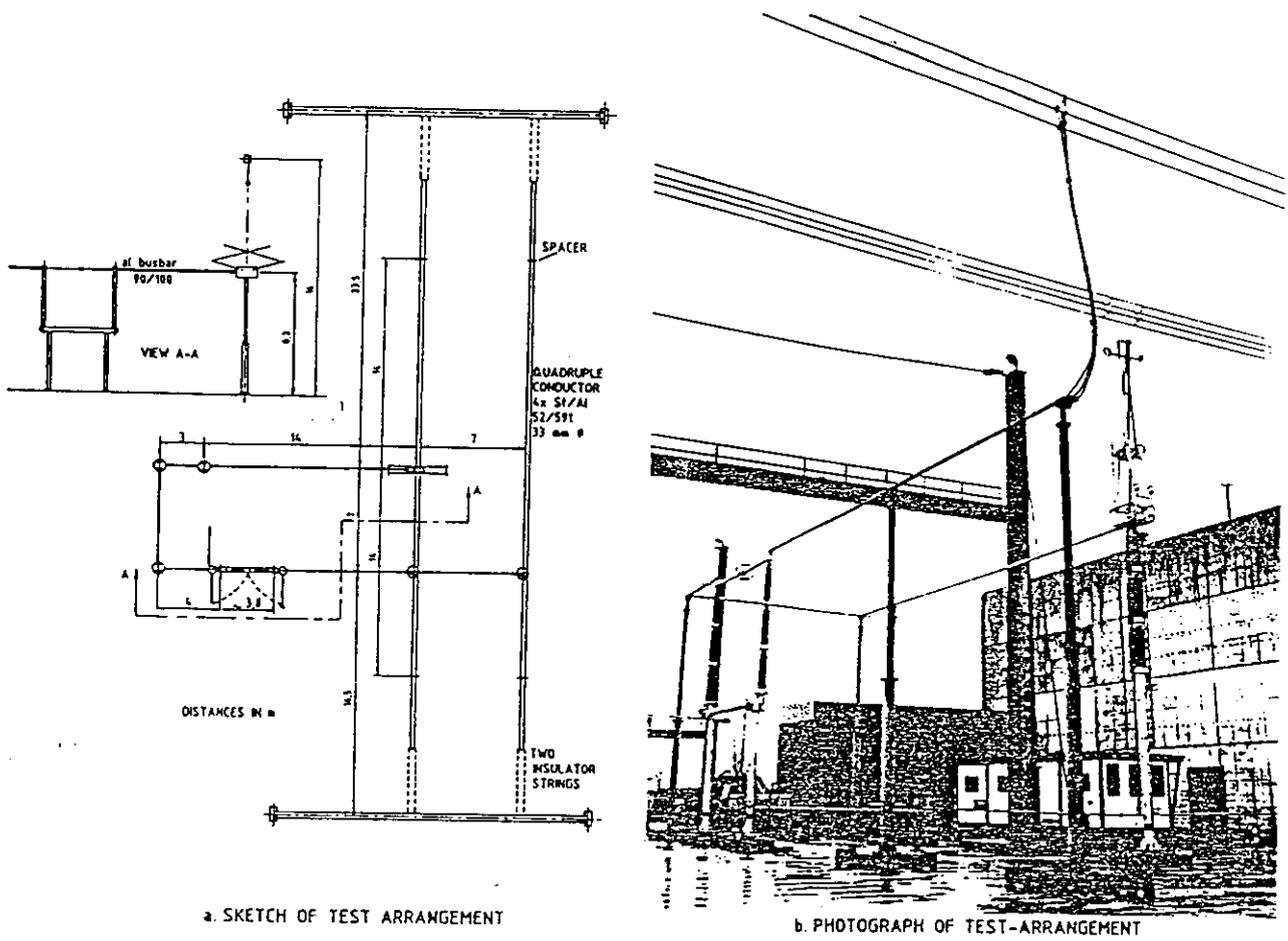
Fig. 2.4   Testing of horizontal disconnector and
pantograph disconnector according to IEC 129,
Figs. 5 and 7 [38]

2.5   Measurements

2.5.1   Methods and Equipment

The problems of measurement are mainly related to the fact that, in order to effectively carry out such measurements, the multi-channel measuring systems (consisting of transducers of mechanical into electrical quantities, e.g., strain gauges, load cells, etc, amplifiers, recording equipment and the required connections and wiring) have to operate in an environment of very high electromagnetic interference. The interference is produced by the very high AC-short-circuit test currents, alternating voltages of some 10 kV and the well-known interference generated by making and breaking operations on secondary equipment.

Practical experience [2,30] has shown that the simplest method to avoid electromagnetic interference and establish potential separation between mechanical/electrical transducers and follow-up units is to employ modulated carrier-frequency systems. A carrier frequency of 5 kHz allows measurements of frequency components up to about 1 kHz, which is usually adequate.

Insulating the measuring equipment from the transducers, which may have to operate at high-voltage, is not the only advantage of transformer potential separation that the carrier frequency measuring systems make possible. Available amplifier and recording equipment is generally not designed to be used under the extreme environmental conditions associated with short-circuit testing. Usually in-line potential separation and inherent channel separation are required to eliminate earth loops, which form a potential source of significant electromagnetic interference.

DC systems may also be used, but require a relatively more complicated technology to achieve the same effect.

General guidelines which should be observed to minimize interference are listed below. More detailed advice can be found in the literature [2,30,103]:

21

- Locate instrumentation as far as possible from the source(s) of interference

- Magnetic and electrostatic shielding of transducers, cable connections and equipment is generally not too important for carrier-frequency operated instrumentation as this type of equipment is insensitive to inductive phenomena of service frequency

- Select suitable single earthing point(s) for measuring circuit(s), screens and equipment. The selection generally involves considering the circuitry of the (multi-channel) equipment to avoid multiple earthing points and earth loops

- Select suitable wiring and cabling with respect to conductor and screen arrangement, in terms of cross-section and conductor arrangement (twisting, weaving etc.)

- Establish a suitable arrangement of measuring cables, e.g. direction, disposal of excessive lengths etc.

The measuring method and equipment according to [30] is presented in Fig. 2.5. In addition, the arrangement illustrated in Fig. 2.5C is possible. The measured signal of a point at earth potential is transmitted via an isolating transformer (Fig. 2.5A) and screened cable to the carrier frequency amplifier and then to the Faraday Cage, in which the measuring devices are located (Fig. 2.6). The isolating transformer provides protection for the equipment.

The measuring signal of a point on an energized part is converted to a light signal and transmitted via the fibre optic cable to the receiver in the screened cage for demodulation and processing (Figs. 2.5B and 2.6).

The use of an additional isolation transformer instead of optic fibre system is also possible. Both systems have been tested in practice and are suitable for these purposes. The measuring quantities are generally bending stresses in the post insulators, steel supports and tubular conductors in a rigid bus system and are measured by strain gauges.
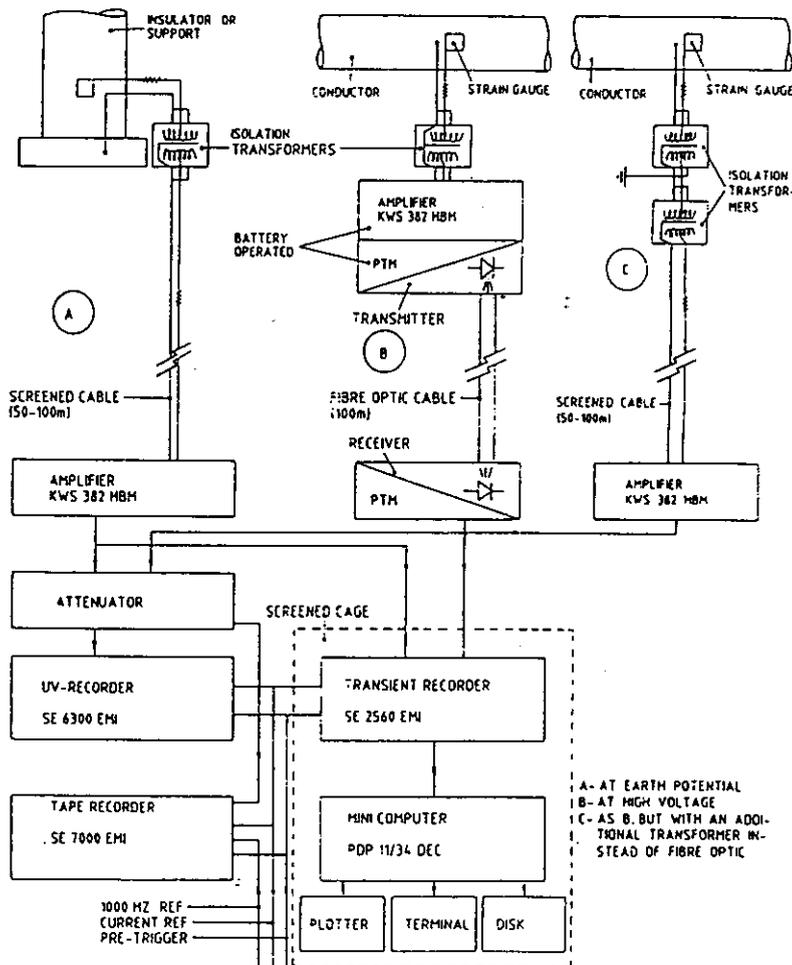
Fig. 2.5   Measuring System
(The specific measuring equipment illustrated
is provided as an example of a properly
functioning measuring system and not as an
endorsement of the particular components.)

22

Fig. 2.7   Device for measuring of tension in Flexible
            conductors and insulator-strings

STRAIN-GAUGE BRIDGE
SENSITIVE IN ONE DIRECTION

DIMENSIONS IN mm
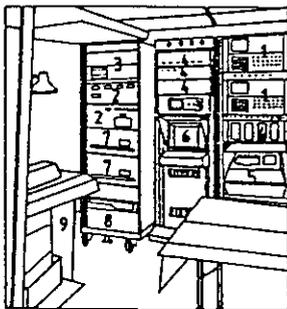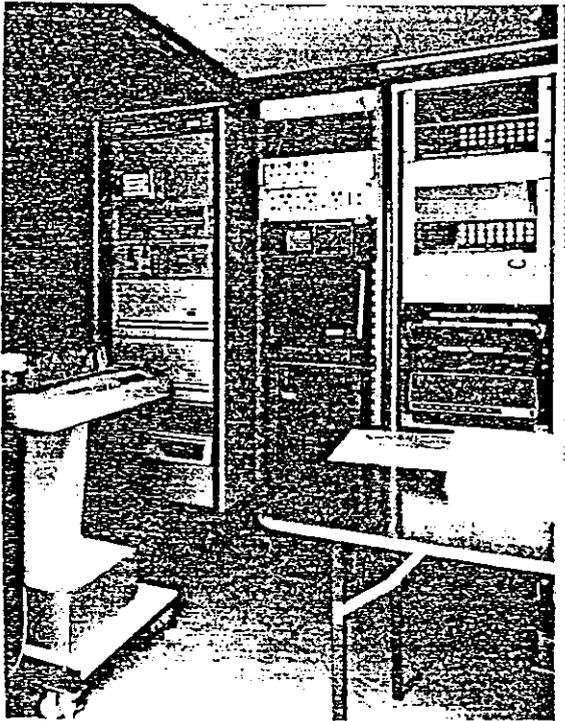
1. FAST TRANSIENT RECORDER
2. VERY FAST TRANSIENT RECORDER
3. MONITOR
4. OPTIC FIBRE-RECEIVERS
5. UV-RECORDER
6. TERMINAL, KEYBOARD
7. COMPUTER DISC
8. MINI COMPUTER
9. PRINTER

Fig. 2.6   Inside view of a part of a shielded room con-
            taining measuring instrumentation

In the case of flexible conductor arrangements, the ten-
sions in (sub)conductors and insulator strings are the
most important stresses. For this purpose a special
device, as illustrated in Fig. 2.7, can be built into the con-
ductor or insulator string. The measuring bridge is
placed in the device. The measuring equipment is
placed in a transportable Faraday Cage where the
sensitive digital apparatus is shielded from electromag-
netic interference.

Displacement measurements are also an important
quantity, especially in the case of flexible conductors.
Displacement can be measured by means of:

-    electro-optical displacement transducer
-    ultrasonic position sensors
-    electrical displacement transducer
-    accelerometer built into the tubular conductor
-    high speed film photography
-    high speed videography (about 1000 pictures per
     second), which makes it possible to record bundle
     pinch phenomena.

Finally, temperatures can be measured by means of op-
tical fiber based thermometers. This type of
thermometer measures temperature using optical techni-
ques and single nonconducting optical fibres between
the point of measuring and the instrument. The probe
consists of an optical fibre with a temperature sensor at
one end. The sensor is illuminated through the fibre
from a light emitting diode in the instrument. The light
stimulates the sensor and emits light with a wavelength
depending on temperature. This wavelength is con-
verted into electrical signals in an optoelectronic detec-
tor. The outputs from the instrument are analog voltage
or current signals compatible with RS-232C or IEEE-488
interfaces.

2.5.2   Data Registration and Processing

Measured data registered by digital recorders according
to Figs. 2.5 and 2.6 can be presented immediately by
UV-recorders or stored on disc in mini- or micro-
computers for subsequent processing and presentation.
(See also [30])

2.5.3   Measuring Points and Calibration

Measuring devices and strain gauge bridges should be
placed on conductors and components where maximum
stresses are to be expected and/or particularly on sensi-
tive locations where stresses cannot be easily predicted.
The measuring devices must be calibrated. The device
for measurement of tensions (Fig. 2.7) can be calibrated
in the laboratory and strain gauge bridges on post in-
sulators and steel supports can be calibrated as il-
lustrated in Fig. 2.8.

Static and dynamic calibration of post insulators, both
separately and together with the steel supporting struc-
tures is necessary to obtain mechanical data such as
stiffness EJ and frequencies. Accurate values for these
data are necessary for calculation of dynamic stresses
and strength.

23
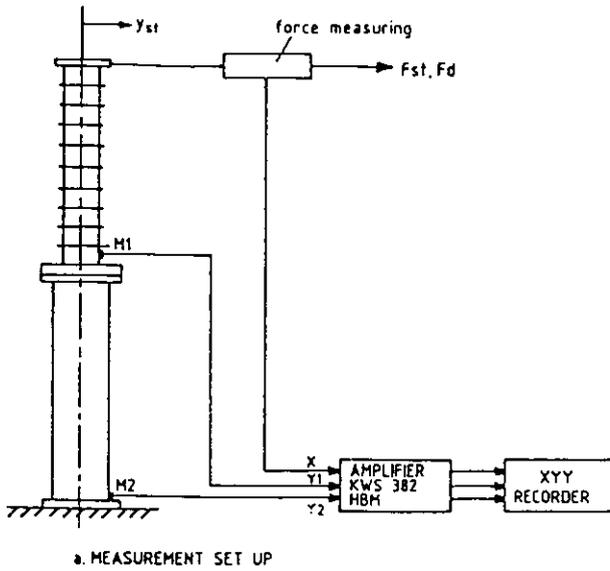
a. MEASUREMENT SET UP
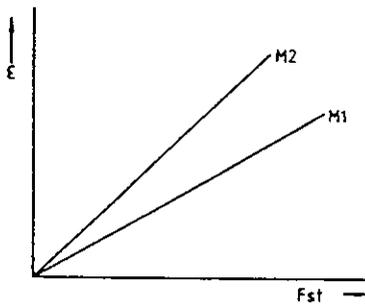
b. DETERMINATION OF STRAIN (ε) IN RELATION TO THE STATIC FORCE Fst

Fig. 2.8 Schematic view of calibration of measuring point on insulator (M1) and steel-supporting (M2)

As the post insulators are particularly sensitive components of rigid bus systems, the determination of their strength and dynamic behaviour is very important. Some results of investigations on post insulators and their strength are given in [26]. From the static force F_{st} according to Fig. 2.8 and displacement Y_{st}, the static stiffness of post insulators can be determined. Measurement of the dynamic response force F_d, for which the frequency may vary, can serve to determine the natural mechanical frequency of the system.

If dynamic calibration is not possible, then the mechanical frequencies of insulators can be determined from the static calibration as follows. From static measurements according to Fig. 2.8 we obtain

$$C = \frac{F_{st}}{Y_{st}} \qquad (2.1)$$

The static deflection of a beam according to Fig. 2.9a can be calculated according to

$$Y_{st} = \frac{F_{st} \cdot \mathcal{A}^3}{3 \, EJ_o} \cdot \frac{1}{v} \qquad (2.2)$$

From equations (2.1) and (2.2), we obtain

$$EJ_o = \frac{C \, \mathcal{A}^3}{3} \cdot \frac{1}{v} \qquad (2.3)$$

The mechanical harmonic frequencies of a beam according to Fig. 2.9a can generally be calculated according to

$$f_n = \frac{\gamma_n^2}{2\pi \cdot \mathcal{A}^2} \sqrt{\frac{EJ_o}{m_i}} \qquad (2.4)$$

where

$$J_o = \frac{\pi}{64} \cdot d_{max}^4 \qquad (2.5)$$

$$m_i = p \cdot \frac{\pi}{4} d_{max}^2 = \frac{M_i}{\mathcal{A}_i} \cdot \frac{3}{v^2 + v + 1} \qquad (2.6)$$

Substituting equations (2.3) and (2.6) in (2.4) gives

$$f_n = \frac{\gamma_n^2}{2\pi} \cdot \sqrt{\frac{C}{M_i} \left(v + 1 + \frac{1}{v}\right)} \qquad (2.7)$$

where:
γ_n = Eigen values according to Fig. 2.9c
C = spring constant according to Eqn. (2.1)
M_i = total mass of insulator column in kg
$v = \frac{d \min}{d \max}$:

2.6 Mechanical Tests on Insulators

In open air substations, insulators are the most fragile components in terms of short-circuit stresses. This is, of course, a result of the lack of a plastic phase (yield) prior to destructive material elongation (strain) or fracture in the case of porcelain.

Strain insulators, as typically employed in substations, do not experience problems in this respect since their loadings are usually much less than their ratings. (Strain insulators with ratings in the same order as the breaking strength of the conductors are readily and economically available.) This cannot be said of post insulators subjected to bending loads in the case of short-circuit. These are typically used in substations for rigid bus supports; but also disconnectors, breakers, arresters, measuring transformers, transformer bushings and GIS bushings.

The cross-sections required to withstand a given bending load increase rapidly with the voltage level as the bending moment is proportional to post height or length of the cantilever arm.

Narrower margins of safety have to be tolerated in this case because of the high cost and limited strength capabilities of post insulators. This puts an increased importance on the need for accurate calculation techniques and detailed knowledge of the material properties and mechanical characteristics of post insulators and their support structures.

24
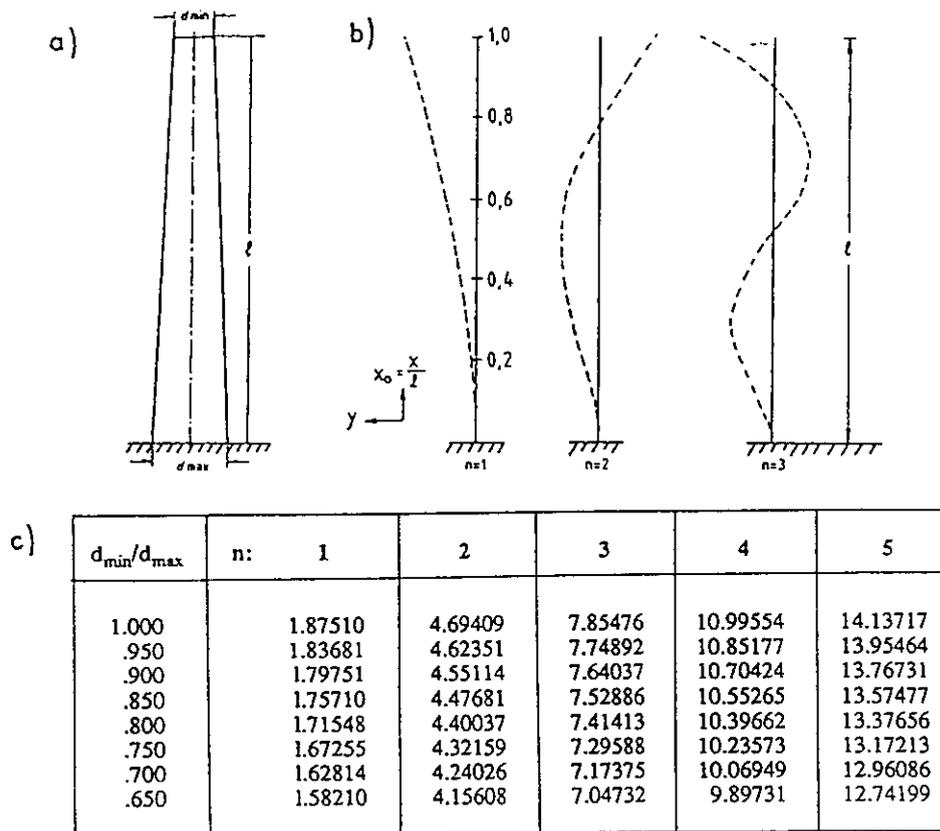
Fig. 2.9 Eigenvalues of a beam with clamped and free
ends (γ_n) with diameters at the ends d_{max} and
d_{min} respectively
a) Beam (clamped - free)
b) Some modes of oscillation
c) Eigenvalues γ_n (n=modenumber)

d_{min}/d_{max}	n: 1	2	3	4	5
1.000	1.87510	4.69409	7.85476	10.99554	14.13717
.950	1.83681	4.62351	7.74892	10.85177	13.95464
.900	1.79751	4.55114	7.64037	10.70424	13.76731
.850	1.75710	4.47681	7.52886	10.55265	13.57477
.800	1.71548	4.40037	7.41413	10.39662	13.37656
.750	1.67255	4.32159	7.29588	10.23573	13.17213
.700	1.62814	4.24026	7.17375	10.06949	12.96086
.650	1.58210	4.15608	7.04732	9.89731	12.74199

2.6.1 Structure-mechanical Properties and Characteristics

There is no need to describe details of the assessment of the properties, listed below, of the individual structural parts and their materials. These data are obviously indispensable for modelling insulators:

- geometrical form ⎫
- mass density ⎬ > mass distribution
- masses ⎭
- Young's moduli

The static and the dynamic performance of insulator models can be checked against measurements of stiffness and Eigenfrequency characteristics as discussed in section 2.5. Only the case of the actual loading, i.e. bending, need be considered. The measurements of stiffness and Eigenfrequency can, and should, be done in the same test setup (Fig. 2.8). These may relate to just one value of displacement corresponding to one value of static bending force applied. The value of this force and of the corresponding displacement shall be approximately equal to those applied in routine testing. These measurements can be done together by releasing the insulator in the deflected position (first Eigenform) to oscillate into zero position (first Eigenfrequency).

Similar measurements and tests on other components and combinations of components subjected to dynamic bending forces, for example steel columns, towers, portals, cross arms, etc., are possible and are increasingly useful the more complex the structure considered.

2.6.2 Withstand Limits

When one has obtained, by some method, estimates of the short-circuit loads and/or stress values, they must be compared with estimates of the permissible loads and stresses. Testing is of particular importance in establishing the strength of insulators, and the dynamic, as opposed to the static, nature of the short-circuit loading must be considered. For most practical cases, the assumption of quasi-static insulator behaviour may be adequate to allow operation within permissible bending loads.

Beyond the quasi-static case, actual material stresses must be compared with permissible values. Tests are indispensable in assisting the development and proof of methods to assess material stresses in insulators and to find permissible values of stresses for the short-circuit range of the general dynamic case. In addition, both material strength properties and the overall strengths of insulators can be expected to display considerable statistical variability. Therefore, the number of tests needed to establish withstand values must consider statistical significance requirements.

Based on the above, three types of tests can be identified:

(a) Type and acceptance tests on insulators
(b) Special tests on insulators
(c) Material tests on specimens.

2.6.3 Type and Acceptance Tests on Insulators

The only strength data that the manufacturer supplies is the "Minimum Breaking Load" (MBL) of an insulator. This can be considered as a guaranteed value for static loading which is generally derived from statistical test results [35]. The statistical basis for the MBL is not defined by standards, varies considerably, and is frequently not provided by the manufacturer. The higher the voltage level, i.e. the cost of an insulator, the oftener this value is checked in acceptance tests on individual lots of insulators. These full-load acceptance tests give a good indication of the quality control consistency achieved and the maximum achievable level of safety.

2.6.4 Special Tests on Insulators

Mechanical tests as described in [26,27,53], involving extensive strain-gauge and displacement measurements and comparison of static and representative short-circuit insulator loadings, can contribute considerably to the assessment of insulator response to different loadings and the parameters that influence it. Such studies on real insulators, can support or confirm the applicability of material specimen measurements. These tests have brought forth important results that must have influence on the further studies in stress assessment and the practical solution of the problem of strength assessment.

Due to stress concentrations (usually at the points of highest global stress), it is necessary to apply stress-concentration factors (>1), which are particular to the insulator type and location in the insulator, to derive discrete stress values from the bending moment and the core diameter. Further static and dynamic tests, to define stress-concentration factors more precisely are highly recommended.

2.6.5 Material Tests on Specimens

The costs of tests on full-size insulators, as described above, whether destructive or not, are so high that it is evident that only the minimum required data will be obtained. As with the application of other materials, e.g. metals, designers have to rely to an extent on strength values derived from tests on material specimens [99,101].

2.7 Conclusions

The mechanical stresses caused by short-circuit current in substations can be calculated according to various calculation methods which will be described in subsequent sections. Calculations methods are necessary at the design stage; but for optimal and reliable design, their accuracy should be confirmed by tests for the following reasons:

- The construction of a substation including its components, apparatus, connections and fittings is a complicated mechanical system, which may be too complex for accurate calculation.

- The data required for advanced calculations may not be available.

Therefore, laboratory tests, especially full-scale tests on sections of a real substation setup, are justified in some cases. The values of the short-circuit loading and design strength can be varied and an optimal and reliable design obtained. In addition, the electrical, mechanical and thermal testing of the particular components and apparatus can be combined to reduce the total cost of the testing.

Measurement data obtained during such tests provide supplementary technical information, which is useful in confirming and extending the capabilities of calculation methods.

3 RIGID BUS SYSTEMS

3.1 Introduction

An arrangement of rigid busbars in one plane is commonly used in modern HV and EHV open air substations. The structure must be strong enough to withstand the significant mechanical stresses created by short-circuit current flow. These stresses appear in the tubular conductors and in the supporting structures composed of insulators and substructures.

The verification of calculation methods used for design, and recommendations for proper design procedures were the tasks of CIGRE Working Group 23.02. This Working Group published its first report describing measurement methods and a preliminary comparison of test results in 1973 [2]. At the 1976 CIGRE Session, a second report on comparison of calculated and measured values was presented [3]. Lastly, the results of a full comparison between calculated and measured values was presented in [4]. This comparison showed satisfactory consistency of results thereby confirming the accuracy of several calculation methods. Parametric studies and conclusions regarding simplified calculation methods were published in [5] and computer aided approaches in [8]. The results of CIGRE WG 23.02 investigations have been incorporated in IEC 865/86 [39].

3.2 Electromagnetic Short-Circuit Force

For the dimensioning of HV and EHV arrangements, the stress in the conductors and insulators of the outer phases L1 and L3 (Fig. 3.1) resulting from a three-phase short-circuit is decisive [5]. The worst case time function of the electromagnetic forces acting on conductors L1 or L3 during a three-phase short-circuit per unit length $F'_{L1}(t)$ = $F'_{L3}(t)$ is given by Equation 3.1a and for a phase-to-phase short-circuit $F'_2(t)$ by Equation 3.1b, see also Fig. 1.4:

$$F'_{L1}(t) = F'_{L3}(t) = C' \cdot \frac{\sqrt{3}}{2} \left\{ \frac{\sqrt{3}}{4} - \frac{1}{2} \cos(2\omega t - 2\gamma_z) \right.$$

$$+ e^{-\nu\tau} \left[\cos(\omega t - 2\gamma_z) - \frac{\sqrt{3}}{2} \cos\omega t \right]$$

$$\left. + e^{-2\nu\tau} \left[\frac{\sqrt{3}}{4} - \frac{1}{2} \cos2\gamma_z \right] \right\}$$

$$= C' \cdot e_{L1}(t) = C' \cdot e_{L3}(t) = C' \cdot e_{k30} \quad (3.1a)$$

$$F'_2(t) = C' \cdot \frac{3}{4} \left[\frac{1}{2} - \frac{1}{2} \cos(2\omega t - 2\gamma_z) + 2e^{-\nu\tau}\sin(\omega t - \gamma_z)\sin\gamma_z \right.$$

$$\left. + e^{-2\nu\tau}\sin^2\gamma_z \right]$$

$$= C' \cdot e_2(t) = C' \cdot e_{k2} \quad (3.1b)$$

where,

$C' = \frac{\mu_0}{2\pi a} \cdot (\sqrt{2}i_{k3})^2$, the reference force per unit length, (3.2)

γ_z = arctan X/R, the impedance angle

X/R= reactance to resistance ratio

$$\tau = \frac{L}{R} = \frac{X}{\omega R} \quad (3.3)$$
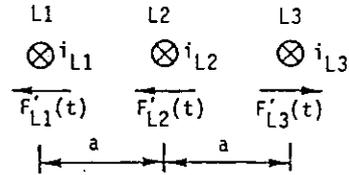
Fig. 3.1   Conductor arrangement and reference directions

The peak forces are proportional to the square of the factor κ for the peak short-circuit current (equation 1.5).

The peak short-circuit forces per unit length are:

- Three-phase short-circuit, conductor L1 or L3

$$F'_{L1p} = F'_{L3p} = \frac{3+2\sqrt{3}}{8} C' \kappa^2 = 0.808 C'\kappa^2 \quad (3.4)$$

- Phase-to-phase short-circuit

$$F'_{2p} = 0.750 C' \kappa^2 \quad (3.5)$$

- Three-phase short-circuit, conductor L2

$$F'_{L2p} = \frac{\sqrt{3}}{2} C' \kappa^2 = 0.866 C' \kappa^2 \quad (3.6)$$

The functions (3.1a) and (3.1b) can be broken down into partial functions with different mechanical effects

$$e(t) = \underbrace{e_0 + e_{2\omega}(t)}_{\text{steady state}} + \underbrace{e_g(t) + e_\omega(t)}_{\text{decaying}} \quad (3.7)$$

where

e_0 = a constant term (arithmetic mean of e(t) in the steady state)

$e_{2\omega}$ = undamped oscillation at double electrical frequency

e_g = exponential term, decaying with time constant τ/2

e_ω = oscillation with electrical frequency, decaying with τ

Figure 3.2 shows the components of the electromagnetic force according to Eqs. 3.1a and 3.7. The corresponding force for the conductor L2 is given in Fig. 1.4a (Chapter 1).

3.3 Dynamic Response of the System

The dynamic effects of the electromagnetic force can be described with the aid of factors:

$$\left. \begin{array}{c} v_F(t) \\ v_o(t) \end{array} \right\} = \frac{\text{Stress in dynamic case}}{\text{Stress in static case}}$$

where

$v_F(t)$= factor for insulator stress

$v_o(t)$= factor for conductor stress
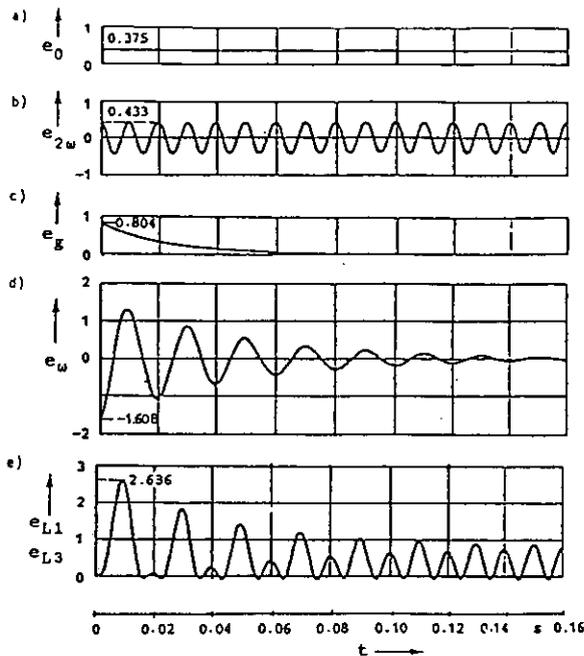
Fig. 3.2 Worst case time functions of electromagnetic forces (eq. 3.1a) related to reference force C' according to eq. 3.2. Conductors L1 or L3, R/X = 0.07

a) e_o = constant term

b) $e_{2\omega}$ = undamped oscillation at double the electrical frequency

c) e_g = exponential term, decaying with time constant $\tau/2$ ($\tau = L/R$)

d) e_ω = oscillation with electrical frequency, decaying with time constant τ

e) $e_{L1}(t)$ = $e_{L3}(t) = e_o + e_{2\omega}(t) + e_g(t) + e_\omega(t)$

For static reference values, the electromagnetic force is assumed to be constant and equal to its maximum momentary value. The maximum momentary values of $v_F(t)$ and $v_\sigma(t)$ are characterized in the following paragraphs by V_F and V_σ. The dynamic behaviour of structures during short-circuit, for a range of structural frequencies, are illustrated in Figs. 3.3 and 3.4 due to the forces of Fig. 3.2.

If the frequency of the mechanical fundamental oscillation or of a mechanical harmonic oscillation is equal to the simple or the double electrical frequency, resonance enhancements of the stress will occur. Figure 3.3 shows the factor $v_F(t)$ for line-to-line short-circuits for the mechanical fundamental Eigenfrequencies f_c = 1.7 Hz, 10 Hz, 25 Hz, 50 Hz, 100 Hz and 150 Hz. A comparison of Fig. 3.3a with Figs. 3.3b to 3.3g, shows that the time function of the dynamic insulator stress is similar to that of the acting force for only the higher mechanical fundamental frequencies f_c > 150 Hz. For mechanical frequencies $f_c \geq$ 250 Hz, there is a practical coincidence of the two time functions and the maximum value of factors V_F and V_σ are approximately equal ($V_F = V_\sigma \approx$ 1). For low mechanical frequencies and frequencies out of the resonance ranges, V_F <1 and V_σ < 1. This comparison also shows that even if the maximum instantaneous value of the electromagnetic force occurs approximately 10 ms after the appearance of the fault, the maximum value of the dynamic stress occurs for f_c<150 Hz much later and depends on the mechanical fundamental frequency.
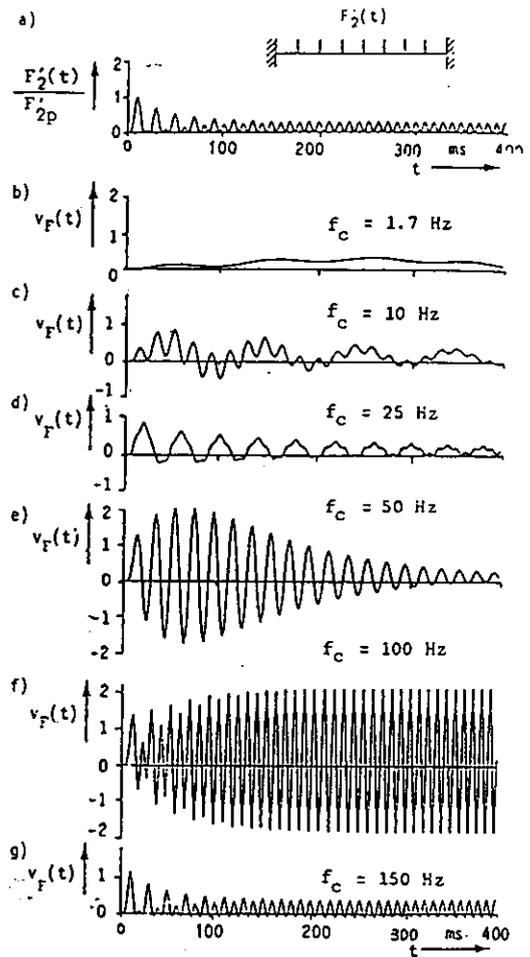
Fig. 3.3 Electromagnetic force per unit length for line-to-line short-circuit $F'_2(t)$ related to the peak value F'_{2p} (figure a) and coefficient $v_F(t)$ for different mechanical fundamental frequencies f_c (figures b to g). R/X = 0.07, Λ = 0.2 [1, Appendix IV]

In Fig. 3.3c, f_c / f = 10/50 = 0.2. For f_c / f = 0.185, there is a resonance of the third harmonic oscillation with the 50 Hz term of the electromagnetic force. But the 50 Hz harmonic oscillation is also excited for the value f_c / f = 0.2, which is close to the resonance value. Figure 3.3e shows the 50 Hz resonance of the mechanical fundamental frequency. Because the term $e_\omega(t)$ of the electromagnetic force is decaying, the corresponding factor $v_F(t)$ also decays after it reaches its maximum value.

Figure 3.3f shows that for the 100 Hz resonance, where the magnitude of the term $e_{2\omega}(t)$ is constant, the maximum instantaneous values of the factor $v_F(t)$ are limited to a maximum value which depends on the value of the mechanical damping decrement Λ. Without damping, these values would increase linearly with time.

The dynamic effects of the electromagnetic force terms of Fig. 3.2 are very different and do not result from the maximum instantaneous values of these terms.

28

Figure 3.4 shows the factors V_σ, for conductors with both ends fixed, as a function of the ratio f_c / f during a three-phase short-circuit, for the phases L1 or L3. In order to compare the different curves, factors $V_\sigma 0$, $V_\sigma 2\omega$, $V_{\sigma g}$, $V_{\sigma \omega}$, and $V_{\sigma 0+g}$ are related to the same static value as the factor V_σ. From comparison of Figs. 3.4 and 3.2, it is clear that, especially in the low mechanical frequency range (typically for HV and EHV structures $0.02 < f_c / f < 0.2$), the dynamic effect of short-circuit forces cannot be estimated from the maximum instantaneous values. For example, $f_c / f = 0.1$ corresponds to $V_\sigma 0/V_\sigma 2\omega = 27.8$ even though the maximum instantaneous value of $e_{2\omega}$max is greater than e_0, $e_0/e_{2\omega}$max $= 0.866$.
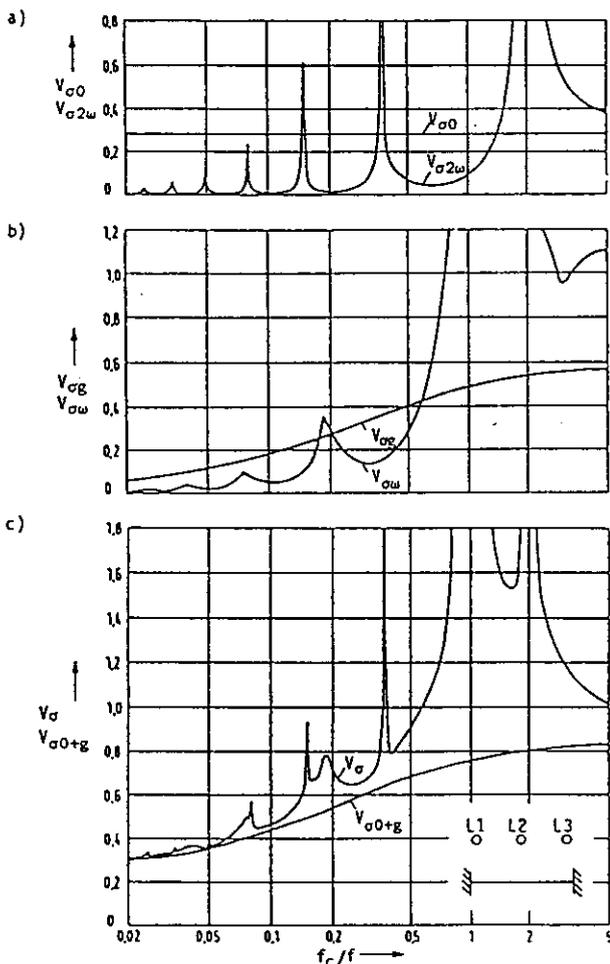
Fig. 3.4   Factors V_σ for dynamic stress of the conductors for the different time functions of electromagnetic forces of Fig. 3.2 [74].
a) $V_\sigma 0$ when only e_0 is acting,
   $V_\sigma 2\omega$ when only $e_{2\omega}(t)$ is acting
b) $V_{\sigma g}$ when only $e_g(t)$ is acting,
   $V_{\sigma \omega}$ when only $e_\omega(t)$ is acting
c) $V_{\sigma 0+g}$ when only $e_0 + e_g(t)$ is acting,
   V_σ when $e_{L1}(t) = e_0 + e_{2\omega}(t) + e_g(t) + e_\omega(t)$
   is acting

Factors $V_\sigma 0$ and $V_\sigma 2\omega$ are independent of the ratio R/X. The term $e_{2\omega}(t)$ causes enhancements in the 100 Hz resonance ranges. The effect of this term outside the resonance ranges and for low mechanical frequencies is very small. Figure 3.4b shows the effect of the terms $e_g(t)$ and $e_\omega(t)$ on the factor $V_{\sigma g}$ and $V_{\sigma \omega}$ for R/X = 0.07. These factors depend on the ratio R/X. Fig. 3.4c illustrates that in the range of the usual HV and EHV structures and outside the resonance ranges, almost all of the dynamic stress is due to the terms $e_0 + e_g(t)$. These results are also valid for the corresponding factors V_F.

3.4   Calculation Methods

Bus structures with rigid conductors consist of parallel conductors, supported by insulators and their substructures (that is, beams within the terms of mechanics), as illustrated in Fig. 3.5. Time variant electromagnetic forces act on the conductors during short-circuits; and the whole structure performs forced oscillations for the short-circuit duration and free oscillations after the clearing of the fault. Different dynamic deflections and stresses (usually bending stresses) appear at every point of the structure. The maximum bending stress in the conductors and in the insulators is of particular interest.

Currently, two classes of methods are in general use:

- simplified methods based on simplified models (e.g. modified static) which yield fast estimates of real results suitable for everyday design purposes.

- advanced methods based on relatively realistic models, which are more cumbersome to use but which can be used to give accurate results for complex configurations

Methods of the first group are especially useful for hand calculation but are also sometimes programmed. They are relatively easy and presently are the most commonly used design methods. Application of the advanced methods is computer aided. They are especially desired in cases where more precise knowledge of busbars or supporting structure response to short-circuit current forces is required.

3.4.1   *Simplified Methods*

Description

These methods are modified static methods [1,5,39,45,49,56]. A simplified calculation can be performed in the following two steps:

1. Static Calculation - for rigid supports, stress values and deflections can be easily determined by well-known static analysis methods. The electromagnetic force per unit length is assumed to be constant and equal to its absolute maximum according to equations 3.4, 3.5 and 3.6.

2. Dynamic Calculation - the dynamic stress values are obtained by multiplication of the static stress values with factors V_F for the insulator stress and V_σ for the conductor stress; the deflection can be calculated in the same way, if desired, using the factor V_σ for approximation (V_F and V_σ were defined in section 3.3.).

29
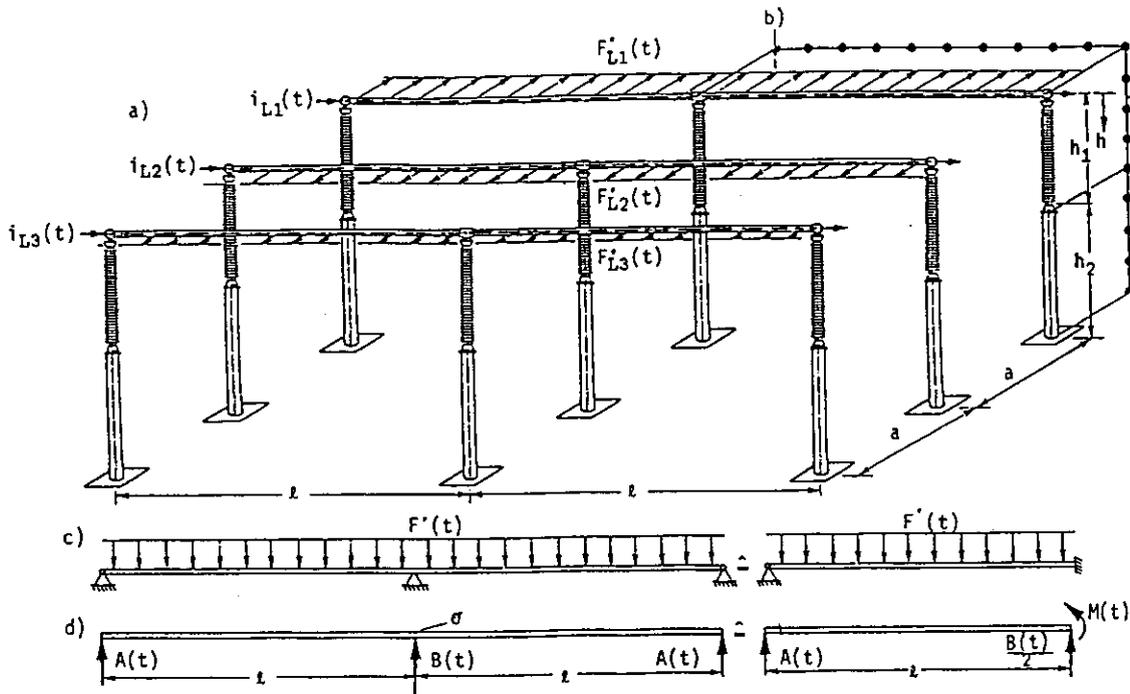
Fig. 3.5   Three-phase rigid bus system with two spans
a)   Physical arrangement
b)   Model for numerical calculation methods,
     m_i mass element. E modulus of elasticity, J
     moment of inertia
c)   Model considering the insulators and the
     supports as rigid
d)   Forces and moments at the conductor sup-
     porting points

The parametric studies carried out in [5] show that the most important parameter for the calculation of the dynamic short-circuit stress is the mechanical fundamental frequency. In the case of rigid supports, the mechanical fundamental frequency f_c can be easily determined from equation 3.8 or Fig. 3.6; whereas for elastic supports, special computer programs are used. In publications [75,84] a method is developed to calculate the fundamental mechanical frequency in the case of elastic supports, without computer programs, using curves [84]. As discussed in [5] conventional high-voltage substations can be assumed to have rigid supports.

$$f_c = \frac{\gamma^2}{2\pi \ell^2} \sqrt{\frac{EJ}{m'}} = \frac{\gamma'}{\ell^2} \sqrt{\frac{EJ}{m'}} \qquad (3.8)$$

where,

f_c = mechanical fundamental frequency (Hz)
γ' = factors according to Fig. 3.8c

Figure 3.7 shows factor V_F as given by various authors. To calculate the static reference values, the absolute maximum of the electromagnetic force under the conditions of a three-phase fault was used for all curves. According to equation 3.6, the maximum occurs on the inner phase L2. The factors V_σ are similar to V_F [5]. Fig. 3.7 illustrates that the factors V_F become larger as the mechanical frequency increases. Frequency indepen-

dent factors, which are shown horizontally in Fig. 3.7, are therefore unsuitable since they may lead to considerable over-dimensioning or even under-dimensioning.

Multiphase autoreclosure at the optimally worst time with respect to mechanical vibration of high-voltage test bus increases the stress significantly as compared to the case without autoreclosure [1,18,19]. Such increases range up to 95%. The results of parametric studies covering the whole range of relevant mechanical frequencies are given in [63]. The maximum stress increases can be determined with the aid of the factor V_r.

$$V_r = \frac{\text{dynamic stress with autoreclosure}}{\text{dynamic stress without autoreclosure}}$$

Figures 3.8a and 3.8b show the factors V_F, V_σ and V_r, which are proposed in [5] and which form the basis of the simplified method IEC865 [39]. The development of this simplified calculation method is based on extensive parametric studies using several numerical and analytical methods [5] and measurements [3,4].

The stress can be effectively reduced if the short-circuit duration is considerably less than half the period of the mechanical fundamental frequency. Curves for V_F and V_σ for practical use are developed in [77,82] and given in [32,82].

30
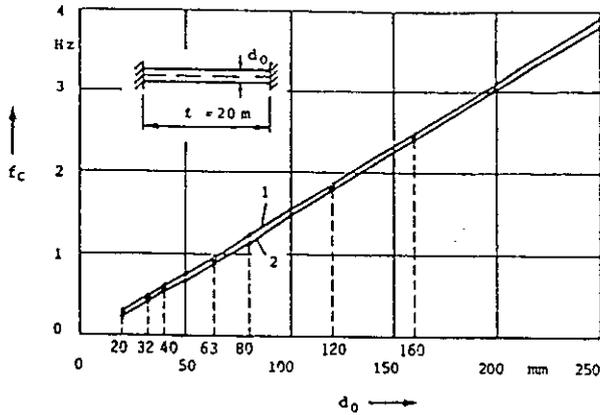
Fig. 3.6 Fundamental Eigenfrequencies f_c of stiff aluminum tubular busbars, fixed at both ends, 20 m long, as a function of outer diameter d_0 [5]. Equation (3.8) is used to calculate f_c
1 - smallest standardized wall thickness
2 - largest standardized wall thickness

Note: As the frequency is inversely proportional to the square of length l, the values for other lengths can be obtained from Fig. 3.6 by simple conversion with l^2. The fundamental frequencies for different boundary conditions can also be obtained simply; if the conductor is supported at one end and fixed at the other, the frequencies are multiplied by factor 0.689, and by factor 0.441 if both ends are supported.
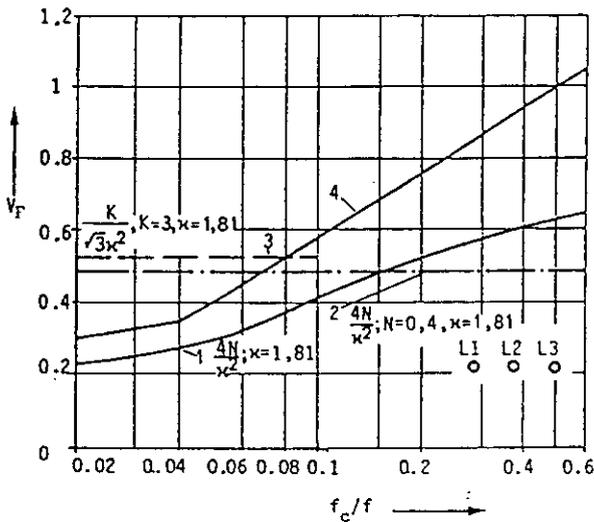
Fig. 3.7 Factors for calculation of dynamic insulator stress resulting from three-phase short-circuit according to various authors
1 Corresponding to factors N from [49]
2 Rough calculation with constant N [1,17]
3 Corresponding to factor K = 3 [1,21]
4 Proposed in [5] and included in IEC 865/86 [39]
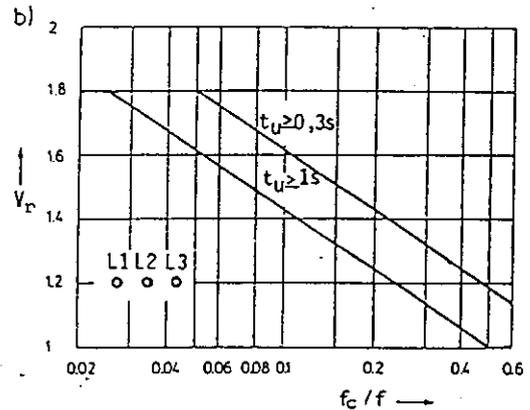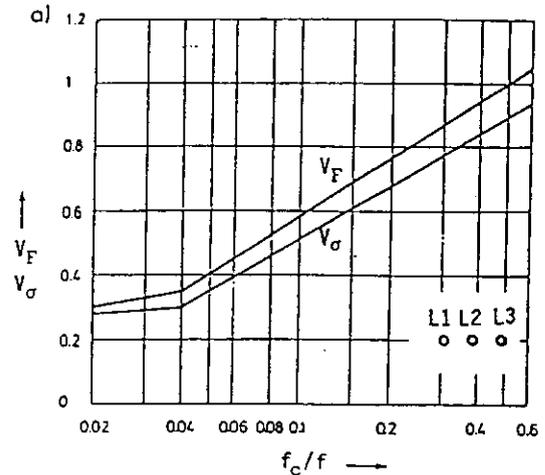
n = 1	n > 1 equidistant spans	γ'
△————△	·	1.57
⫫————△	△———△ · △	2.45
⫫————⫫	△—△⸳△—△	3.56

Fig. 3.8 Factors V_F, V_σ, V_r and γ for calculation of dynamic stress [5]
a) Factors V_F and V_σ, $0.035 \leq R/X \leq 0.17$, $\kappa \geq 1.6$. Factors for $R/X > 0.17$ are given in [74]
b) Factor V_r, t_u is the dead time
c) Factor γ' for calculating the fundamental mechanical frequency by equation (3.8)

Calculation example

An example structure is shown in Fig. 3.9. The electromagnetic peak force and static stress are determined as reference values for the inner phase. The dynamic stress is calculated for the most heavily stressed outer phases, L1 and L3, using the V factors (V_F, V_σ, V_r).

The calculation for a three-phase short-circuit is carried out as given below:

31
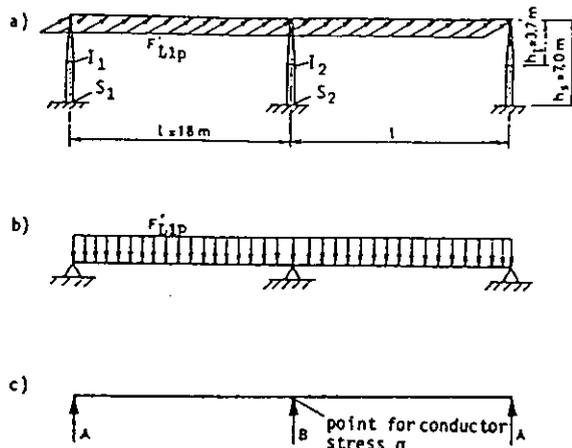
Fig. 3.9 Structure for the example
a) Two span arrangement
b) Model for rigid support structures
c) Forces A,B on the top of the insulators and stress σ in the conductor

Input data:
Symmetrical three-phase short-circuit current I''_{k3}
= 80 kA (rms)

Impedance ratio	R/X = 0.07
Tubular conductor	
Mass per unit length	m' = 7.84 kg/m
Modulus of elasticity	E = 7.0·10⁴ N/mm²
Outside diameter	d_o = 160 mm
Inside diameter	d_i = 148 mm
Span length	$\mathcal{l}$ = 18 m
Insulator 380 kV	
Height	h_l = 3.7 m
Support height	h_s = 7.0 m
Centreline distance of conductors a = 5 m	

a) electromagnetic peak force is calculated according to equations:

$$C' = \frac{\mu_0}{2\pi a} \cdot (\sqrt{2} \cdot I''_{k3})^2 = 512 \text{ N/m}$$

$$\kappa = 1.02 + 0.98 \cdot e^{-3 R/X} = 1.81$$

$$F_{L2p} = 0.866 \cdot C' \kappa^2 = 1453 \text{ N/m}$$

b) static stress (A, B, σ according to Fig. 3.9c) is given by:

$$A_{st} = \frac{3}{8} F_{L2p} \cdot \mathcal{l} = 9808 \text{ N}$$

$$B_{st} = 2 \cdot \frac{5}{8} F_{L2p} \cdot \mathcal{l} = 32693 \text{ N}$$

$$J = \frac{\pi}{64} \cdot (d_o^4 - d_i^4) = 862 \text{ cm}^4$$

$$W = \frac{J}{d_o/2} = 108 \text{ cm}^3$$

$$\sigma_{st} = \frac{F_{L2p} \cdot \mathcal{l}^2}{8W} = 545 \text{ N/mm}^2$$

c) dynamic stress without three-phase autoreclosure is calculated from:

$$\gamma' = 2.45 \text{ from Fig. 3.8c}$$

$$f_c = \frac{\gamma^2}{2\pi \mathcal{l}^2} \sqrt{\frac{EJ}{m'}} = \frac{\gamma'}{\mathcal{l}^2} \sqrt{\frac{EJ}{m'}} = 2.10 \text{ Hz} \qquad (3.9)$$

$$\frac{f_c}{f} = \frac{2.10}{50} = 0.042$$

From Fig. 3.8a, $f_c/f = 0.042$

$$V_F = 0.36$$
$$V_\sigma = 0.31$$

Hence

A_{dyn} = $A_{st} \cdot V_F$ = 3.5 kN
B_{dyn} = $B_{st} \cdot V_F$ = 11.8 kN
σ_{dyn} = $\sigma_{st} \cdot V_\sigma$ = 169 N/mm²

The bending moment on the bottom of the first insulator:

$$M_{dynI1} = A_{dyn} \cdot h_l = 13.0 \text{ kNm}$$

The bending moment on the bottom of the first support:

$$M_{dynS1} = A_{dyn} \cdot h_s = 24.5 \text{ kNm}$$

The bending moment on the bottom of the middle insulator:

$$M_{dynI2} = B_{dyn} \cdot h_l = 43.7 \text{ kNm}$$

The bending moment on the bottom of the middle support:

$$M_{dynS2} = B_{dyn} \cdot h_s = 82.6 \text{ kNm}$$

d) dynamic stress caused by unsuccessful three-phase autoreclosure. It can be seen from Fig. 3.8b that V_r = 1.8 for $f_c/f = 0.042$ and $t_u = 0.3$ s.

The stress values A_{dyn}, B_{dyn}, σ_{dyn}, M_{dynI1}, M_{dynS1}, M_{dynI2}, and M_{dynS2} calculated under c) above should therefore be multiplied by 1.8.

3.4.2 Advanced Methods

General remarks

The application of advanced methods requires the use of computers. The relevant computer programs are typically developed by specialists in numerical analysis, rather than by HV and EHV substations design engineers. Therefore substation design engineers require general information regarding which computer methods may be applied and the corresponding results to be expected; and computer specialists require brief information about the substation bus problems and recommendations concerning the proper choice of the method and programs.

In [8] mechanical and mathematical models of busbar structures are presented, as well as a general classification of possible solution methods. Since the problem can be treated as a linear problem of transient structural dynamics, a variety of methods may be applied. The following is a summary of [8] and [4].

32

Mechanical and mathematical models

Real bus structures can be reasonably modelled by a frame consisting of bars, uniform (conductors, steel pillars) or nonuniform (support insulators), with distributed or concentrated masses. Mechanical and electrical data required in calculations and to characterize these bars (stiffness, mass, Eigenfrequencies) are established from their geometry and material properties, if known, and if not, from experimental measurements.

If any data are missing, one may use as a first approximation, relations between traction, torsion and bending properties corresponding to circular cross-sections. Note that by neglecting some special effects (for example, local loss of stability in tubular rigid conductors), the mechanical effects caused by short-circuit currents in HV and EHV substations may be described with sufficient accuracy for engineering purposes, by the simple linear theory of dynamic structures. In addition, the study of earthquake effects may be considered by a similar approach.

Due to physical assumptions, real structures are represented by a space frame consisting of a certain number of similar bars subjected to bending, tension and torsion. In engineering practice, a whole space frame is sometimes simplified to one beam [52]. In such a case, the analytical approach is very effective. Further, subsequent simplifications may be introduced; for example, one concentrated mass (ordinary differential equation) or massless beam (static solution only). The models form a theoretical base for the simplified methods which may be used to find a rough approximation of real results.

Solution approaches

Two basic problems of dynamic nature are usually considered:

1. Free vibrations where Eigenfrequencies and Eigenforms are required.

2. Transient problems, which are the main point of interest in this chapter.

An attempt at a general classification of solution approaches is presented in Fig. 3.10 [8].

Finite element methods with step-by-step time integration are presently in most common use because of their numerous advantages, viz: generality, commercially available software, etc. Because of the linearity of the problem, some general purpose computer programs (ASKA, RAMSES, SAMCEF, SAP IV, STARDYNE) for dynamic analysis of structures may be successfully applied for calculations of mechanical effects in HV and EHV substation bus systems. Cost savings for analysis may be achieved in practical design cases where configurations and structural data are standardized and relatively simplified, medium accuracy and specially oriented programs may be applied.

3.4.3 Calculation Approaches

Several programs which have been used by WG 23.02 are briefly described as follows.

ASEA, Sweden
Computer program SAP IV [90], is used to analyze the superposition of modes of oscillation resulting from the various natural frequencies of the mechanical system.
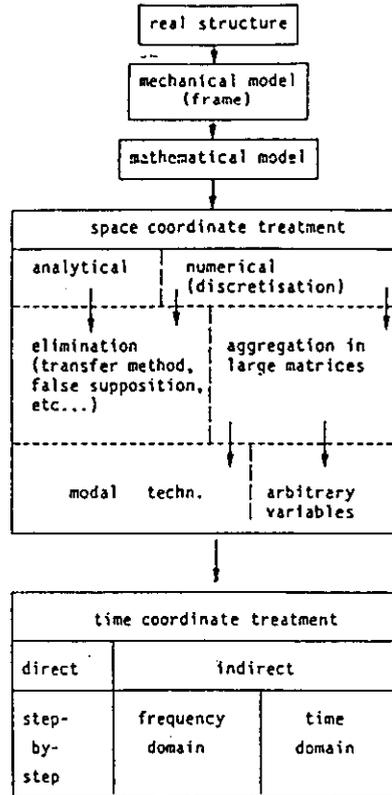
Fig. 3.10 Approaches to transient problems

The physical model for the supports is comprised of mass-spring elements. Conicity of the insulators is allowed for.

ENEL, Italy
All elements of the system (conductor, insulators, steel pillars) are assumed to be ideal elastic elements with a uniform distribution of masses. The displacements of the conductors and the insulators are calculated separately, using the method of finite difference approximation. At each time step, the displacements of the supports and the busbars at the connection points are constrained to be equal. The model of the supports consists of cylinders for the insulator and the steel pillar [72].

Imatran Voima, Finland
The structure is subdivided into concentrated masses and elastic bending springs. The "STARDYNE" program is employed (which is similar to "SAP IV"). The model for the supports comprises mass-spring elements. Insulators are considered to be cylinders.

KEMA, Netherlands
The differential equations of the coupled system (busbars and supports) are solved numerically. The conductors are assumed to be ideal elastic elements with distributed masses and the supports are represented as simple mass-spring elements.

Ontario Hydro, Canada
The structure is assumed to be a beam mounted on elastic supports. The masses of the system are assumed to be concentrated on each support. The basic frequency of structure is determined from the characteristic data of the various elements by hand calculation.

The design stress is determined by means of factors obtained from the fundamental frequency of the structure and the ratio R/L of the system impedance according to [49].

Siemens, Germany
Step-by-step integration of the differential equations describing the mechanical system, using the "SAP IV" program [90]. The model for the supports comprises a suitable number of mass-spring elements. Conicty of the insulators is allowed for.

SSPB, Sweden
The coupled system of conductor and supports is described as a two-mass oscillator. Only the fundamental natural frequencies of busbars and insulators were taken into consideration. Steel support columns are neglected.

Erlangen University, Germany
All of the components of the mechanical system are composed of a suitable number of concentrated masses and springs without mass. The system is described by means of transfer matrices [54]. The model for the supports comprises a suitable number of mass-spring elements. Conicity of the insulators is allowed for.

Liege University and TRACTEBEL, Belgium
All elements of the system (conductor, insulators, steel pillars) are assumed to be ideal elastic elements with a uniform distribution of masses. The finite element method was used. Transient analysis is carried out by modal superposition. The computer program used is S.A.M.C.E.F. [100].

Louvain University, Belgium
The elements of the mathematical model are ideal elastic beams with a uniform distribution of mass and concentrated masses. The vibration frequency behaviour of each element is calculated analytically and is used to obtain the Eigenmodes of the entire system.

EDF, France
The plane structure formed by the assembly of busbars, post insulators, and lattice supports is divided into ideal elastic beams. The beam bending vibration equation is used, neglecting deformations due to shearing stress, inertia of rotation and damping. The solution is obtained using finite differences, centered in space and over time. The computer program used is VIBRAPORTIC, which is briefly described in [19].

All of these calculation techniques give good results [4]. They are primarily finite element based programs. Acceptable results can be obtained with four element representations of insulators and eight element models for conductors, although the influence of discretization is perceivable. More elements are needed when the lowest frequency is less than 3 Hz or when the possibility of resonance exists. The typical data required for calculations and an example of results are given in Appendix 1.

3.5   Parametric Studies

Parametric studies have been carried out by analytical and numerical methods [5,32,74]. The influence of electrical and mechanical parameters on the dynamic short-circuit stress throughout the range of relevant mechanical frequencies was determined, namely:

- the time functions of the electromagnetic forces
- short-circuit duration
- unsuccessful autoreclosure

- mechanical resonances
- mechanical damping
- boundary conditions for the conductor

- the elasticity of the support structures
- unequal distances between supports
- the number of spans

3.5.1   Electrical Parameters

The worst case time functions of the electromagnetic forces of conductor L2 are very different from conductors L1 or L3 (see Chapter 1, Fig. 1.4). From the electromagnetic forces and investigation of their dynamic effects, it follows that:

- In the range $f_c / f > 1$ (typical of medium and low-voltage busbars structures), the conductor and insulator stress is greater for phase L2 than for phases L1 and L3.

- In the range $f_c / f < 1$ (ranges of resonance with $2f$ being ignored), the stress for L2 is considerably smaller than that for L1 or L3. In the HV and EHV substation range it is up to about 50% smaller, although the momentary maxima of the electromagnetic force are even greater for L2 than for L1 or L3.

- When the short-circuit duration $T_k \leq 0.1$ s, phase L2 stress in the HV and EHV busbars range $f_c / f \leq 0.2$ is always lower than phases L1 and L3 stress.

- The phase-to-phase short-circuit stress is somewhat smaller than the three-phase short-circuit stress in the conductors and insulators of the outer phases L1 and L3. Measurement of phase-to-phase short-circuit stresses is more convenient than for three-phase short-circuit stresses; however, the information given by measured data from phase-to-phase tests can be applied to phases L1 and L3 for the three-phase short-circuit condition, but not to phase L2 (see also Chapter 2).

The time functions of the electromagnetic forces also depend on the ratio R/X (equations 3.1a, 3.1b, 3.3). The V_F and V_σ curves for R/X = 0.035 ($\kappa = 1.90$), and R/X = 0.150 ($\kappa = 1.64$) cover the usual HV and EHV structure range. Significant differences only arise in the resonance ranges and only slight deviations occur outside these ranges [5].

Resonance enhancements can be reduced by restricting the short-circuit duration. The stress outside the resonance ranges can effectively be reduced only if the short-circuit duration is considerably less than half the period of the mechanical fundamental frequency. Curves for V_F and V_σ for practical use are developed in [77,82] and given in [32,82].

In multiphase autoreclosure on HV and EHV test stations, considerable increases in stress, compared with the case without autoreclosure, have been measured [1,18,19]. Such increases range to 95%. The results of parametric studies covering the whole relevant range of mechanical frequencies are given in [63]. Maximum stress increases can be determined according to [39] with the aid of the factor V_r which is also given in subsection 3.4.1.

34

3.5.2 Mechanical Parameters

Resonance damping and boundary conditions

The influence of mechanical resonances, mechanical damping and boundary conditions at the ends of buses can be summarized as follows [5]:

- Apart from the fundamental oscillation resonances, harmonic oscillation resonances also affect the dynamic stress. These cannot be taken into account with a model of a one or two mass oscillator. The resonance enhancements are generally lower for conductor stress than for insulator stress.

- Mechanical damping is only of major significance in the resonance ranges; outside these ranges it is very slight, even with the comparatively high logarithmic damping decrement $\Lambda = 0.2$. For tubular busbars the value $\Lambda = 0.05$ is appropriate [55]. Mechanical damping can be ignored apart from the case of multiphase autoreclosure. In numerical calculation methods, stability considerations may well make it worthwhile to take damping into account; however in this case, the calculation should be performed with a small damping value so that any resonance present can be discerned.

- Different boundary conditions for the conductor ends cause shifts in the resonance ranges. Outside these ranges the stresses alter only slightly.

Supports, number of spans and unequal distances

Investigations performed on typical high voltage arrangements with different mechanical properties of the supports and different boundary conditions [5,61] show:

- Elastic supports cause a shift in the harmonic oscillation resonances and a reduction of the resonance enhancements as compared to the rigid support arrangement. The stress outside these resonance ranges, above all in the mechanical frequency range $f_c / f \leq 0.1$, is not significantly influenced by the elasticity of the supports.

- The maximum dynamic bending moment in the supports increases approximately linearly with distance h [20]. For Fig. 3.5 the maximum bending moment at the base of the insulators is $A_{max}\cdot h_1$ or $B_{max}\cdot h_1$ and at the base of the substructures correspondingly $A_{max}(h_1 + h_2)$ or $B_{max}(h_1 + h_2)$.

- Investigation shows that the influence of the number of spans n is not large if $n > 3$; therefore multispan arrangements can be suitably represented by three spans.

- Arrangements with unequal distances between supports can generally be treated with sufficient accuracy if all spans are assumed to have the largest occurring distance between supports. Thereby, at most, the end insulators are stressed as severely as the inner insulators. Very short distances between supports, measuring less than 20% of adjacent distances between supports, are best avoided. If this is not possible, the conductors can be decoupled by means of flexible joints.

3.6 Conclusions

The simplified calculation method as presented and according to [39] is feasible and expedient for design purposes in most cases. This method is based on extensive parametric studies using numerical and analytical methods and was verified by measurements in HV and EHV substations carried out by WG 23.02. The application of the IEC 865 method is easy and the accuracy for most practical structures is adequate.

Advanced methods are needed mainly for:

- parametric and sensitivity studies
- optimum design of standard structures
- computations for unusual structures
- computations for uprating existing substations for higher short-circuit currents

Advanced methods offer the primary advantage that complex structures may be analyzed in detail including both the busbars and the support structure. When structural data are accurately known, high and controlled calculation accuracy may be achieved. However, in practical situations, data for foundations, insulators and joints are not well known and additional measurements may be needed to ensure accurate final results. General purpose program systems for structural dynamics may be adapted for bus system design, and as well, various specific, less costly programs have been developed which allow fast computations for cases which are not too complex.

Users of advanced calculation methods must recognize that the assumed boundary conditions for the bus system and other structural data are inevitably imprecise and that this can cause considerable deviations in calculation results for mechanical frequencies and the stresses. In order to achieve reliable results, the model data should be varied within the range of possible inaccuracies. In practice, typical substations have a large number of bus arrangements; therefore, such sensitivity studies are costly and inconvenient even with modern computing equipment. This demonstrates the practical advantages of simplified methods such as the IEC 865 calculation method.

4 FLEXIBLE BUS SYSTEMS

4.1 Introduction

The analysis of flexible busbar systems is much more complicated than that of rigid bus systems because these structures experience significant displacements in response to the short-circuit forces which depend on the displacements of the conductors and this results in a highly nonlinear behaviour. As well, the complete conductor, insulator and support structure system must be considered in the analysis. During the 70's, the members and experts of WG 23.02 began development of methods, (for example using finite element methods) to calculate the dynamic response of flexible busbar systems to short-circuits. In addition to the use of advanced methods, extensive efforts were expended to develop simple solution methods which would give good estimates of the results for parameter and sensitivity analysis.

As a result, several methods for the calculation of short-circuit effects in busbars with flexible conductors have been developed which differ very significantly in terms of the models used to represent the bus systems, the numerical calculation techniques, their capabilities and complexity. Most of the calculation methods use computer programs, which present different options, possibilities and computer requirements. The methods are divided into four classes, namely, simple, medium, advanced and bundle pinch. For each of these methods, definitions, range of application, required data and general results are described in the following paragraphs and Appendix 3.

The typical bus configurations to be analyzed have been classified as described in Section 1.4 and Figure 1.8:

- Case A: horizontal strain bus connected by insulator strings to steel structures
- Case B: vertical connections to span (droppers)
- Case C: connections between components (similar to case A, but with shorter spans and lower static tensions)
- Case D: jumpers

A simplified representation of the so-called pure cases A and C is illustrated in Figure 4.1.1.

4.1.1 Simple Method

This class of calculation methods uses simple analytic representations of bus short-circuit effects which can be accommodated with hand calculation and/or pocket calculators. They give maximum values and no information about time history or evolution of the phenomena. These methods require only general data, for example span length, static tension, distance between phases, structure stiffness, cable mass, short-circuit current and duration. These methods may be derived for spans longer than 20 m from (or are extensions of) the IEC method.

Cases C, D, and pure case A (no droppers) can be accommodated. These methods typically provide only the swing out tension, falling down tension, and a maximum tension to be considered for dimensioning. An envelope of displacements is available (not the trajectory) allowing for a rough, conservative approximation of the clearance between phases.
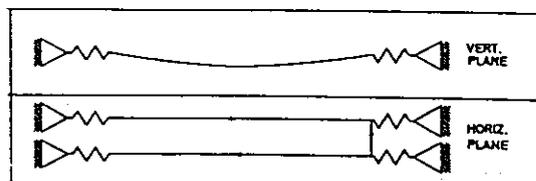
Fig. 4.1.1 "Pure" case A or C (see Fig. 1.8) (without droppers and the supports being considered as massless springs)

4.1.2 Medium Methods

Limiting the complexity of the problem by reducing the number of degrees of freedom or making simple approximations, allows mathematical models involving the solution of a system of a few differential equations using step-by-step time integration. This is the first type of medium method. The calculation can generally be performed in a short time on a personal computer, with a modest memory (a few tens kB) requirement. Because of the approximations inherent with these methods, several important limitations remain.

Bus configurations can also be represented by a simple system involving time and space integration. This is the second type of medium method. In this case, the calculation requires more computer storage space and computation time, depending on the model and on the complexity of the method used.

Medium methods can accommodate "pure case A", C and D bus configurations. The short-circuit duration is taken into account. Time-integrated methods give a time-history of tensions and displacements for the middle of bus spans, while time and space integrated methods give more detail. Droppers (case A+B) can only be considered as added masses and bus systems which deviate from the pure case A cannot be represented. As a result, resonance problems between conductors and supports are generally not detected [10]. The results are approximate, but can be adequate depending on safety factors, the conservatism used and the structure.

General structural data and time-history information (short-circuit duration, time constants, reclosure, etc) are required. As well, heating rate and expansion coefficients can be taken into account. The general result of these types of methods is a more quantitative time-history of tensions and displacements which permits clearance calculations and an improved understanding of the phenomena.

4.1.3 Advanced Methods

Another approach is the accurate modelling of the structure using finite elements for the conductors and supporting structures. Using such methods to compute the dynamic response of the structures, including their non-linear behaviour, it is possible to obtain highly accurate

36

results, limited only by the degree of detail used in the modelling and the availability of reliable basic structural data. As with the rigid bus case, with some adaptations, several general purpose finite element programs can be used.

The calculation typically requires a minicomputer with at least 300 kB of memory and one hour CPU for a typical calculation running on a 1 Mips (million instruction/second) machine. The main restriction is the cost.

These methods can be applied to any structural configuration and forcing function including, for bus design, cases A, B, C, D as well as case A+B. Space and time integrations can be performed to any degree of accuracy, limited only by the computational time available. However, analysis of bundle conductor pinch effect is not available from all programs and requires substantial computer time, particularly if it is included with swing effects in a global calculation. This subject is discussed in greater detail in section 4.4. The main limitation of advanced methods is the availability of accurate structural data. For example, the stiffness of apparatus or exact length of droppers, etc, are sometimes difficult to obtain. In addition, for the general design situation, the structures may exist only on paper at the design stage when detailed structural data are required, and the results tend to be sensitive to the data in some cases. The typical data required includes, for example, configuration data for the bus, droppers, support structures, connections, material elasticity, mass, heat capacity, expansion coefficients, time variation of short-circuit current and so on. Nondestructive measurements on partly installed structures can improve the situation, by giving better knowledge of such parameters including the stiffness and dynamic behaviour of the components of the structure.

The time history of tension and displacement for all components of the structure (cable, supports, droppers, apparatus) are obtained. Step-by-step computations provide sets of structural data for the complete structural response as a function of time and the views of the deformed structure which facilitate the understanding of exactly what happens to bus systems during and after short-circuits.

4.1.4 Bundled Conductor Pinch Effect Calculation

As with other aspects of bus analysis, a range of methods is used to analyze bundled conductor pinch effect, using simple, medium or advanced methods [12,106]. Because pinch effects occur more rapidly than swing effects, following initiation of a short-circuit, pinch effects are commonly analyzed separately from swing effects. This phenomenon and the methods for its analysis, are described more completely in section 4.4; however simple or medium methods require only a few seconds on a typical desk top personal computer. Pinch effect can also be calculated at the same time as swing effects if an advanced method is used. In this case the computer time will be increased; but the whole problem will be solved at the same time.

As with analysis of the other short-circuit bus effects, the accuracy of calculation results depends on the accuracy of the data. In the case of bundle pinch, a particularly important factor is the equivalent dynamic spring rate of the hardware connections, support insulators and apparatus. Empirical values can be used. As with the previously described short-circuit effect calculation methods, bundle pinch calculations require similar data, namely, stiffness of supporting structure, cable mass and elasticity, number of subspans, bundle spacing, short-circuit current.

The primary results of bundle pinch effect calculations are peak tension in the conductors and the compression forces on spacers.

The following sections provide more detailed descriptions of simple, medium and advanced methods for swing effect calculations. In addition, bundle pinch effects are described and finally, a parametric analysis is provided to give insight into the interrelationships and sensitivities of design parameters.

4.2 Simple Calculation Method

4.2.1 General Information

Stranded conductors, as used in substation bus systems, are assumed to have no flexural strength and are therefore normally under tensile force only, in static equilibrium with the load imposed by their own weight. As long as gravity represents the only load, the conductor of span L1 is on the vertical xz plane on which the anchor points A_1 and B_1 are located (Fig 4.2.1). The smaller the sag b_c, the larger the tensile forces P and Q. For the simple method of calculating mechanical short-circuit effects, this premise also applies to very short spans and large conductor cross-section. As well, bundles with two subconductors per phase (Fig. 4.2.3) are assumed to behave approximately the same as single conductors of double the cross-section and mass for swing effect calculations. These calculations are not affected by bundle pinch. (Bundle pinch calculations are described in section 4.4.)
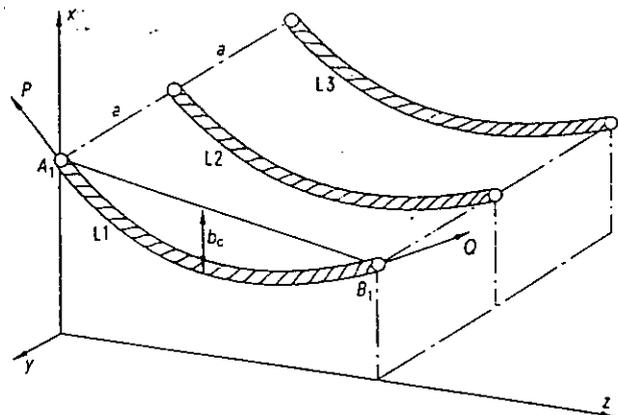
Fig. 4.2.1 Nearly horizontal spans of flexible conductors (single or twin) in side by side three-phase configuration

The simple method of calculating mechanical short-circuit effects is based on the configuration illustrated in Fig. 4.2.1. The short-circuit loads act in the horizontal y-direction and cause the spans to swing out of the vertical xz plane. Because of the inertia of the bus system, the response of the bus is much slower than the time functions of the short-circuit forces (Fig. 1.4). Therefore, for the simple method, the short-circuit loads can be represented by the mean values of the short-circuit forces:

Line-to-line short-circuit load

$$F' = \frac{\mu_0}{2\pi a} \, I_{k2}^2 \, (1+m)$$

Three-phase short-circuit load on outer conductors L1, L3

$$F_0 = 0.75 \cdot \frac{\mu_0}{2\pi a} \, I_{k3}^2 \, (1+m)$$

Three-phase short-circuit load on centre conductor L2

$$F_m \to 0$$

F' and F_0 are of the same value because typically $I_{k2}^{''}$ = ($\sqrt{3}$/2) $I_{k3}^{''}$. Since $\mu_0 = 4\pi \cdot 10^{-7}$ Vs/Am and taking 1J=1 Nm the common formulae (in N/m) for practical use is

$$F_0 = 0.15 \, I_{k3}^2 \, (1+m)/a$$

and one obtains a short-circuit load/dead load ratio of

$$r = \frac{0.15 \, I_{k3}^2 \, /a}{(g_n m_s n_s)} \, (1+m) = r_0(1+m) \qquad (4.2.1)$$

In (4.2.1)

I_{k3} = Three-phase initial symmetrical short-circuit current in kA.

m = Factor from Fig. 4.2.2.

r_0 = Minimum of r, if the short-circuit current appears without the decaying component i_{DC} of Fig. 1.1.

The reference time T' for taking m from the figure is

$$T' = T_{k1} \text{ if } T_{k1} \le T_r/4$$

$$T' = T_r/4 \text{ if } T_{k1} > T_r/4 \text{ or } T_{k1} \text{ is unknown}$$

T_{k1} is the short-circuit duration; at repeated short-circuits it is the duration of the first current flow

T_r is the period (in s) of pendulum oscillation of a span with sag b_c (in metres) and load ratio r_0:

$$T_r \approx 1.79 \, \sqrt{b_c} \, (1+r_0^2)^{-0.25} \qquad (4.2.2)$$

The arrangement shown in Fig. 4.2.1. is clearly a very much simplified representation of the real structures which are illustrated in Fig. 1.8 and classified as Case A, Case C and Case D. The short-circuit behaviour of these real configurations can be substantially influenced by the mass and stiffness of their characteristic components: steel structures, insulator strings, post insulators, connected apparatus etc. The simple method of calculating mechanical short-circuit effects takes into account these considerations by adjusting the basic ideas to represent individual substation sections, resulting in "Adjusted Simple Methods". At the present time, such work has been completed for connections between components (Fig. 4.2.3), (that is for Case C). Case C is important in the substation design field because:

- Normally the post insulators and/or apparatus represented by Case C are the mechanical weak points of substations resulting from the relatively low allowable bending stress of such equipment.
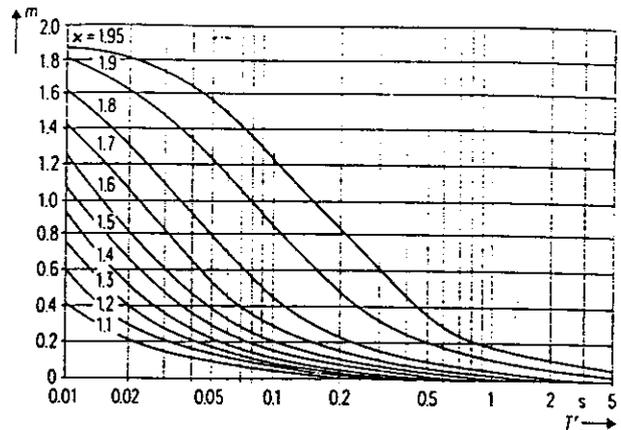
Fig. 4.2.2 Factor m, the DC (aperiodic) component contribution to thermal effects [39] and short-circuit loads of flexible conductors. κ factor for peak short-circuit current, see equation (1.5)

- Many experiments were necessary for development and verification of the simple method. Case C involves few parameters and is bounded by the post insulator strength for maximum span lengths of about 20 m. These simple configurations are relatively easy to test with acceptable costs.

- Although the simple method for Case C is not recommended for Cases A and D, until adjusted versions have been developed, designers may wish to use this method with suitable caution in specific cases. The significant errors which might occur through the use of this approximate approach may be acceptable in some cases if the cost of high safety factors is not too great, or if the consequences of structural failures in the form of ductile yielding (as opposed to brittle porcelain failure in Case C) are acceptable.
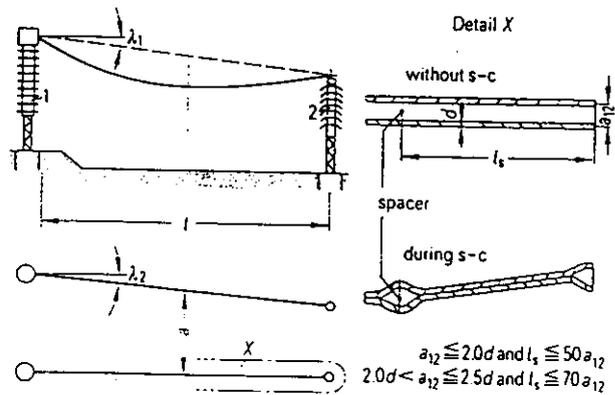
Fig. 4.2.3 Connections between components (case C). Actual application range of the simple method: 1.2 components whose elasticity is covered by a standard elasticity constant S=10^5 N/m. Almost horizontal span $|\lambda_1| < 15°$ Almost parallel conductors $|\lambda_2| < 8°$ Either single or twin conductors corresponding to detail X

38

For pure Case C (Fig. 4.2.3.) some additional remarks are beneficial:

- The span length l, is only indirectly limited by the mechanical loads allowed for components 1, 2.

- With the recommended spring constant $S=10^5$ N/m, the simple method always provides reliable results. That is, the use of this value obviates the necessity of determining the elasticity values of the components; but the support components are assumed to have some elasticity. The simple method is adjusted to comply with Case C using the elasticity S [47].

- Detail X, shown in Fig. 4.2.3 illustrates a twin conductor bundle for Case C. Designers must estimate bundle pinch forces in such configurations to establish that the peaks in force at the beginning of a short-circuit caused by pinch effect (indicated by t_{pi} in Fig. 1.5) are smaller than the subsequent swing forces determined by equations 4.2.6 and 4.2.13 (indicated by t_t and t_f in Fig 1.5). This is typically the situation for Case C because of the amount of slack allowed in connections between apparatus.

4.2.2 Physical Description

Rigid pendulum

During phase-to-phase or three-phase short-circuits two of the spans (for example, L1 and L2) swing away from each other. Assuming that they remain evenly shaped and retain their parabola fairly closely (Fig. 4.2.4a), they can be considered to act like rigid pendulums (Fig. 4.2.4b) with a period of oscillation (for small angles δ and constant sag b_c) given [104] by:

$$T = 5.62 \sqrt{b_c/g_n}$$

$$T = 1.79 \sqrt{b_c} \qquad (4.2.3)$$

with b_c in m and T in s

During the short-circuit duration T_{k1} a maximum angle $\delta=\delta_k$ is attained and the distance between the centers-of-gravity a_{ss} is greater than the static phase spacing a and consequently the mean short-circuit force as calculated with equation 4.2.1 is reduced.

The oscillatory motion thus establishes a mean short-circuit load/static load ratio of

$$\bar{r} = k_d r \qquad (4.2.4)$$

δ_k and k_d in Figs. 4.2.5 and 4.2.6 are obtained by the trial and error method. Should the value T_{k1}/T lie outside the range depicted in Fig. 4.2.5 (in accordance with the caption), the designer should note that the $\bar{r}$ curves can be extended symmetrically (mirror image) about the Δ.

However spans during short-circuits do not behave like free, ideal pendulums; they sustain radial displacements for some time within the δ_k range. For this reason, designers should assume to be conservative, that for very long duration short-circuits, not depicted in Fig 4.2.5, the maximum decay angles δ_m in accordance with Fig 4.2.7, will be attained on or after termination of the current flow.

Note that the designer must decide whether T_{k1} is the duration of an individual short-circuit (for example in an experiment) or the upper bound of the durations to be
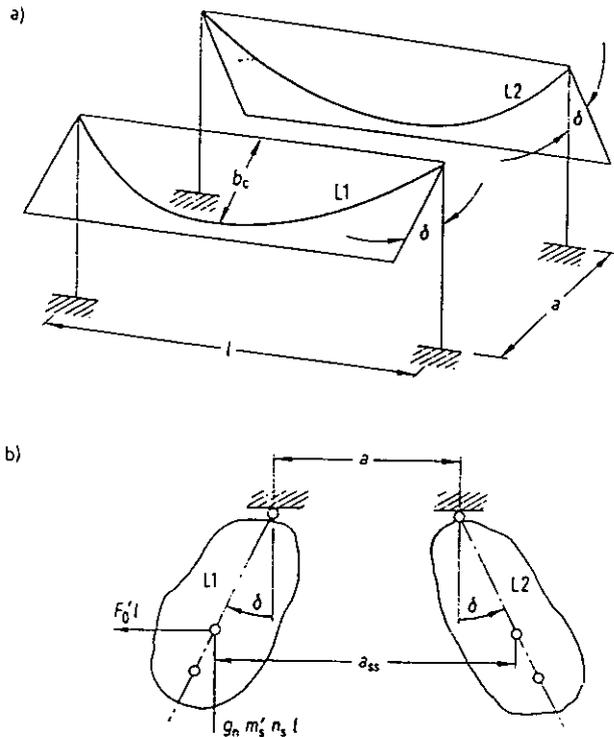
Fig. 4.2.4 Spans L1, L2 side-by-side and their simple method images (rigid pendulums) during line-to-line short-circuit. (A three-phase short-circuit produces in the spans L1, L3 of Fig. 4.2.1 the same angles δ.)
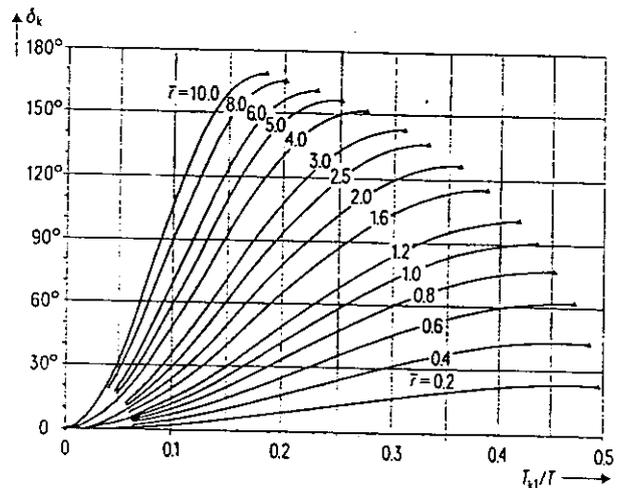
Fig. 4.2.5 Decay angle δ_k
- located on an $\bar{r}$-line, if the normalized short-circuit duration T_{k1}/T is within the T_{k1}/T range of the $\bar{r}$-line (δ_k occurs at current breaking moment T_{k1})
- corresponding with a boundary marker Δ, if T_{k1} is unknown or the normalized short-circuit duration T_{k1}/T exceeds the T_{k1}/T range of the $\bar{r}$-line (δ_k occurs before current breaking)

39
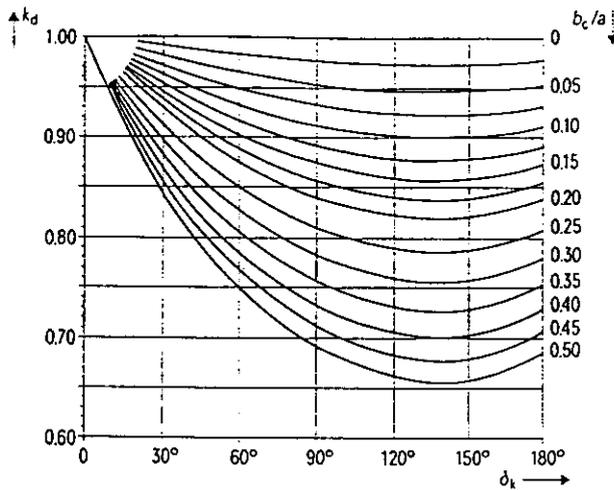
Fig. 4.2.6 Factor k_d
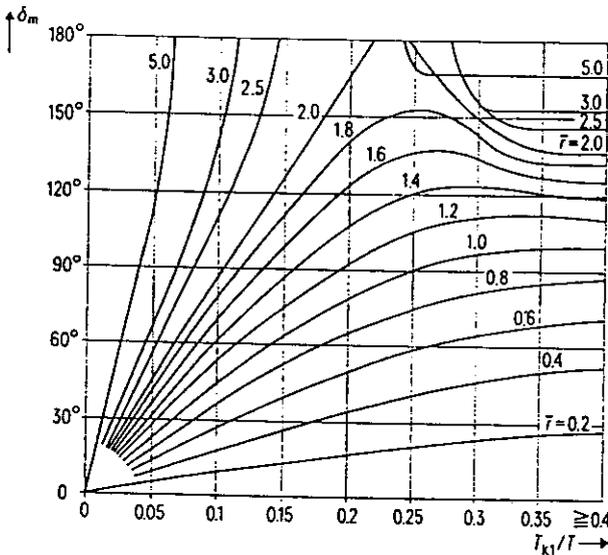
Fig. 4.2.7 Maximum decay angle δ_m

expected in a substation. For an individual T_{k1}, read δ_m at the $\bar{r}$ line intersection with T_{k1}/T. An extreme T_{k1}, represents the worst case if T_{k1}/T is on the left hand side of the $\bar{r}$ line vertex. For extreme T_{k1} and if T_{k1}/T is on the right hand side of the $\bar{r}$ line vertex, the worst case is represented by the δ_m of the $\bar{r}$ line vertex. When T_{k1} is unknown, multiply the T_{k1}/T value of the $\bar{r}$ line vertex by the T of the structure. If the resulting T_{k1} is shorter than the conceivable short-circuit durations, use the δ_m of the $\bar{r}$ line vertex. Otherwise assume a realistic extreme value for T_{k1} for diagram usage.

δ_m is the decisive parameter for span motions.

-   When $\delta_m < 70°$, the span passes through the first reversal point from which it returns to the steady-state position with damped oscillations (Fig. 4.2.8a). During or on termination of the current flow, the radial load is at a maximum $(g_n m'_s n_s \cos\delta + F_o \sin\delta +$ centrifugal force), which causes both maximum

tensile force F_t and maximum sag b_{ct} that are calculated in accordance with the following paragraphs. The surface area required for span motions is depicted (right side of Fig. 4.2.8) but without a time factor because the simple method of calculation does not permit time parameterization of the location curves.

-   For $70° < \delta_m \leq 180°$, the span drops from the position indicated by δ_m. The tensile-force oscillations intrinsic to the span continue roughly in the direction of the suspension points (Fig. 4.2.8b). When the span reaches the bottom of its descent, at t_f, the tensile forces attain their maximum value F_f (eq. 4.2.13). The span continues to oscillate; but succeeding force peaks are generally smaller as a result of damping.

-   For $\delta_m > 180°$, the short-circuit forces have imposed such a high velocity on the span that it rotates once or several times prior to dropping (Fig. 4.2.8c). At the bottom of the descent tensile-force peaks of approximately the same order as the maximum drop force F_f may occur at approximately equal intervals corresponding to the span natural frequency. If these intervals coincide with the duration of the periods of the support structures (for example, component 1 in Fig. 4.2.3), the tensile forces can be accentuated by resonance. (This effect has been observed in experiments.) The simple method of calculation cannot furnish more precise (quantitative) data on this aspect because the method does not permit calculations as a function of time.

Maximum tensile force during short-circuit:

If the displacement angle on termination of the short-circuit $\delta_k < \arctan r$, then the additional load referred to the gravitational load attains a maximum value of

$$\varphi = 3(r \sin \delta_k + \cos \delta_k - 1) \quad (4.2.5a)$$

if $\delta_k \geq \arctan r$

$$\varphi = 3(\sqrt{1+r^2} - 1) \quad (4.2.5b)$$

The radial load φ causes maximum tensile force during the short-circuit given by

$$F_t = k_z F_{st}(1 + \varphi\psi) \quad (4.2.6)$$

where
$k_z = 1.00$ for single conductors (n=1)
$k_z = 1.10$ for twin conductors (n=2) (in accordance with Fig.4.2.3)
$F_{st} =$ static conductor tension
$\psi =$ see Fig. 4.2.9

Experiments have confirmed that insulators, support structures and connected apparatus will experience tensile forces during short-circuits as calculated from equation 4.2.6, although for the conductors themselves, tensile peaks up to 1.5 F_t can occur. Therefore, corresponding ratings for these bus components should be established.

To obtain ψ from Fig. 4.2.9, the span factor ζ is required:

$$\zeta = \frac{(g_n m'_s n_s \ell)^2}{24 F_{st}^3} \cdot \frac{1}{1/\ell S + 1/n_s A_s E} \quad (4.2.7)$$

40

where (insofar as not previously explained)
A_s = subconductor cross section

Equation (4.2.6) and Fig. 4.2.9 are based on the well known change-of-state equation for a span if the radial load changes from $R_{st} = g_n m'_s n_s$ in $R_t = g_n m'_s n_s (1+\varphi)$ so that:

$$L_t - L_{st} = (F_t - F_{st}) \left(\frac{\ell}{n_s A_s E} + \frac{1}{S} \right)$$

while on the curve lengths of the parabolas

$$L_t = \ell + \frac{\ell^3}{24(F_t/R_t)^2} \qquad L_{st} = \ell + \frac{\ell^3}{24(F_{st}/R_{st})^2}$$

The following then applies

$$\varphi^2 \psi^3 + \varphi(2+\zeta)\psi^2 + (1+2\zeta)\psi - \zeta(2+\varphi) = 0$$

so that ψ can be determined analytically (under the proviso that $\psi > 0$).
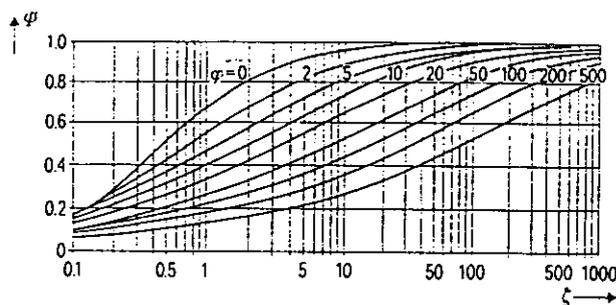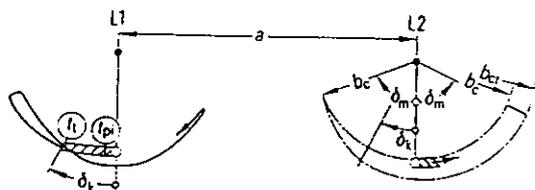
a) Oscillations of the span at $\delta_m < 70°$
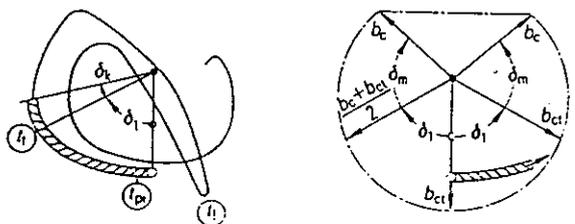
b) Oscillations and drops of the span at $70° \leqq \delta_m < 180°$
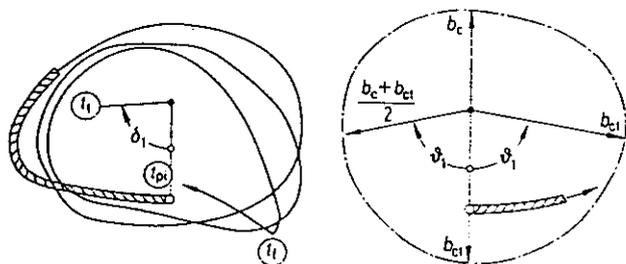
c) Rotations of the span at $\delta_m \geqq 180°$

Fig. 4.2.8 Short-circuit location curves in the centre of the spans (depicted for the left-hand phase L1 of two adjacent phases L1, L2) and determination of the surface area required (depicted for the right-hand phase L2).
/////// locus during and
———— locus after current flow
t_{pi}, t_t, t_f instants of conductor force peaks (Figs. 1.5 and 5.3.1)
b_c, b_{ct} initial static sag b_c, maximum sag b_{ct} according to Equation (4.2.8)
δ_k, δ_m, δ_1 decay angles, δ_k according to Fig. 4.2.5, δ_m according to Fig. 4.2.7, $\delta_1 = \arctan r$

Fig. 4.2.9 Factor ψ

Maximum sag during the short-circuit:

The sag b_{ct} required for Fig. 4.2.8 is

$$b_{ct} = C_F C_D b_c \qquad (4.2.8)$$

The factor C_F is an empirical value established from tests and covers the change in the shape of the conductor curve. The following applies:

$$\begin{array}{ll} C_F = 1.05 & \text{if } r \leq 0.8 \\ C_F = 0.97 + 0.1r & \text{if } 0.8 < r < 1.8 \\ C_F = 1.15 & \text{if } r \geq 1.8 \end{array} \qquad (4.2.9)$$

The factor C_D allows for sag increases caused by elastic and thermal elongation of the conductor and is calculated by

$$C_D = \sqrt{1 + \frac{3}{8} \left(\frac{\ell}{b_c} \right)^2 (\varepsilon_\sigma + \varepsilon_\theta)} \qquad (4.2.10)$$

The elastic elongation may be calculated from

$$\varepsilon_\sigma = (F_t - F_{st}) \left(\frac{1}{n_s A_s E} + \frac{1}{\ell S} \right) \qquad (4.2.11)$$

For thermal elongation the following applies:

$$\varepsilon_\theta = \left(\frac{I'_{k3}}{n_s A_s} \right)^2 T \beta \qquad (4.2.12)$$

The value for T is as required for Fig 4.2.2 and the values of the materials are as follows:

$\beta = 0.88 \times 10^{-13}$ m⁴/(kA²s) Copper conductor
$\beta = 0.27 \times 10^{-12}$ " All aluminum conductors ACSR with Aℓ/St > 6
$\beta = 0.17 \times 10^{-12}$ " ACSR with Aℓ/St ≤ 6

Maximum Tensile force after the short-circuit:

When $\delta_m > 90°$ oscillation (Fig. 4.2.8b) or rotation of the span (Fig. 4.2.8c) terminates with dropping of the conductor. On termination of the drop, the potential energy

$$E_{pot} = (g_n m'_s n_s \ell) (2b_c/3) 2\sin^3 (0.5\delta_m)$$

is converted into elongation energy

$$E_{elo} = \frac{1}{2} \left(\frac{1}{n_s A_s E} + \frac{1}{S\ell} \right) (F^2_{t(th)} - F^2_{st})$$

41

That is, the theoretical tensile force $F_{f(th)}$ caused by the drop is based on the assumption that at the instant of peak tension, the span is at rest (its kinetic energy is zero) and the strain energy can be equated to the potential energy. Application of the factor ζ given in (4.2.7) results in

$$F_{f(th)} = F_{st} \sqrt{1+8\zeta \; \sin^3 (0.5 \; \delta_m)}$$

Since additional kinetic energy is generally available at the start of the drop, (that is the velocity at δ_m is not zero), tensile forces greater than $F_{f(th)}$ were observed during experiments. A safety factor is therefore added to $F_{f(th)}$, so that the equation for the tensile force caused by span drop becomes

$$F_f = 1.2 \; F_{st} \sqrt{1+8\zeta \; \sin^3(0.7\delta_m\text{-}36°)} \qquad (4.2.13)$$

for $\delta_m > 70°$ and with $\delta_m = 180°$ for rotation.
F_f is to be used (unlike F_t) for all components of the span.

4.2.3 Applications

The simple method presented above provides estimates of the maximum tensions and displacements of a bus system caused by short-circuits. The calculation steps should be carried out sequentially in the numerical order of the equations and diagrams as given. In principle, the simple method requires the same data (including the short-circuit duration) as any other method.

The short-circuit duration T_{k1} depends on the system protection time, which is a variable depending on system design requirements and statistical effects that occur during the service life of a substation. In practice, designers commonly assume that short-circuits occur with variable durations and estimate the "worst case" from analysis of historical operating records. If the short-circuit duration T_{k1} is not known, the simple method produces the worst case result corresponding to the specified short-circuit current level. This corresponds to [39] which deals with:

- the evaluation of F_t for a single conductor with a maximum radial load φ given by equation 4.2.5b

- the evaluation of F_f on the basis of equation 4.2.13:

$$F_f = F_{st}\sqrt{1+4r\zeta} \quad \text{if } 0.6 < r < 2 \qquad (4.2.13a)$$

$$F_f = F_{st}\sqrt{1+8\zeta} \quad \text{if } r \geq 2 \qquad (4.2.13b)$$

Finally, consistent with the IEC Standard, designers should consider the span temperature range because

- The tensile forces F_t during a short-circuit are maximal for the coldest conductors. These maximum forces should be determined for the lowest temperature for the substation.

- The higher the span temperature the higher the span displacements and tensile forces after the current flow. Therefore high ambient temperatures and corresponding conductor temperatures (typically 60°C) are considered appropriate [39,41].

4.2.4 Example

Flexible busbar connections with two aluminum conductors, steel reinforced, (ACSR 560/50 mm²) per phase are planned for a 245 kV outdoor substation. The span length is l=11.5 m and the horizontal phase spacing $a = 3$ m.

The conditions depicted in Fig. 4.2.3. detail X are fulfilled with $a_{12} = 7$ cm center-line distance between the subconductors and with one spacer at the mid point of the span.

The anchor points at each span end are insulators on a steel substructure, that is, in accordance with Fig. 4.2.3, with a stiffness of $S=10^5$ N/m.

The steady-state maximum tension per phase at -5°C, with ice load, is 2000 N, so that at -20°C the tension is 1465 N and at 60°C it is 1220 N.

Regarding the short-circuit level, the following applies:

- the three-phase symmetrical short-circuit current (rms) I''_{k3} = 40 kA

- the factor for peak short-circuit current $\varkappa = 1.8$

- the mechanical short-circuit stresses are to be determined for an unknown short-circuit duration T_{k1}, as well as for $T_{k1} = 0.05$ s, $T_{k1} = 0.16$ s and $T_{k1} = 0.8$ s.

The following data are also available and are necessary for the calculation:

Conductor cross section	$n_sA_s = 1.22\cdot10^{-3}$ m²
Conductor weight	$n_sm'_s = 3.91$ kg/m
Young's modulus	$E = 6.20\cdot10^{10}$ N/m²
Sag -20°C/60°C	$b_c = 0.43$ m / 0.52 m

Supplementary calculated variables:

Temperature in °C:		-20	60
r_0	Eq (4.2.1)	2.09	2.09
T_r in s	Eq (4.2.2)	0.772	0.849
T in s	Eq (4.2.3)	1.18	1.29
ζ	Eq (4.2.7)	2.92	5.06

Table 4.2.1 demonstrates that for short-circuit durations 0.25s < T_{k1} < 0.32 s, the drop of the span leads to the worst case tension F_f = 9430 N. Therefore, insulators with ratings exceeding 10 kN, with no safety factor provided, are necessary according to [39]. At 0.193 s after initiation of the short-circuit, the maximum swing force (6920 N) occurs. Therefore, the connectors for this bus should be rated on the basis of 1.5 $F_{tmax}/2$ = 5.2 kN per conductor.

4.2.5 Future Extensions

As already mentioned, test results for the verification of simple methods for applications in the field of Case A and Case D would be desirable. However, in the absence of this, designers must recognize that the simple method is not a universal tool like the advanced calculation methods.

42

Table 4.2.1
Tabular compilation of the Calculations Performed for the Example

Short-circuit duration T_{k1} in s :	unknown		0.05		0.16		0.80	
Conductor temperature in deg:	-20	60	-20	60	-20	60	-20	60
T Fig. 4.2.2 Eq. (4.2.12)	0.193	0.212	0.05	0.05	0.16	0.16	0.193	0.212
m Fig. 4.2.2	0.232	0.211	0.800	0.800	0.280	0.280	0.232	0.211
r Eq. (4.2.1)	2.57	2.53	3.76	3.76	2.67	2.67	2.57	2.53
T_{k1}/T, T Eq. (4.2.3)	Δ	Δ	0.042	0.039	0.136	0.124	0.678	0.620
δ_k in deg Fig. 4.2.5	132	130	9	7	51	43	132	130
k_d Fig. 4.2.6	0.860	0.840	0.980	0.980	0.914	0.910	0.860	0.840
$\bar{r}$, Eq. (4.2.4)	2.21	2.13	3.68	3.68	2.44	2.43	2.21	2.13
δ_m in deg Fig. 4.2.7 span curve Fig. 4.2.8	>180[1]	>180[2]	75	66	164	141	140	139
	rotation		fall down	pendulum	fall down		fall down	
φ Eq. (4.2.5)	5.27	5.16	1.73	1.35	5.11	4.66	5.27	5.16
ψ Fig. 4.2.9	0.63	0.71	0.74	0.83	0.63	0.73	0.63	0.71
F_t in N, Eq. (4.2.6)	6920	6290	3670	2850	6790	5880	6920	6290
b_t in m, Eq. (4.2.8)	0.75	0.81	0.61	0.67	0.74	0.79	0.75	0.81
F_f in N, Eq. (4.2.13)	8680	9430	2180	-	8440	7940	7270	7790

Δ = final value of r-curve according to Fig. 4.2.5 reading rule
1 = 0.20 s < T_{k1} < 0.30 s
2 = 0.25 s < T_{k1} < 0.32 s

The aim for Case (A+B) is to integrate into the pure Case A, all of the influences caused by portals, droppers and insulator strings. The representation of droppers (Case B) will not be detailed sufficiently that details on their tensions and displacements will be calculated; but their influence on the main span will be included to some extent. In the present state, it has been established that single insulator strings have only a small influence on the current method and therefore its application is acceptable for such Cases A.

For Case D, no such extensions are planned for the future, because such configurations require, in particular, data on the space required for conductor motion. This can be determined fairly accurately with the current simple method; but an additional space requirement must be imposed, which would be determined by the motion of the insulator strings of Case A or at least calculated by an approximate method. Excessive space requirements can easily be avoided, (for example, by raising the loop weight [18]). In general, the tensile forces in configuration D do not have much influence on the tensile force maxima of configuration A. Therefore apart from the effects on the lower level equipment connected by droppers, in practice it is not essential to calculate the tensile forces of configuration D.

4.3 Medium Calculation Methods

4.3.1 Introduction

Between the hand calculations of simple methods and detailed modelling of advanced methods, is a wide range of computational techniques termed, "medium methods". These methods can be subdivided in two categories:

1. The first category is characterized by methods which avoid space integration and reduce data requirements by making simple assumptions about the geometry of the cable before, during and after short-circuits. Several methods, based on pendulum models (for example, distributed and concentrated pendulum models), fall into this first category. They are called pendulum models or "time-integrated methods".

2. The second category is characterized by methods which accommodate time and space integration. By accepting some limitations concerning the modelling of connections between cables, droppers, and so on, it is possible to design methods which perform space as well as time integration. They are less general than advanced methods, because they cannot include each component of the structure in as much detail as designers could require. Several specific programs fall into this second category, for example, CONEX and SACS/DACS. They are called "time and space integrated methods".

43

The main objective of medium methods is to reduce engineering and computer requirements and therefore costs, while maintaining adequate accuracy of results for design purposes. The convenience of medium methods is obtained at the expense of calculation precision, flexibility for analysis of special arrangements and availability of detailed results for connections, supports, etc. Table 4.3.1 summarizes the medium methods presently available.

The types of bus configurations solved by medium methods are the pure Case A type as described in section 4.1. This problem is a dynamic nonlinear problem; the nonlinearity referring mainly to two aspects, namely:

- the substantial deflections of the bus, including conductors and string insulators

- the dependence of the magnitude of short-circuit force on the relative positions of the short-circuit current carrying conductors.

4.3.2 Time Integrated Methods

Time integrated methods are mainly based on pendulum models. As shown in Fig. 4.3.1, the span, including conductors, strain insulators and supporting structures, are transformed into a simple elastic pendulum with 2, 3 or 4 degrees of freedom. The differences between the various methods involve the number of degrees of freedom, whether the mass of the pendulum is distributed along the pendulum arm or concentrated at the end of the pendulum arm and whether the equations are integrated to give the complete time-history or integrated only during short-circuit and then balanced to give maximum tension. In all cases, the results are presented in the form of time-histories of tensions and displacements at the middle of the span.

Distributed pendulum

This model (PENDO2), which has been described in [78], is gaining general acceptance and has been adopted in simplified form for slack conductors by IEC 865 and VDE 0103 [39,41]. See section 4.2 and Appendix 3 for application of a simple method of calculation.

Model and assumptions:

- Each point of the conductor is assumed to receive the same resultant force.

- Representation of the length variation of the catenary during a short-circuit event is a central part of the model.

- The mass of the pendulum is distributed uniformly along the length of the pendulum arm.

Integration of the dynamic equations:

- Time integration is performed only until the first maximum peak of tension is reached. Then an energy balance gives the peak tension for the fall of the bus span. Therefore, the complete trajectory and time history of tension of the span is not available.

Concentrated pendulum

Several models based on concentrated pendula have been designed, as shown in Table 4.3.1. One of these [13] has been used for the parameter analysis of short-circuit effects presented in section 4.6.

General assumptions:

- The shape of the conductor span is assumed to be a parabola throughout its motion.

- The stiffness of the pendulum arm is a function of the tension in the cable.

- The electromagnetic force is assumed to be that created by two conductors of finite length, located at the instantaneous position of each gravity center, and to act in the direction defined by a line joining the gravity centers of the two conductors.

- The conductors are assumed to be incompressible, which implies that the lowest value of the tension is limited to zero.

SWING T

Model and assumptions:

- The model and equations have been described in [69].

- Figure 4.3.1 shows the pendulum with two degrees of freedom:
  b = sag of the parabola
  δ = swing angle

- The concentrated mass is located at the radius of gyration of a suspended parabolic representation of the span, which is 2/3 of the sag of the span.

- The mass of the pendulum consists of the mass of the cable and a certain part of the mass of the strain insulators. It is calculated from the initial sag and tension using the following formula

$$M = 8 \, b \, F_{st} / g_n \mathcal{L}$$

(4.3.1)

$$b = b_c + b_i$$
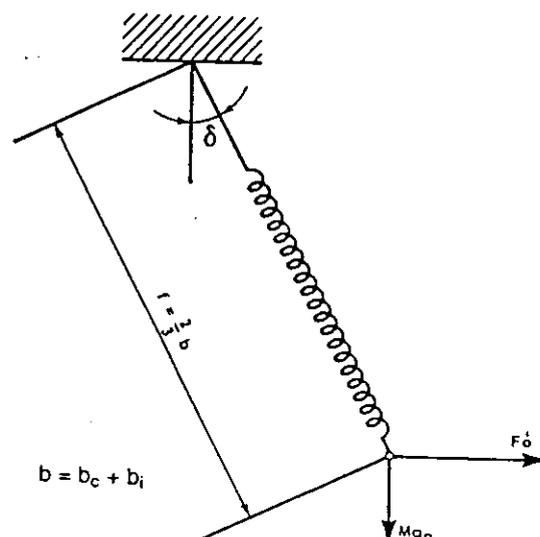
Fig. 4.3.1 Two Degrees of Freedom Pendulum

44

Table 4.3.1

Synoptic View of Available Programs
(Medium Methods)

A1 designation	CONEX	PEND02	PENDBL	PENDULUM	SACS/DACS	SWINGT
A2 developed and available from	EDF Paris France	Univ Erlangen Germany	Tractebel Brussels Belgium	Univ Liege Belgium	ASEA AB Vasteras Sweden	Ontario Hydro Canada
A3 references	[9]	[78]	[9]	[9]	[9]	[69]
A4 data generation 1=manual 2=automatic 3=interactive	1	1	1	3	1,2	1
A5 time descretiz 1=explciit 2=implicit	1,2	1	1	1	1	1
A6 time step 0=manual 1=automatic	1	1	1	1	1	1
A7 damping 0=no 1=yes	1	0	0	0	1	0
A8 output 1=printed 2=graphic	1,2	1	1,2	1,2	1,2	1,2
A9 source code 1=FORTRAN 2=PASCAL	1	1	1,2	1	1	1
A10 core memory	600-1200K	very low	80K	very low	250K	80K
B1 mass 1=concentrated 2=distributed	1,2	2	1	1	1	1
B2 elements 1=axial force only 2=elastic plastic 3=linear plastic 4=unextensible insulators 5=scc heating	1,3,5	1,3	1,3,5	1,3,5	1,3	1,3
B3 displacements 1=large (nonlinear) 2=small (linear)	1	1	1	1	1	1
B4 space discretiz 1=finite elements 2=finite differences	2	2	2	2	1	2
C1 supports model 1=arbitrary shape 2=truss, full structure 3=reduced to frame 4=reduced to spring & mass 5=reduced to spring	4	5	5	4,5	5	5
D1 electric forces 1=distributed 2=phase-phase interactions 3=autoreclosure	1,2,3	1,2	1,2,3	1,2,3	1,2,3	1,2,3
D2 static loads 1=gravity 2=ice 3=wind	1,2	1,2	1,2,3	1,2,3	1,2,3	1,2,3

- Because the frequency of swing-out motion is assumed to be low compared to the natural frequency of the structures, the structures are represented by mass-less springs.

- The mass of the span is connected to a fixed pivot point by a nonlinear spring, representing the relationship between tension and sag. Assuming that the conductor remains in a plane and maintains the shape of a parabola throughout the motion:

$$F = F_{st} + (8/3\ell) (b^2 - b_0^2) / (\ell/AE + 1/S) \qquad (4.3.2)$$

- Swing equilibrium gives the first equation. It describes the rotational equilibrium between inertia of the concentrated mass, located at 2/3 of the sag = F(sag and the second derivative of swing angle), the gravity load = F(swing angle) and the short-circuit load = F(time, sag and swing angle):

$$2/3\,M\,(b\,\ddot{\delta} + 2\,\dot{\delta}\,\dot{b}) = -Mg_n \sin\delta + F_o\,\ell_F \cos\delta \qquad (4.3.3)$$

- Spring equilibrium gives the second equation. It describes the equilibrium between inertia of the concentrated mass = F(second derivative of sag), the spring force = F(sag), the gravity load = F(swing angle), the short-circuit load = F(time, sag and swing angle) and the centrifugal force = F(the first derivative of the swing angle):

$$2/3\,M\,(\ddot{b} - b\,\dot{\delta}^2) = Mg_n \cos\delta + F_o\,\ell_F \sin\delta - 8bF/\ell \qquad (4.3.4)$$

Integration of dynamic equations:

- The set of equations, as described above, consisting of two second order ordinary differential equations and one nonlinear algebraic equation, are solved simultaneously using the Runge-Kutta-Gill method.

PENDBL

Model and assumptions:

- The model [9] is similar to that used by SWINGT, with the addition of the representation of thermal expansion of the conductors under short-circuit current heating.

- Two pendula are used to model two phases. This gives 4 degrees of freedom and 4 differential equations, but allows for different characteristics of the two phases (for example, initial tension or sag) or level of anchoring points and therefore for nonsynchronous motion of the two phases and vertical components of the short-circuit forces.

Integration of the dynamic equations:

- The set of equations, as described above, consisting of four second order ordinary differential equations and two nonlinear algebraic equations, are solved simultaneously using the Runge-Kutta method of the sixth order with Fehlberg automatic step size control.

PENDULUM

- The model and equations have been described in [9,105]. Figure 4.3.2 shows one phase of the pendulum with 4 degrees of freedom as used in PENDULUM. Different swing angles for the conductors and the insulators and support structures defined by a mass and spring system (instead of a simple spring) are represented.

- This model can represent two different phases if the data for each are not identical. It includes a new pendulum arm, which makes it possible to take the insulator chain into account and include the rotational inertia effects of the span.

- The parabola of the cable (without the insulators) is assumed to remain in a plane, which rotates from the vertical plane, as in the other pendulum models, but in this model, the end points of the conductors can also move on a circular locus.

- The insulator chains are assumed to be inextensible and their conductor connection ends can move on a circle. This movement can be described by one degree of freedom, namely the angle of rotation, relative to the plane of the pendulum. Thus, the length of the arm is constant.

- The anchoring points can include both mass and stiffness, allowing for a correct reproduction of the frequency of the first symmetrical Eigenmode of the supporting structure. It is difficult to include the effect of other phases in this stiffness.

- The model, with separate degrees of freedom for insulators, may be very sensitive to resonance problems between the conductors and insulators, which results in overestimating tensions in certain cases. If the length of insulator chain and the mass of structure are set to zero, this model reduces to the PENDBL model.

Integration of dynamic equations:

- A set of three nonlinear, fully coupled, second order differential equations must be solved. This number increases to five if the inertial effect of supporting structures is included. The equations are integrated using an "improved" fourth order Runge-Kutta method with an automatic step size control.

4.3.3 Space and Time Integrated Methods

SACS/DACS

Model and assumptions:

- The method has been described in [9] and consists of two analyses:
  - SACS includes the static analysis of a flexible cable suspended at each end
  - DACS performs a dynamic analysis for a two phase short-circuit on the same suspension bus

- Figure 4.3.3 shows the 3-dimensional calculation model. The nodes are assumed to remain in a plane perpendicular to the axial direction of the suspension bus at its initial position.

- As a result of portal elasticity, the model assumes that an axial movement of the plane can be superposed.

- The strain insulators are always located between the first two or last two nodes of the spans.

- The suspension bus can be simulated by about 20 different component parts, each having its own characteristics. In fact, the discretization can be finer (a 100 calculation node array is recommended).

46

$$d = \frac{2}{3} b_C$$

A   SPRING-MASS EQUIVALENT STRUCTURE.
B   INSULATOR STRING LIKE RIGID BODY.
C   BUSBAR.
D   GRAVITY CENTER OF PARABOLA
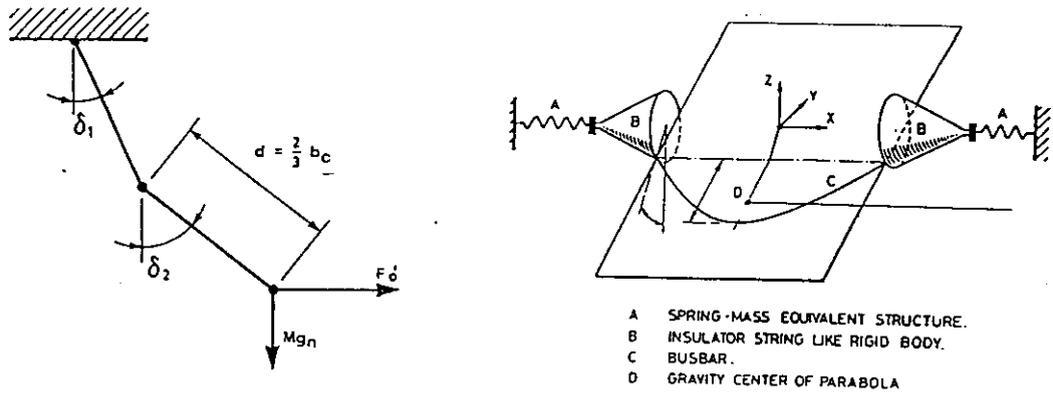
Fig. 4.3.2 Four Degrees of Freedom Pendulum
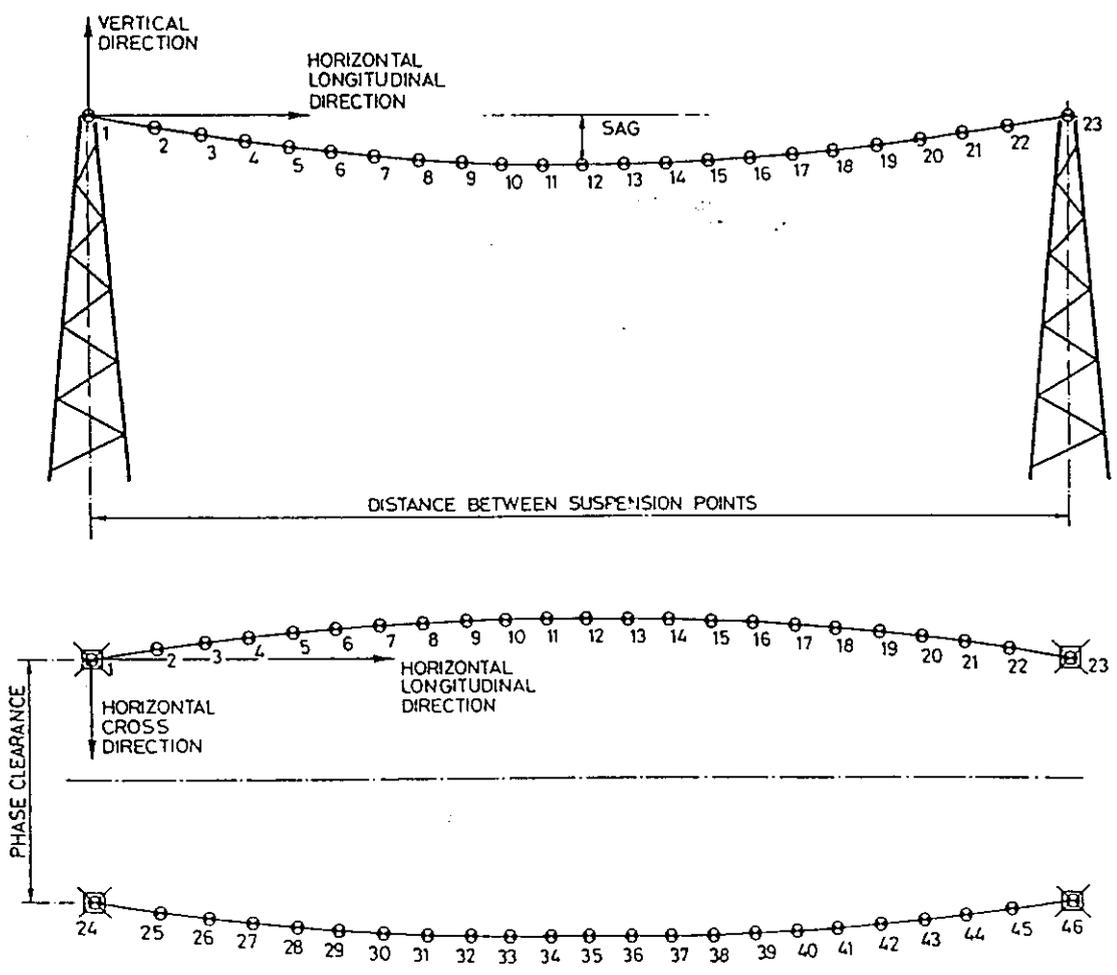
Fig. 4.3.3 Modelling of a structure for
SACS/DACS Analysis

47

- Concentrated masses can be located at nodes to simulate droppers.

- Elasticity of insulators and suspension bus is included. Flexibility is assumed to be infinite.

- Horizontal and vertical loads are supported, allowing for wind and ice loading calculations.

Integration of dynamic equations:

- The time-history response in two directions is computed using a fourth order Runge-Kutta method with an adaptive time step or by a modified Euler backward method. Reduction of the time-step can be obtained by using a mean value for the short-circuit current time function.

- The short-circuit forces are calculated by integrating the contribution of each part of the electrical circuit at each time step. If the sag is small, an approximation can be made by neglecting the displacement of the conductor during the period of current flow, which results in a slight loss in accuracy.

CONEX

Model and assumptions:

- The model has been described in [19]

- The conductors are assumed to be perfectly flexible.

- The suspension hardware is assumed elastic and flexible.

- The dead end support is simulated by an equivalent mass and spring.

- The method includes energy dissipation due to air friction and to friction forces between the strands of the conductor.

- Thermal expansion of the conductor resulting from its heating during short-circuits has been introduced. This heating is assumed to be adiabatic.

- The equations include:
  - dynamic representation of the conductor under external and internal (friction) forces
  - conservation of mass (related to elongation of the stressed conductor)
  - representation of the elasticity of the material, including thermal expansion of heated conductors
  - dynamic representation of bending and torsion of the towers (supporting structures).

Integration of dynamic equations:

- The system of equations is hyperbolic. Care must be taken to maintain stability of the numerical method, in relation to time and space increments and to propagation velocity of longitudinal waves in the conductors.

- The time-history response of the structure is calculated for a two phase short-circuit using a finite difference method. The method is explicit in time for each point of the conductor and implicit for the insulator strings and portal frames.

4.3.4 Calculation Procedure

Set of Data

For the first type of medium methods, the data set is reduced to characteristics of components, dimensions of structures and parameters of short-circuits. For the second type of methods, more information must be given for the geometry as a result of the extended capabilities of these methods. Appendix 3 gives an example of the required data for the first type of medium method. The data required by the second type of medium method are very close to those required by advanced methods, depending on the capabilities used.

Interactivity and User Friendliness

As a result of the simplification of calculation methods, it is possible to obtain programs which run interactively and which allow for easy, computer-aided, data entry. Thus, medium methods are simple to use, results are obtained at low cost and in a few seconds (for first type of methods), and designers can perform several calculations to get the worst case or to test the design sensitivity. Space and time-integrated methods (section 4.3.3) may also be used in a similar way, although with higher costs.

Graphic Enhancements

Certain programs (for example, PENDBL) provide immediate illustration of the trajectory of the conductors (Fig. 4.3.4), and of the clearance between phases (Appendix 3). A plot of the variations of tensions in the conductors can also be displayed (Appendix 3), which clearly indicate the maximum values. These features are important, because they give the designer tangible knowledge of the dynamic behaviour of the bus conductors under short-circuit conditions. A plot of the results is always more effective than a list of numerical values.

Set of Results

As mentioned in section 4.3.2, for time integrated medium methods, the results are limited to mid-span displacements and the tensions of the conductors as a function of time. For space and time-integrated methods, more information can be obtained, as a result of the extended capabilities of these methods. Appendix 3 gives a typical example of the results obtained from the first type of methods.

4.4 Bundled Conductor Pinch Effect Calculation

4.4.1 Introduction

Normal or emergency ampacity, and (in HV and EHV systems) corona loss and radio noise requirements typically can only be satisfied for flexible bus systems through the use of more than one conductor per phase. Traditionally, the number of conductors per phase, conductor size and bundle spacing, for such bus systems, have been determined primarily from ampacity and radio noise specifications. Two, three and four conductor per phase designs are typical in HV and EHV systems. As is well described in Chapter 1 of this brochure, currents flowing in conductors generate forces acting between the conductors. For bundled conductor systems, the relatively close bundle spacing and typically large short-circuit currents can result in very significant conductor

48
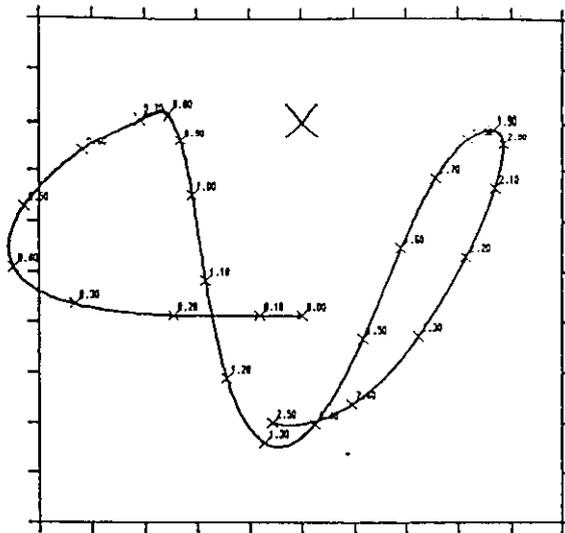
Static pull	:	7.65	kN
Maximum tension	:	19.51	kN
Corresponding time	:	1.329	s
Initial sag	:	0.970	m
Max. displ. left	:	0.959	m
Max. displ. right	:	-1.393	m
Max. displ. down	:	-1.620	m
Max. displ. up	:	0.040	m
Minimum clearance	:	0.645	m

Fig. 4.3.4 Example of output from PENDBL
I_{k2} = 29.4 kA for 0.8 s

forces. As illustrated in Fig. 4.4.1, the forces acting on the conductors cause a rapid acceleration of the conductors towards each other until they clash together. This rapid pinching together of the conductors causes an effective shortening of the conductor length available for the bus span which results in a rapid increase in conductor tension. This rapid increase in conductor tension, which occurs typically in the range 10-50 ms after fault initiation, is transmitted to the span support points (insulators, hardware and support structures) as an impulse loading. Figure 4.4.2 shows a typical oscillogram of a short-circuit current waveform and the corresponding phase tension. The support structures respond dynamically to this rapid increase in phase tension and interact with the bus span in a complex fashion depending on their mass, stiffness and other parameters. Components of the increased tension are also applied to any bundle spacers which may be present [48]. For EHV substations, bundle and phase spacings are such that the dynamic bundle pinch tensions acting on the hardware, insulators and support structures can exceed the tensions generated by the swinging motion of the phases. In lower voltage substations, phase spacings and bundle spacings are typically reduced and as a result bundle pinch tensions may not be the dominant factor.

Of concern to designers are the compressive loadings on bundle spacers, possible damage to conductors caused by clashing and the impulse loading of the bus support system. As a result of these concerns, a number of experimental and/or theoretical studies have been carried out. Because of the complexity of the dynamics of the bundle pinch effect and its interaction with the support structures, generalized analytical representation has not yet been accomplished. The most accurate method to determine bundle pinch tensions is through full scale high-current testing [e.g. 30]. Unfortunately, the cost to carry out such testing for the range of bus configurations encountered in practical substation designs, makes this approach impossible. As a result, designers have resorted to a number of simplified and approximate methods to estimate bundle pinch effects. Several of these methods are briefly described in the following section.

4.4.2 Calculation Methods

Calculation methods fall into three broad categories, namely: standardized recommendation, simplified and advanced calculation methods. These three approaches will be discussed in the following paragraphs. Because of space limitations, full detail cannot be provided. Readers interested in detailed presentations of these approaches are directed to the references.

Standard Methods

The only known standard dealing with bundle pinch is the German Standard VDE 103 [41]. The method is based on experimental evidence and simplified analysis and is applicable to slack conductors supported on pin type insulators. The standard cannot be applied to all cases. Evaluation of the literature or measurement is suggested for non-standard cases.

Simplified Methods

A number of approaches have been developed to represent, in simplified form, the highly complex processes acting in the bundle pinch effect. The first approach can be broadly categorized as the static balance method. Methods such as Atwood et al [46], Serizawa [50], the EDF recursive technique and a static balance method developed at the Instytut Energetyki in Warsaw, Poland fall into this category. In these methods, the electromagnetic forces acting on the conductors are resolved according to the pinched bundle configuration and balanced with the phase and conductor tension components. Recursive or iterative techniques are used to establish the bundle configuration parameters (for example, the length of conductor in contact and conductor tension) for which the electromagnetically induced forces are balanced with the conductor tension. These methods may or may not include simplified representation of the support structures, insulators and hardware. The simple static balance method is described below.
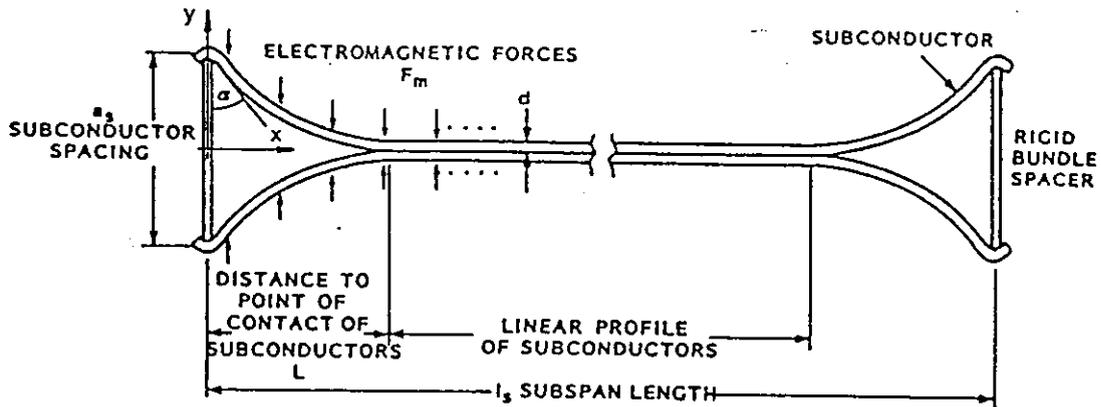
Fig. 4.4.1 Position of subconductors of one subspan during bundle pinch

33 cm BUNDLE SPACING	PEAK CURRENT	87.6 kA	PEAK TENSION CENTRE PHASE	67.6 kN
7 SUBSPANS	INITIAL rms CURRENT	34.9 kA	HORIZONTAL DISPLACEMENT OF GIRDER	11.2 mm
INITIAL TENSION - 12.5 kN	FINAL rms CURRENT	32.7 kA	BENDING STRAIN IN TOWER LEGS	
NO SPRINGS	NUMBER OF CYCLES	5.7		

- EAST 148 MICROSTRAIN
- WEST 136 MICROSTRAIN
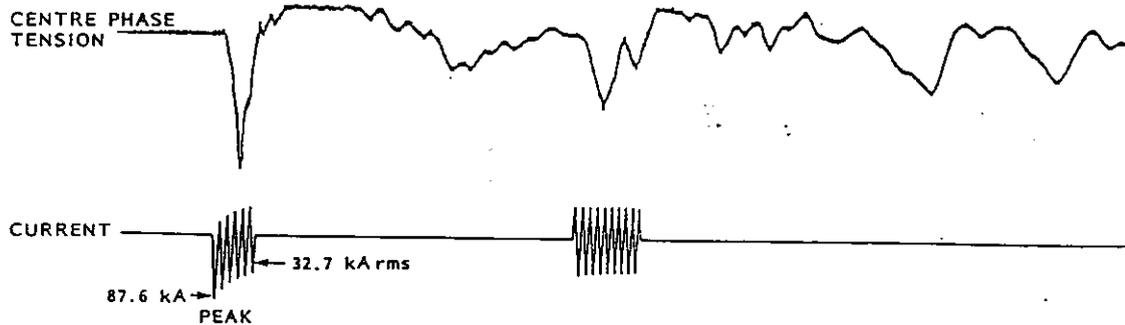
Fig. 4.4.2 Oscillogram of a typical bundle pinch tension

Simple Static Balance Method

The simple static balance method involves the following simplifying assumptions. 1. The response of the conductors is instantaneous. That is, the dynamics of the phenomenon are neglected. 2. Joule heating and acoustic energy losses are neglected. 3. The flexibility and dynamic interaction of support structures and insulators is neglected. 4. The conductors make contact during the short-circuit. 5. The subconductors assume a parabolic shape (see Fig. 4.4.1) in the portions of the subspan in which the conductors do not make contact. The tension in the subconductors can be estimated using the following two approaches.

Based on the electromagnetic forces:

$$F_{s1} = \frac{F_m}{\cos \alpha}$$

Based on mechanical relationships or Hooke's Law:

$$F_{s2} = F_{s1} + EA(\Delta \ell / \ell_s)$$

where

F_m	=	Electromagnetic force, N
F_{s1}	=	Static tension in one conductor of bundle, N
E	=	Young's Modulus, N/m^2
A	=	Conductor cross-section, m^2
$\Delta \ell$	=	Change in length of the conductor, m
ℓ_s	=	Subspan length, m

The electromagnetic force is estimated using the classical Ampere relationship:

$$dF_m = \frac{0.2\, i_p{}^2}{2\, y} \quad dx$$

50

Based on the parabolic shape of the non-contacting portion of the subspan (see Fig. 4.4.1):

$$y = \frac{d}{2} + \left(\frac{a_s - d}{2}\right)\left(\frac{x-L}{L}\right)^2$$

The electromagnetic force is obtained from:

$$F_m = \int_0^L dF_m = 0.2\, i_p^2 \frac{L}{\sqrt{d(a_s - d)}} \arctan \sqrt{\frac{a_s - d}{d}}$$

where i_p is the peak short-circuit current in kA and a_s, d, L and a are defined in Fig. 4.4.1

$$\cos \alpha = \frac{a_s - d}{2\sqrt{L^2 + \left(\frac{a_s - d}{2}\right)^2}}$$

$$F_{s1} = \frac{0.4\, i_p^2 L \sqrt{L^2 + \left(\frac{a_s - d}{2}\right)^2}}{(a_s - d)\sqrt{d(a_s - d)}} \arctan \sqrt{\frac{a_s - d}{d}} \quad (4.4.1)$$

and

$$F_{s2} = F_{st} + \frac{2\,EA}{\mathcal{l}_s}\left[\sqrt{L^2 + \left(\frac{a_s - d}{2}\right)^2} - L\right] \quad (4.4.2)$$

These two equations can be equated and solved for the unknown quantity, L, and the conductor tension calculated from:

$$F_t = 2\,F_s \sin \alpha = 2\,F_s \frac{L}{\sqrt{L^2 + \left(\frac{a_s - d}{2}\right)^2}}$$

Energy Balance Method

A second simplified approach involves a balancing of energy at the instant of maximum bundle pinch. The Ontario Hydro method [69] falls into this category. In this method, the conductors are assumed to lie in a horizontal plane. The strain energy in the conductors, plus the kinetic and potential energy in the supporting structures at the instant of maximum bundle pinch is equated to the energy expended on the bundle during the pinch by the electromagnetic forces. The resulting non-linear equation is solved for the distance to the point of contact of the conductors by Newton's method. Assuming that at peak tension the conductors adopt the parabolic and linear profile shown in Fig. 4.4.1, and that the work done on the linear section of the conductors is dissipated by the impact, the work done on subspan i by the electromagnetic forces during bundle pinch (neglecting current offset) is given by:

$$W_c^i = -0.8 \int_0^L \int_{a_c/2}^{\frac{d}{2} + \left(\frac{a_s - d}{2}\right)\left(\frac{x-L}{L}\right)^2} \frac{i_p^2}{2y}\, dy\, dx$$

The change in kinetic and potential energy of each support structure at the instant of maximum bundle pinch is given by:

$$U_t^n = \frac{1}{2} S_t^n \left[x(t_c)\right]^2 - \frac{1}{2} S_i^n (x_i^n)^2 + \frac{1}{2} M_t^n \left[\dot{x}(t_c)\right]^2$$

Where $x(t_c)$ is the displacement of the structures at the time of impact, (estimated by modelling the support structures as simple one degree of freedom spring-mass systems subjected to a forcing function derived from approximations of the force observed in tests). x_i^n is the initial static displacement of support structure n. M_t^n is the effective mass of support structure n and S_t^n is the stiffness of support structure n. The maximum displacement of the structure can be found by equating the potential energy at the instant of maximum displacement to U_t^n. The equivalent static load on the structure is calculated simply from the maximum displacement and the static stiffness of the structure. The increase in strain energy in the conductors in subspan I resulting from tension is given by:

$$U_c^i = \int_0^{\frac{\mathcal{l}_s}{2}} \frac{F_p^2 - F_{st}^2}{2EA}\, dx$$

and resulting from bending is given by:

$$U_B^i = \frac{\pi E/\gamma^2 d^4}{32\, L^2} \int_0^L \frac{dx}{\left[1 + \frac{\gamma^2}{L^2}(x-L)^2\right]^{5/2}}$$

$$\gamma = \frac{2}{L}(a_s - d/2)$$

An expression for the maximum tension F_p in terms of L is obtained by equating the increase in length of the conductor caused by the increase in tension, to the increase in length required by the parabolic and linear profile (as shown in Fig. 4.4.1), while taking account of the change in span length caused by the deflection of the support structures. Finally the equation:

$$\sum_{n=1}^{2} U_t^n + \sum_{n=1}^{n_{sb}} (U_c^i + U_B^i - W_e^i) = 0$$

where n_{sb} = the number of subspans

is obtained by equating the change in the strain energy in the conductors and the kinetic and potential energy in the structures at the instant of maximum bundle pinch to the work done by the electromagnetic forces. This equation can be solved by Newton's method for L, which is subsequently used to obtain the peak conductor tension using the expression described in the previous paragraph. This method, as it is presently used, is somewhat conservative as it neglects energy dissipated as heat and noise and energy absorbed by the span raising in response to the increased tension. The compressive load in bundle spacers is also obtained from the geometry of the conductors in the vicinity of the spacers as illustrated in Fig. 4.4.1.

Recent studies have also shown that it is necessary to include in the analysis the strain energy absorbed by the suspension insulators and hardware. This assembly is modelled by a simple massless spring having a dynamic stiffness (based on measured data) of 5250 N/mm. Figure 4.4.3 illustrates a composite comparison of measured versus calculated results [86].
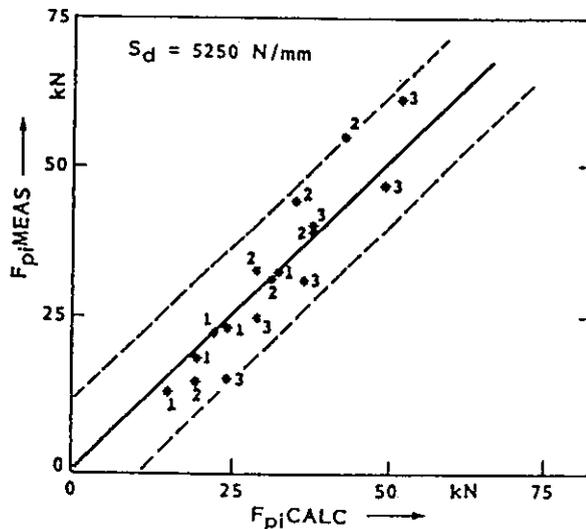

Fig. 4.4.3 Measured versus calculated peak conductor tensions for Ontario Hydro 1974 test results [86]. 330 mm bundle spacing, 61 m span. S_d is the dynamic stiffness of the insulator string assembly. The number beside the symbol • indicates the number of subspans. Fault currents range from 13 kA to 50 kA but are not identified on the plots. Perfect correlation between measured and calculated results exists for points on the solid diagonal. The dashed lines indicate ± 11 kN deviation from the solid diagonal.

Solution of Dynamic Equations

The third simplified approach involves solution of the formal dynamic equations of motion of the bundle conductors. Each conductor in the bundle is assumed to form a parabola in a rotating plane, both before and after pinch. In contrast to the previously described models, this approach represents a two parameter, or degree of freedom, model. This method was first developed in [85] but abandoned apparently as a result of numerical instability. Recently this approach has been successfully pursued using the unconditionally stable, Newmark time integration procedure [79]. Numerical solution of the dynamic equations provides the conductor tension and contact distance as functions of time. Also, the equilibrium values of the conductor tension and contact distance have been deduced in static form from the dynamic equations.

Advanced Methods

The final approach for calculating bundle pinch effects is the use of advanced detailed calculation methods. Early work on this approach was reported by Schaffer [51]. The conductors were modeled as elastic strings with uniformly distributed mass which were represented for short-circuit conditions by a set of nonhomogeneous hyperbolic partial differential equations. By means of space and time discretization, a system of coupled, ordinary differential equations of second order is obtained which is solved by numerical integration. Finite element analysis leads to the same set of equations for the case of lumped masses. The space and time increments may be selected to satisfy numerical convergence requirements. Calculated maximum bundle tensions using this approach agree within 30% of measured values except for cases with reduced spacing and relatively few spacers, where small absolute differences in low tension peaks result in relatively large deviations.

The use of modern finite element analysis is particularly suited for detailed dynamic analysis. Although the use of such methods is very cumbersome, they are needed if the complexity of the phenomenon is to be adequately represented. The use of such methods will allow, for example, the accurate and detailed modeling of the conductors, the connecting hardware and the support structures. Because of the nature of the forces, the rapid movement of the conductors and the resulting impulsive loading of the support structures, detailed modeling of the dynamic response of the conductors, hardware and support structures and their interactions is necessary. Work on the development of such models is being carried out in several countries; however, only limited results have been produced to date [12].

Although the development of advanced methods including analysis of bundle pinch effects is needed, their ultimate use as practical design tools will probably be limited. Techniques such as finite element analysis are very powerful and with effort such techniques can be developed to represent very accurately the response of specific bus configurations (see also Section 4.5). The use of such techniques typically require substantial amounts of detailed structural and mechanical data which is difficult and expensive to obtain at best or impossible to obtain at worst, for future arrangements for which designs are being made. And lastly, as indicated above, the use of such advanced methods is presently very cumbersome and therefore time consuming and expensive for practical design purposes.

4.4.3 Application

The application of bundle pinch calculation techniques would be best illustrated through detailed numerical example. However, most calculation techniques (even the simplified methods) are performed by computer programs. Therefore, the application of these calculation techniques will be illustrated by a numerical example using the Simple Static Balance Method and by the results of parameter studies.

Simple Static Balance Example

Configuration Data:
 Conductor ACSR 54/19
 Diameter d=0.0356 m
 Cross-section A=995x10⁻⁶ m²
 Young's Modulus E=7.033x10¹⁰ N/m²
 Bundle spacing a_s=0.381 m
 Length of subspan ℓ_s=18.796 m
 (there are three equal subspans in a span of 56.388 m)
 Initial tension F_{st}=13970 N
 Peak short-circuit current i_p=100 kA

52

Inserting these values in equations 4.4.1 and 4.4.2 and equating gives:

$$131605 \, L \, \sqrt{L^2 + 0.0298252}$$
$$= 13970 + 7446089 \, \{\sqrt{L^2 + 0.0298252} - L\}$$

This equation is solved for L giving L=0.975 m. Using this value in either equation 4.4.1 or 4.4.2 results in the subconductor tension F_s= 127000 N. The normalized peak tension F_s/F_{st} =9.09 and the force acting on the support F_t=2 F_s sin α = 250100 N.

Parameter Studies

Although simplified methods, by definition, are somewhat approximate depending on the specific simplifications made in their development, they are adequate for the purpose of investigating the sensitivities of the phenomenon to parameter variations. Such a study was recently reported [12] in which the EDF recursive method and the Ontario Hydro energy method were used. As well, an additional study using the simplified dynamic model [79] with the same data as in [12] has been carried out. Apart from the parameter sensitivity aspect of these studies, it is also interesting to compare results for the various methods. Four conductor sizes, two bundle spacings, five subspan lengths, three sets of support structure data and three current levels were selected. The reader is referred to [12] for details of the parameters and results of the sensitivity study. Figure 4.4.4 compares the results of the two methods in [12] and the results of the method in [12] for these data. This figure illustrates the ratio of peak bundle pinch tension to the pre-fault static tension, F_p/F_{st}, as a function of the number of subspans. For bundle conductors with wide conductor spacing and for short-circuit current greater than 80 kA (peak), differences are less than 30% of the maximum value. Figure 4.4.5 illustrates typical compression forces as a function of number of subspans for the four conductor sizes.

Figures 4.4.4 and 4.4.5 illustrate typical results for bundle pinch tensions. The ratio F_p/F_{st}, for wide bundle spacings, ranges from about 4 to as high as 20 depending on the short-circuit current, the number of subspans and the type of conductor. The ratio increases as the number of subspans increases; although as the number of subspans is increased, eventually a maximum F_p/F_{st} will occur beyond which, if the number of subspans is further increased, the ratio F_p/F_{st} decreases. This effect (not normalized) is illustrated in Fig. 4.4.6. If the bundle spacing is reduced, the ratio F_p/F_{st} ranges from about 1.5 to 6, again depending on the short-circuit current, the number of subspans and the type of conductor. Clearly the ranges of the ratio F_p/F_{st} indicate that peak tensions generated by bundle pinch can be significant. These peak tensions act directly on the conductors, the connecting hardware and the support insulators and these components are required to have ratings exceeding these peak instantaneous loads. The loading of the support structure (described in section 5.3.2) resulting from these impulsive loads is highly complex. Generally the strength rating of components in the support structures can be reduced if analysis is carried out to include consideration of the dynamic response of the structures.

4.4.4 Conclusions

In general terms, theoretical and experimental studies indicate the importance of bundle pinch effect in regard to bus hardware and support structure loadings. For flexible bus spans, reduced spacing between sub-
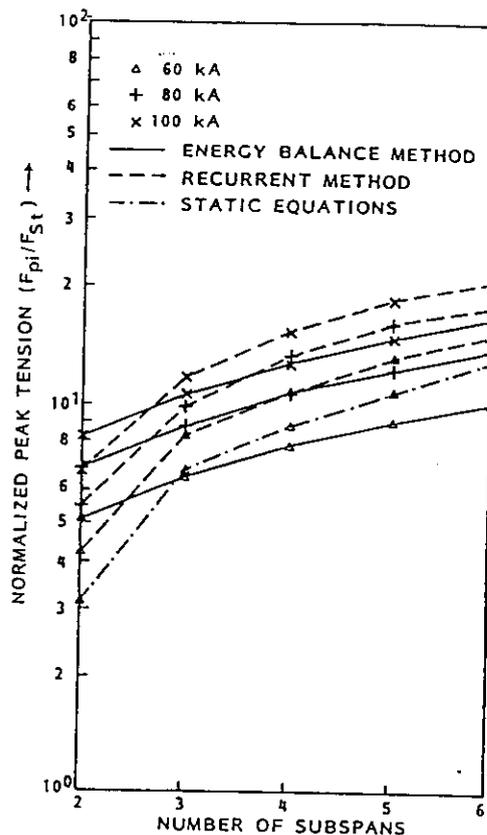

Fig. 4.4.4 Comparison bundle pinch calculation methods results from an ASC(91) conductor, 381 mm bundle spacing and static tension of 13.97 kN
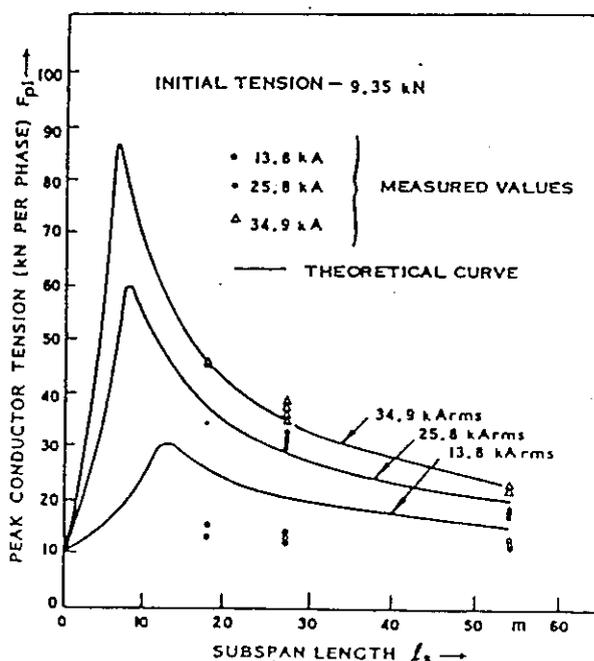

Fig. 4.4.5 Typical variation of peak bundle pinch tension for a range of subspan lengths

53
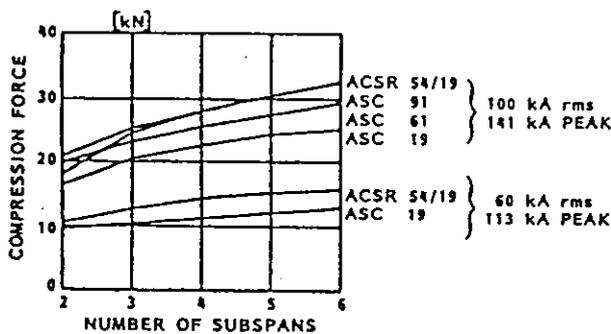
Fig. 4.4.6 Compression forces on spacers calculated using the recurrent method.

conductors, consistent with thermal and ampacity requirements, is recommended. In addition, it is recommended that as few bundle spacers as possible be used, consistent with the maintenance of adequate conductor separation under maximum load current conditions. (Maximum subspan length can be determined from static analysis, including consideration of conductors sticking following short-circuits.) In addition to the thermal considerations, subconductor contact under normal load conditions is undesirable because the alternating electromagnetic forces result in a vibration which produces arcing and radio noise. For flexible jumpers, two approaches are suggested; either allow adequate slack to accommodate any possible pinch effect or provide enough spacers that significant pinch is prevented.

4.5 Advanced Calculation Methods

4.5.1 Introduction

The occurrence of short-circuit currents in substations with flexible conductors leads to large transverse conductor motions. These motions cause an increase in conductor tension, resulting in dynamic loadings on several components of the bus structure. For severe short-circuit conditions, extreme conductor motions result which lead to highly nonlinear dynamic behaviour. As described in the previous sections, designers have the option of considering testing and simple or medium calculation methods. However, in some cases there is a need for more detailed results which leads to the possibility of using advanced dynamic nonlinear simulation analyses. These analyses can be used for cases A, A+B, C, D (as illustrated in Fig. 1.8) and can provide the designer the possibility to evaluate relatively easily, stresses and strains anywhere in a substation and for a range of substation parameters and configurations. This capability contrasts with simplified methods and experimental testing, where detailed studies are restricted to a limited number of locations and configurations.

This section provides a guide for design engineers on the application of advanced computer methods for the evaluation of mechanical effects of short-circuit currents in HV and EHV substations. Specific attention is given to the following:

- calculation of electromagnetic short-circuit forces by advanced analysis
- modelling of conductors and structures
- computer methods for simulation of electrodynamic behaviour of flexible conductors
- examples of application.

State-of-the-Art In Advanced Computer Calculations

In recent years, the detailed analysis of complex structures has become possible through the use of digital computers operating on discrete models. However, precise evaluation of the mechanical effects (displacements, stresses) caused by short-circuit current in substations with multiple, flexible conductors is not a trivial problem. It cannot be solved in a satisfactory way by the direct application of any of the presently available general purpose computer programs, although these can possibly be adapted, e.g. ADINA [97], NONSAP [93]. SAMCEF [100] has the capability of direct application using the submodule SAMCEF-CABLE, which was produced specifically for suspended cable analysis by the program developer. As well, some attempts have been made to prepare special purpose programs for the examination of short-circuit effects (for example, STANAN [60]). An advanced computer-aided approach allows for a much better simulation of the real structure (through more detailed physical modelling and more powerful mathematical analysis) than is the case for any simple method.

Application of advanced calculations costs between 1 and 2 CPU hours on a medium sized mainframe computer. As well, the modelling, data preparation and structural representation for analysis by advanced programs involves a significant investment in engineering time. The overall cost is justifiable, depending on the relative significance of mechanical short-circuit effects in the design of any specific substation.

4.5.2 Short-Circuit Forces In Advanced Analysis

The electromagnetic force acting between any two current carrying elements (including elements in the same conductor) is calculated using the formulas 1.6 to 1.8.

In a finite element context, the spatial distribution of forces can be calculated numerically in a consistent manner on the basis of the shape functions utilized to construct the mechanical model, as described in [98]. The finite difference approach [60] may also be used. Integration of the forces is done by taking into account, for single conductors, the spatial distribution of forces, which is dependent on the motion of the cable and which undergoes relatively slow changes compared with those of the time distribution. Thus the spacial distribution need not be updated at each step of the time-integration process. The elementary contributions resulting from remote elements decrease in proportion to their distance and it is possible to stop the integration when the relative incremental contribution becomes less than a given tolerance.

Short-circuit current data needed for calculation of the short-circuit forces are described in section 1.2. In addition, a definition of the short-circuit current path is required.

For bundle conductors, the short-circuit forces depend on both conductor-to-conductor and phase-to-phase interactions. The conductor-to-conductor electrodynamic forces are particularly important in this case because of the relatively close spacing and they depend on the actual configuration of the bundle during the short-circuit. The conductor motion within a bundle changes relatively fast in comparison to the interphase motion. Hence for the description of the short-circuit current the harmonic function, given in Chapter 1, must be used and an accelerated updating of the short-circuit forces during the time integration should be applied.

54

4.5.3 Modelling of Conductors and Structures

Brief Descriptions of Typical Real Structures

Typical flexible bus configurations include strain buses with single or bundled conductors, insulator strings, steel towers or gantries, apparatus (insulators, connectors, drop leads, hardware and so on), substructures and foundations. For a more detailed description the reader is referred to section 1.4 of this brochure. The buses are secured to the steel structures by insulator strings and the individual spans are supported such that axial movement is permitted. The strain insulators are either of the cap-and-pin type (glass or porcelain) with many elements, or they are of the longrod type (porcelain) with few elements.

For steel structures, the lattice type predominates over the solid-web types. The bases of supporting structures which only have to bear vertical loads may be hinged. The foundations are designed to meet all given loads but they do not remain motionless in the earth if large short-circuit forces occur. Referring to the apparatus, the reduction in stiffness caused by coupling links should be noted. For instance, a complete insulator assembly is more elastic than the porcelain column. For optimum calculation accuracy, the availability of measured data, such as deflections and spring constants, is imperative.

Mechanical Model Used in Calculations

For calculations, the actual structure mentioned above is replaced by an ideal representation, called a mechanical model. It consists of bars, cables and possibly rigid bodies. Two kinds of bar elements are distinguished, namely truss and beam elements. Truss elements are straight bars which are only subject to axial forces (tension or compression). Their connections are hinged. Beam elements can transmit arbitrary forces and moments (that is, besides axial forces, they may be subjected to bending and torsion forces). In calculations, truss elements are characterized by cross-sectional area, mass density, Young's modulus and Poisson's ratio. In the case of beam elements, torsional and bending moments of inertia are also needed.

Conductors and Insulators

Conductors play the key role in the success of any mechanical model of a substation. Under the influence of short-circuit forces they display a strong nonlinear behaviour including large displacements and rapid changes of shape in the neighbourhood of spacers. Conductors are modelled by tensioned cables that may be considered as a chain of cable elements of the required order. Insulators are represented by a chain of rigid or semi-rigid bodies. Jumpers and droppers, if considered, are also modelled like cables or assumed to be concentrated masses. Usually multiple conductors are considered in detail with their motion restricted by bundle spacers represented by truss elements.

To save costs, calculations for bundle conductors can be done in two steps. In the first step all bundle details are incorporated and the analysis is continued until the bundle pinch effects are finished. (For a more detailed description of this phenomenon one is referred to section 4.4.) In the second step, the bundle is replaced by an equivalent single conductor and the relatively slow interphase conductor motions are analyzed. Note that for the transition from step 1 to 2 special purpose options for the remodelling of the program are needed. Due to a

lack of comparison between experiments and calculation results of phase-to-phase bundle interactions, this may be the subject of further work.

Droppers

Experience with finite element analysis indicates that interactions of the short-circuit current forces between conductors and droppers are important for an accurate description of the electrodynamic behaviour of droppers. For calculation of these interactions, two methods are recommended:

1. Account for all electromagnetic forces arising between all the elements within the short-circuit current path. In this case the interactions of elements within the same conductor are also considered.

2. Include only the forces arising between the elements in a cable segment "consisting of a group of elements within a conductor or dropper" and all the elements in other segments within the short-circuit current path. In this case the minor effect of the forces arising between the elements within the same conductor or dropper can be neglected.

Portal Structures

A real supporting structure is represented by a space frame (structure composed of beam elements) or trusses (structure composed of truss elements). As a result of the relatively small displacements, structural motion may be described well in terms of linear theory, contrary to the nonlinear theory necessary in the case of conductors.

As with modern design of portal structures, the mechanical properties are determined from finite element analyses. The substructure stiffness and mass matrices can be subtracted from these analyses. This approach leads to a reduction of the size of the finite element modelling of the substation. For existing portal structures, the supporting stiffness matrix can be derived from the measured flexibility matrix which can be added as a substructure stiffness matrix. By adding lumped masses, one can fit the frequencies of the substructure to those of the existing portal structure.

Apparatus

The stiffness properties of connected apparatus only slightly affect the dynamic behaviour of the conductors. Hence apparatus can be modelled by rigid boundaries. The stress and strain caused by dynamic loading on apparatus can be determined from separate calculations, in which the calculated loading history is used as input.

General Features of Mechanical Model

A reasonable electromechanical model of a substation should represent not only large displacements of cables (nonlinear theory) but also temperature and damping effects, various boundary conditions (for example, clamped and free-supported), the type of foundation for the supporting structures, service conditions such as the type of short-circuit, duration of short-circuit current, multiple reclosure, actual short-circuit electromagnetic forces and so on.

A very important problem is the exact system loading caused by electromagnetic short-circuit current forces, including conductor-to-conductor interactions. These

electrodynamic interactions essentially depend on the actual configuration of conductors. In this way electromagnetic and mechanical effects are combined. Portal structures can be modelled with finite elements. However, these can be replaced for analysis purposes by simpler equivalent substructure representations. The theory and calculation methods in the general case of nonlinear dynamics of structures are described in [95-97].

4.5.4 Simulation of Electromagnetic Dynamic Behaviour

Initial Conditions Static Solution

The electrodynamic behaviour initiates from static equilibrium conditions. Hence the sagged conductor and droppers must fulfil these conditions. Before application of the short-circuit forces, the static equilibrium conditions must be determined from static nonlinear analysis, usually performed by FEM or special purpose programs.

Discretization

Practically all calculation methods may be implemented by a computer. However, advanced computer approaches require preliminary discretization of the problem being considered. That is, the actual structure has to be represented by a mechanical model which results in a discretization by finite elements, as discussed in section 4.5.3. In this way, the problem expressed in terms of differential or integral equations is replaced by another problem described in terms of algebraic equations involving discrete quantities (numbers). The dynamics of structures deals with both space and time discretization. At the present time, finite element methods or finite difference methods are generally applied for spatial variations, while time discretization is usually performed by various forward integration methods (for example, [88] and [95]). These are so-called unconditionally stable solution methods. In most programs optimal values for time integration parameters are included as default values.

$$Ku + C\dot{u} + M\ddot{u} = R(t) \qquad (4.5.1)$$

and where $K = K(u)$, C and M are respectively stiffness, damping and mass matrices, u and R displacement and force vectors.

Time Integration

Various step-by-step methods are usually applied to obtain numerical solutions of the above equations. At each step, a nonlinear boundary value problem, formulated as a system of simultaneous nonlinear algebraic equations must be solved. The time step must be selected in coordination with the smallest period of interest in the structure. As the fundamental frequency of the short-circuit current force is two times the power frequency, the time step size has to be about 1/10 of the time period of these forces. Hence the time step will be about 1 ms. However, in substations with single conductors, the lowest Eigenfrequencies, which are excited by short-circuit forces are about 1 Hz. For bus systems with such low natural frequencies, the mechanical response is only slightly affected by the high short-circuit current force frequencies. This allows simplification of the calculation of

the short-circuit forces, as has been indicated in Chapter 1, Eq. 1.10. This process permits a considerable increase in time integration step, which can be raised to 0.01 s to follow the actual force. A detailed description of numerical solution procedures of finite element methods is presented in [95].

Summary of Advanced Method Capabilities and Drawbacks

For the user, the important questions are: "What are the capabilities?" and "What are the problems with the advanced computer approach?" Its main advantages are:

-   The capability to consider relatively complex models precisely enough to get satisfactory agreement with actual conditions.

-   Satisfactory solutions may be obtained in cases that are not predictable by any simple methods (and by experiments if they are possible), such as for structures of a new type or structures with a significant change of parameters.

-   Results may be obtained as a function of time for any quantity wanted, (for example, displacements $u(t)$, stresses $\sigma(t)$ at any required point of the structure). This is not possible for any other calculation method.

-   Results may be presented in graphical form suitable for any design engineer; in well-equipped computer centers, interactive technique may also be applied.

On the other hand there are some clear disadvantages of the advanced computer approach:

-   Computation of dynamic problems may be expensive. Satisfactory results may require times in the order of hours of CPU use for a contemporary mid-size computers.

-   Results are not available immediately.

-   A laborious and time-consuming task of initial data preparation for each problem is required. This may sometimes be decreased if mechanisms for automatic data generation are available.

-   Advanced computer programs are highly complex and not likely to be understood in detail by most designers. Therefore treatment of such programs as a "black box" risks a certain amount of abuse and misuse.

-   Therefore, engineering experience is required for critical evaluation of the final results.

4.5.5 Programs In Practical Use

This section describes some of the most-advanced computer programs which have been adapted and used for numerical analysis of mechanical effects in substations resulting from short-circuit currents. A typical mechanical model, more or less common to these programs, is shown in Fig. 1.8. Table 4.5.1 can be used to compare these programs on the basis of their assumptions, discretization methods and ranges of capabilities.

Table 4.5.1
Comparison of Advanced Computer Programs Analyzing...
Mechanical Effects of Short-circuit Currents in
Substations with Flexible Conductors

Program Name	SAMCEF-CABLE	NONSAP	ADINA	STANAN
General Information				
Data generation: Manual=1, Auto=2	1,2	1,2	1,2	1,2
Time discr: Expl=1, Impl=2	1,2	2	1,2	1,2
Time step: optional = 1	1	1	1	1
Damping: Optional=1, No=0	0	1	1	1
Results (output): displace stresses at any point = 1	1	1	1	1
Code Fortran = 1	1	1	1	1
Core required	256 kB	250 kB	350 kB	450 kB
Conductors and Insulators				
Mass: concentrated (lumped) = 1 distributed (consistent) = 2	1,2	1,2	1,2	1,2
Elements: transmit axial forces only = 1	1	1	1	1
Material: optional, e.g. el-plastic = 1 linear elastic = 2 insulators not extensible = 3	2,3	1,2	1,2	2,3
Short-circuit heating: optional = 1, no = 0	1	0	1	1
Arrangements per phase: single=1, duplex=2 multiplex=n, with spacers=3, with collapse during SC=4 jumpers=5, droppers=6	1,2,3,4 5,6.	1,2,3,4 5,6	1,2,n,3 4,5,6	1,2,3,4
Displacements large=1, small=2	1,2	1,2	1,2	1
Space discr: finite elements=1 finite difference=2	1	1	1	2
Supporting Structures				
Solid web structure: arbitrary shape=1 truss full structure=2 reduces to frame=3	1,2,3	1,2,3	1,2,3	1,2,3
Space discretization: finite elements=1 finite differences=2	1	1	1	1
Electrodynamic Forces				
Distributed = 1 Phase to phase = 2 In bundle = 3 Unsuccessful autoreclosure = 4	1,2,3,4	1,2,3,4	1,2,3,4	1,2,3,4
Other Loadings				
Static: gravity = 1 ice = 2 ground = 3	1,2,3	1,2,3	1,2,3	1,2,3
Dynamic: e.g. earthquake = 1	1	1	1	1

Although most general purpose structural analysis programs may be adapted for the analysis of bus systems under short-circuit conditions, the general purpose programs SAMCEF and ADINA are applicable without program modifications. Options for user supplied loading subroutines are available and users can add specific subroutines for the calculation of the short-circuit forces.

Sources for Programs

1. Program name: SAMCEF
    University of Liege (Belgium)
    Adaption to short-circuit problems
    Sponsored by TRACTEBEL
    References [7,79,105]

2. Program name: NONSAP
    University of California Berkeley (USA)
    Adaption to short-circuit problems
    N.V. KEMA (The Netherlands)
    University of Erlangen and
    University of Karlsruhe (W. Germany)
    References [80,93]

3. Program name: ADINA
    M.I.T. Cambridge (USA)
    Adaption to short-circuit problems
    Siemens (W. Germany)
    ASEA (Sweden)
    N.V. KEMA (The Netherlands)
    Reference [7]

4. Program name: STANAN
    Technical University of Cracow (Poland)
    Adaption to short-circuit problems
    Energoproject (Poland)
    Reference [7]

4.5.6   Preparation of FEM Model

The electrodynamic behaviour initiates from a static equilibrium condition. This condition can be determined from a nonlinear static analysis. This can be performed by special purpose programs. However, when such programs are not available, the following procedure is recommended.

Initial Conditions Determined from FEM Analyses

Model each conductor and its insulators as a stretched string fitted between the supporting structures, as shown in Fig. 4.5.1. Then fit the droppers as stretched strings between its connections to the conductors and the apparatus. To allow for non-zero transverse stiffness, an initial pre-stressing is applied. To satisfy equilibrium with respect to this pre-stressing, additional forces are applied at the ends of the conductors and droppers as shown in Fig. 4.5.1. Subsequently, the gravitational loads are incrementally applied, and at the same time the additional forces are removed.

Next, the desired sag and curvatures of the droppers are established by appropriate contraction or expansion of the conductors and droppers. For this procedure, a fictitious thermal expansion can be used. The procedures recommended above can be well supported by preprocessors, which are available for most general purpose programs. This simplifies the work significantly.
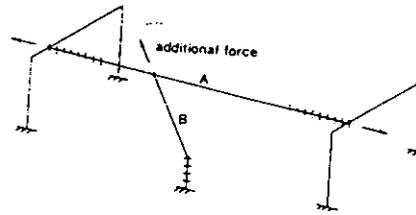

Fig. 4.5.1   Stretched string model which serves as a basis for FEM analysis for determination of the initial static equilibrium conditions

Recommendations for FEM Modelling

Based on experience with advanced analyses of electrodynamic behaviour of flexible single conductors, the following recommendations for the modelling of conductors and droppers are suggested. Conductors should be discretized with approximately 20 nodes. Discretization of the insulator chains depends on their length relative to span length. Droppers can be discretized by 6 nodes. Designers can use either three-dimensional truss elements or higher order elements. The necessary data for the mechanical properties of the conductors and insulators are well documented in Appendix 3.

4.5.7   Applications

In order to verify the capabilities of the numerical methods, comparisons between tests and analyses have been carried out. In the first case the substation tested by Laborelec has been analyzed with ADINA, SAMCEF, STANAN and NONSAP [7]. The required set of data for the analysis of this problem is given in Appendix 3. Some special aspects should be noted. First, STANAN cannot take droppers into consideration, and second, as a result of the lack of beam elements in the nonextended NONSAP program, the portal structure stiffness has to be modelled by mass-spring systems. In spite of these simplifications, a satisfactory agreement between the experimental results and those determined by the numerical methods was obtained.

Some interesting results, for example conductor motion and conductor tension at midspan, are shown in Figs. 4.5.2 and 4.5.3. Some results of more specific interest for the design of substations are given in Appendix 3.

In the second case, a substation tested by EDF was analyzed with some medium and advanced methods (SAMCEF and NONSAP). The calculation results have been described in [10]. Due to the very limited data for the portal structures, they had to be modelled as mass-spring systems. Hence, identical assumptions for tests and calculations were not possible. As well, there were some differences between measured and calculated sags which may be ascribed to limited data for the actual test-span. These differences are clearly significant from the very beginning of the conductor motions, as is

58
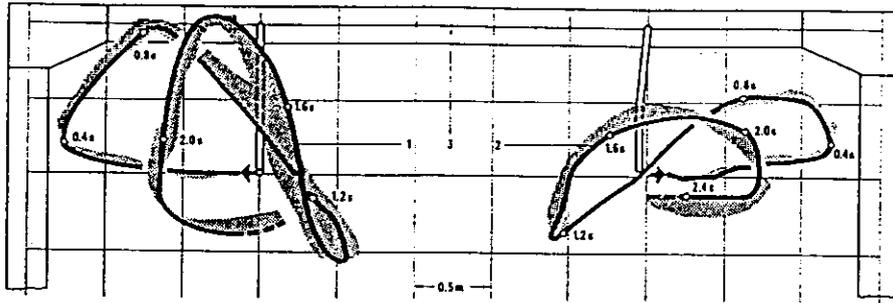
Fig. 4.5.2 Conductor displacements at midspan of Laborelec substation, as presented in [7]. Experimental curves (drawn lines) with the diverging bands of numerical results. 1 west conductor, 2 east conductor, 3 portal structures

Fig. 4.5.4 Conductor displacements of Phase 1 at midspan of EDF substation with a short-circuit duration of 0.122 s

Fig. 4.5.3 Tension in east conductor of Laborelec substation, as presented in [7]. Thin lines experimental curves. 1 ADINA, 2 SAMCEF, 3 STANAN

shown in Fig. 4.5.4, and these continue throughout the final results, as shown in Fig. 4.5.4 for conductor motion and Fig. 4.5.5 for tension at midspan. For this specific case, the results illustrate the significant influence of the modelling and the data used for the calculations. This sensitivity may also be apparent in testing. However, to reveal these sensitivities, extensive testing is required. Hence advanced analysis can be applied to reveal these sensitivities and can be used as a guide for the selection of locations in a test configuration to be monitored during testing.
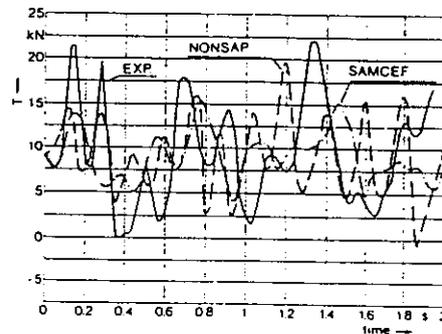
Fig. 4.5.5 Tension in phase 1 conductor, determined for EDF experiment with a short-circuit duration of 0.122 s

4.6 Parameter Analysis

4.6.1 Introduction and General Parameters

The aim of this parameter study is to give design engineers a good qualitative and hopefully intuitive understanding of how short-circuit phenomena are influenced by the respective physical and electrical parameters. Readers new to this field, may be able to obtain a better understanding of the phenomenon by not focusing on a specific case with specific data; but attempt to get an overall view of the influences of various parameters by understanding what happens when they are varied. For example, a parametric study on the choice of subspan length can be very instructive. The analysis described in this section is the result of numerous calculations based primarily on medium methods for single conductors and experimental tests for bundle conductors.

The parameter analyses have been limited to the following two items (Case A, C, D according to Fig. 1.8):

- phase-to-phase interactions (cases A and C, excluding pinch effect), effects on tensions (section 4.6.2) and deflections (section 4.6.3)

- bundle pinch effect (section 4.6.4)

Note that for Case D (jumper) clearance is developed in section 4.6.3 and bundle jumper in section 4.6.4.

The approach is more qualitative than quantitative; nevertheless, it provides useful guidance to the design engineer. The parameters that have been considered are listed in Table 4.6.1 below.

Table 4.6.1
Parameters Included

Current parameters:
- rms short-circuit current magnitude
- network time constant
- duration of short-circuit
- autoreclosure

Conductor parameters:
- initial static tension
- (sub)span length
- interphase distance
- subconductor separation
- number of subconductors
- cross section
- mass
- elasticity modulus

Supporting structure parameters:
- anchoring structure stiffness (spring constant)
- dynamic spring constant (bundle only)
- spacer stiffness

As conductor heating is always associated with short-circuit current flow, this effect has been included in the analysis.

Results of importance for the designer are:

- In cases A and C: swing-out tension "F_t", falling down tension "F_f", and deflections

- For bundled conductor configurations, only the maximum pinch tension "F_{pi}" is discussed.

For the general purposes of parameter analysis, independent consideration of each of the parameters in Table 4.6.1 is awkward because of the compensating interactions between the parameters. Therefore, more general undimensional parameters have been introduced by selectively grouping related parameters from Table 4.6.1. A very limited number of dimensionless parameters gives a better understanding of the interactions between the parameters. As a result of numerous discussions, dimensionless parameters were identified for single conductors: P_1, P_2, P_3 and P_4 [13]; and three for bundles: P_{1s} (a specific case of P_1), P_2 (the same as for single), and P_5 [106]. These factors are described in the following paragraphs.

The Force Factor

Short-circuit forces can cause relatively high acceleration in comparison with the forces of gravity depending on the magnitude of short-circuit current. The ratio between the forces per unit length (short-circuit and gravitational forces) which is equal to the corresponding acceleration ratio, is defined as the first parameter (the force factor):

$$P_1 = F_o / m'g_n$$ (4.6.1)

where $F_o = 0.2 \, I'_{k2}{}^2 /a$ (or $= 0.15 \, I'_{k3}{}^2/a$)   (4.6.2)

The parameter P_1 is identical to r_o defined in section 4.2.1 without any asymmetry influence.

The factor P_1 is only valid for inter-phase effects. For example the weight is the total weight per unit length of one phase: an equivalent single conductor is assumed ($m' = n_s \, m'_s$).

For bundle configurations, the effects between the subconductors of one phase are given by a specific case of P_1 indicated by P_{1s}:

$$P_{1s} = F_{os} / (m'_s \, g_n)$$ (4.6.3)

where $F_{os} = 0.2 \, (I'_{k2}/n_s)^2 \cdot \sqrt{(n_s-1)}/d$ (4.6.4)

with n_s equal to the number of subconductors ($n_s > 1$), and d equal to the diameter of the bundle:

$$d = a_s/\sin(\pi/n_s)$$ (4.6.5)

In practice, P_1 values are in the range 0 to 6 and P_{1s} values are in the range 0 to 100.

The Network Factor

As discussed in section 1.1, the waveform of the short-circuit current can be approximated by a mathematical formula which includes only one time constant, τ. This value is fixed by the network. Obviously, τ is an independent parameter. The dimensionless time parameter P_2 is obtained using the frequency of the current which leads to:

$$P_2 = \omega\tau \qquad (4.6.6)$$

Although P_2 is independent of the asymmetry level of the current, the current waveform asymmetry is an important parameter. The current waveform asymmetry is dependant on the angle of fault initiation which, in practice, is an independent, statistical parameter. For practical design purposes, the conservative assumption of maximum asymmetry is usually made.

Values of P_2 are typically in the range of 5 and 50 (τ from 15 to 160 ms).

Short-circuit Duration Factor

For phase-to-phase interactions, the short-circuit duration is an important parameter. As described in earlier sections, phase-to-phase short-circuits (worst case) can induce significant low frequency displacements. The frequency is related to the oscillation period of the pendulum model of the span. In situations like case A or C, this frequency may be given by the simple pendulum formula:

$$\text{pendulum frequency} = 0.56 / \sqrt{b_c} \qquad (4.6.7)$$

that is, a period of $T = 1.79 \sqrt{b_c}$ $\qquad (4.6.8)$

The maximum swing out of the cable is a function of the duration of the short-circuit and the period of oscillation of the busbar. This leads to a natural choice for the next parameter P_3 which is simply given by:

$$P_3 = \frac{T_k}{T} \qquad (4.6.9)$$

For sags between 0.5 and 2 meters, T ranges from 1.25 to 2.5 seconds. Values of P_3 typically range between 0.015 and 0.3, sometimes higher; but the maximum stress increases until P_3 reaches a maximum of 0.25.

The Structural Factor

The response of the structure to the applied force is not obvious. There is a complex relationship between sag, tension, span length, mass and stiffness of conductors and the anchoring structure. In order to determine the structural behaviour of the complete bus system, a simple approach is taken:

In the case of phase-to-phase interactions, the increase in length of the conductors can be deduced in two ways (expressed as an equivalent single conductor per phase).

from elasticity:

$$\mathcal{L} = \mathcal{L}_0 [1 + (F-F_{st})/EA] \text{ (assuming no heating)} \qquad (4.6.10)$$

from parabola geometry:

$$\mathcal{L} = \mathcal{L}_0 + 2.67 \, b_c^2/\mathcal{L}_0 - 2 \, (F-F_{st})/S \qquad (4.6.11)$$

(S is the spring rate of supporting structure)

thus $(F-F_{st}) \, (\mathcal{L}_0/EA + 2/S) = 2.67 \, b_c^2/\mathcal{L}_0$ $\qquad (4.6.12)$

Thus the next parameter, P_4, is given by:

$$P_4 = 100 \, S \, b_c^2/[F_{st} \, \mathcal{L}_0 \, (S \, \mathcal{L}_0/EA + 2)] \qquad (4.6.13)$$

Note that for case A, $\mathcal{L}_0$ is the length of cable only (excluding the insulator strings). In the P_4 calculation, $\mathcal{L}_0$ can be taken as the span length of the cable busbar. Recalling the simple sag-tension relationship:

$$b_c = m'g_n \mathcal{L}_0^2/(8 \times F_{st}) \qquad (4.6.14)$$

There is a close connection between P_4 and the "span factor" defined in section 4.2.2. In a physical sense, P_4 is a ratio between two stiffnesses, namely:

- the intrinsic stiffness of the cable in series with the anchors: $1/(\mathcal{L}_0/EA + 2/S)$
- the extrinsic stiffness resulting from the initial conditions, mainly the ratio sag to span:

$$F_{st} \, \mathcal{L}_0/b_c^2 = 0.125 \, m'g_n \, (\mathcal{L}_0/b_c)^3 \qquad (4.6.15)$$

In practice, anchoring stiffnesses range between 10^5 and $5 \cdot 10^6$ N/m, and values of parameter P_4 are between 15 and 300.

Bundle pinch effect

A similar development leads to similar equations (written for one subspan using per subconductor data) from the elasticity relationship (see (4.6.10)) and from the geometry:

$$\mathcal{L} = \sqrt{\mathcal{L}_s^2 + \varphi^2} - 2 \, (F-F_{st}) \, (1/S_d + 1/S_z) \qquad (4.6.16)$$

(where S_d = longitudinal stiffness and S_z = spacer stiffness)

$$\varphi = (a_s - d_s)/\sin(\pi/n_s) \qquad (4.6.17)$$

As described in [48], the increase in tension is proportional to the current. In fact, the forces increase with the square of the current; but the length of the conductors not touching (and thus the effective length contributing to the force), decreases simultaneously. The combined action of increasing the force and decreasing the free length, give a simple proportionality relationship between current and tension. Therefore converting this formula to:

$$(F_{pi} - F_{st})/(m's \, g_n \, \mathcal{L}_s) \text{ proportional to } \sqrt{P_{1s}} \qquad (4.6.18)$$

61

Making the same derivations as for Parameter P_4, and taking equations (4.6.10, 4.6.16 and 4.6.18) into account, we derive another new dimensionless parameter,

$$m's \, g_n \, l_s^2 \, (l_s/EA + 2/S_d + 2/S_z)/\varphi^2 \qquad (4.6.19)$$

In order to cover the range of general use the new parameter, P_5 is defined by:

$$\boxed{\begin{array}{l} P_5 = 200 \, [m's \, g_n \, l_s^2 \, (l_s/EA + 2/S_d + 2/S_z) \\ \cdot \sin^2(\pi/n_s)/(a_s-d_s)^2]^{0.333} \end{array}} \qquad (4.6.20)$$

(Note that φ has been replaced by (4.6.17).)

Physical interpretation of P_5 is the same as for P_4 except that in the "extrinsic" stiffness, the sag is obviously replaced by "φ" and the span by the subspan. In practice, values of P_5 are between:

0.5 .. 10	20 100	200.....500
jumper	substation	overhead line

Normalized tension and deflection

The increase of tension is the main concern for the design of the structure. For phase-to-phase interactions, F/F_{st} (with $F = F_t$ or F_t) has been selected as the basis for normalization. Because pinch effect is not a function of initial static tension, normalization in this section for bundle pinch effect is based on $(F_{pi} - F_{st})/(m's \, g_n \, l_s)$.

Another design value for the substations is the clearance. It can be easily deduced from the following normalized deflection: Y_{in} / b_c.

Example of calculation

In the following paragraphs, the parameter values for a typical example bus configuration are calculated. In later parts of this section, the example is continued to illustrate specific aspects of the variation of parameters.

Data:

245 kV substation

span length - 40 m (excluding insulator string)

twin bundle 2x400 mm² ACSR, a_s=0.15 m,

d_s=0.03 m, l_s=10m

weight $m's \, g_n = 15$ N/m per subconductor

interphase distance: a = 3.5 m

sag of cable busbar: $b_c = 0.6$ m

calculated static tension $F_{st} = 10$ kN/phase

anchoring stiffness: S = 1 MN/m (spring constant)

equivalent dynamic spring: $S_d = 10$ MN/m

short-circuit current: $I_{k2} = 40$ kA rms

time constant: $\tau = 60$ ms

duration of fault: 0.2 s (with maximum asymmetry)

Parameter values for interphase effects:

$F_o = 0.2 \cdot 40^2/3.5 = 91.4$ N/m and $m'g_n = 2 \cdot 15 = 30$ N/m

$P_1 = 91.4/30 = 3.0$

$P_2 = (2\pi \cdot 50) \cdot 0.06 = 18.8$

$T_k = 0.2$ s and $T = 1.79 \times \sqrt{0.6} = 1.39$ s

$P_3 = 0.2/1.39 = 0.144$

$l \, S/EA = 40 \cdot 10^6/(6 \times 10^{10} \cdot 2 \cdot 400 \times 10^{-6}) = 0.833$ m/N

$P_4 = 100 \cdot 10^6 \cdot 0.6^2 / [10000 \cdot 40 \cdot (2 + 0.833)] = 31.8$

Parameter values for bundle pinch effect:

$F_{os} = 0.2 \times (40/2)^2/0.15 = 533$ N/m and $m's \cdot g_n = 15$ N/m

$P_{1s} = 533/15 = 35.6$

$P_2 = 18.8$

P_3 and P_4 do not apply for pinch effect:

$l_s/EA + 2/S_d + 2/S_z = 10/(6 \times 10^{10} \cdot 400 \times 10^{-6}) + 2/10^7 + 0 = 617 \times 10^{-9}$ m/N

$m's \, g_n \times l_s^2 /(a_s - d_s)^2 = 104.2$ kN

$P_5 = 200 \, (104.2 \times 10^3 \times 617 \times 10^{-9})^{0.33} = 80$

4.6.2 Effects on Mechanical Tensions

A qualitative approach can be used to determine the effects on the conductor tension caused by variations in electrical and physical parameters. These effects are illustrated by families of curves given in Figs. 4.6.1 to 4.6.3.

Parameters : I_k, a, m', Heating, T_k

The combined interaction of the first four parameters (I_k, a, m', heating) are included in P_1, the most important parameter. As a result, all of the curves in Figs. 4.6.1 to 4.6.3 describe the effect on P_1 (abscissa) caused by all of the other parameters.

Obviously, P_1 should be as low as possible (because a lower P_1 implies a lower normalized tension). From the definition of P_1, an increase of fault current level of a factor 1.25 (for example from 40 to 50 kA) can be fully compensated by an increase in the interphase distance or phase conductor weight by a factor of 1.56.
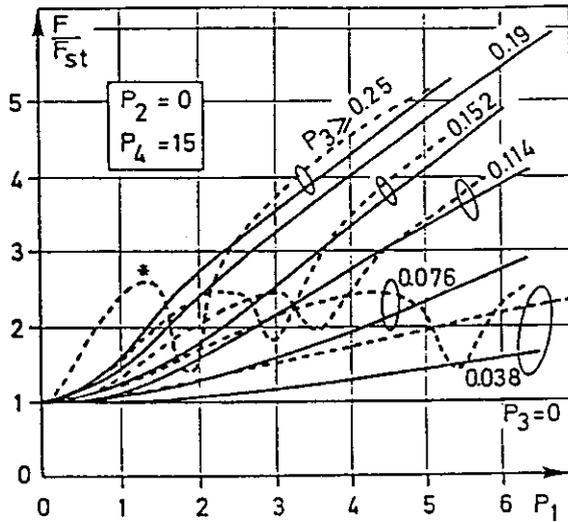
Fig. 4.6.1 Effect of force factor (P_1) on normalized conductor tension for several short-circuit duration factors (P_3)

- - - - F_f (falling down)
———— F_t (swing out)
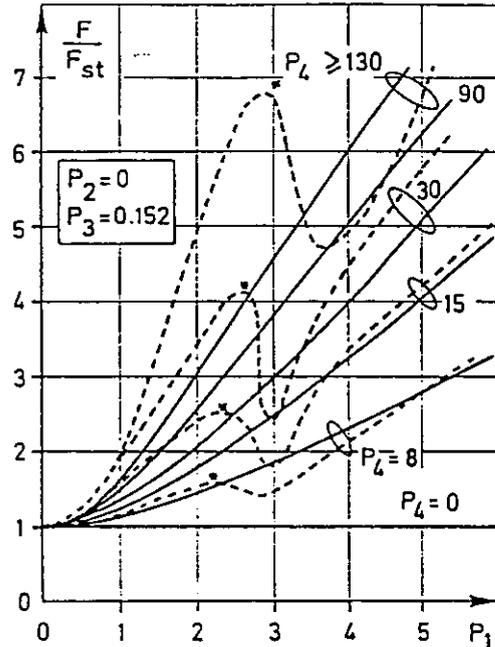
Fig. 4.6.2 Effect of force factor (P_1) on normalized conductor tension for several structural factors (P_4)
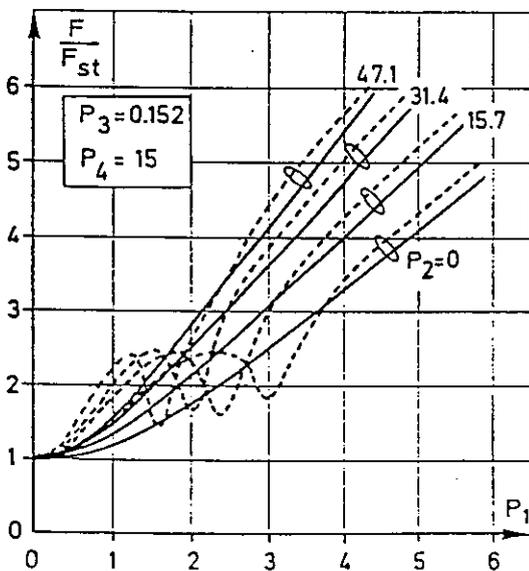
Fig. 4.6.3 Effect of force factor (P_1) on normalized conductor tension for several network factors (P_2)

If the product $P_1 \times P_3$ (input energy) is lower than 0.35 (this value can be found in Fig. 4.6.1), the falling down maximum tension is higher than the swing out maximum tension. Both maximum stresses are of the same order of magnitude for a very limited range of P_1 where a circular movement of the cable does not give any falling down effect.

Figure 4.6.4 illustrates the effect of P_3 (relative time duration of the fault). Swing out maximum F_t, for a given P_1 (relative short-circuit force), increases with the time duration of the fault until this time is equal to a quarter of the period of the pendulum oscillation of the cable busbar. Beyond this value ($P_3 = 0.25$), a saturation effect is apparent. This is logical because at this moment, the cable has just reached its maximum horizontal displacement limited by elasticity. If the short-circuit duration is greater than T/4, natural movement of the cable is disturbed by the electromagnetic force action. Generally, this case will cause lower stresses because swing out is not amplified and falling down pattern is disturbed. This is fully compatible with the "worst case" of the simple method developed in section 4.2 (see example in table 4.2.1).

63
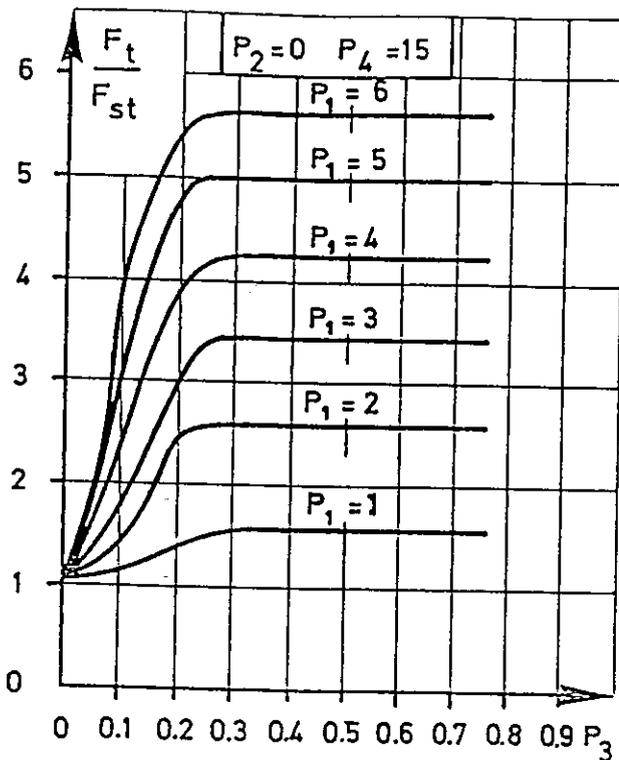
Fig. 4.6.4   Effect of short-circuit duration factor (P_3) on normalized conductor tension for several force factors (P_1)

Parameter : τ

For a given short-circuit force (P_1 fixed) there is an increase of the swing out stresses when the power system time constant increases, as illustrated in Fig. 4.6.3. The increase is the result of increased input energy. In addition, as indicated previously, swing out tension is significantly affected by the extent of the current waveform asymmetry. The network time constant varies at different locations in the power system. At a given location in the network, network time constant and P_2 are fixed; but the level of asymmetry depends on the time of initiation of the fault. As stated earlier, the time of short-circuit initiation is an uncontrolled statistical parameter for which designers typically make the conservative assumption that in all cases maximum current offset occurs.

Parameters : S, S_d, b_c, F_{st} and l_o

The structural parameter P_4, has a fundamental relationship with the fall of span maximum tension (Fig. 4.6.2). The ratio between the fall of span and swing out maximum (F_f / F_t) decreases very quickly with P_4. High anchoring stiffness is generally not recommended. If necessary for other purposes, anchoring stiffness can be balanced by high initial tension. Increasing P_4 (for example by using a higher anchoring stiffness) also has a sensitive effect on the swing out maximum tension. For $P_1 = 4$, an increase in anchoring stiffness of 100% results in an increase in swing out stress of about 25%.

The ratio of sag to span also has a significant influence on P_4. If this ratio is held constant, P_4 remains quasi-constant independent of the span length. In such cases, span length has no influence on the normalized stress (see example in section 4.6.5).

Autoreclosure

The problems associated with unsuccessful autoreclosure cannot be studied in detail by simple methods because the response varies depending on the new initial conditions at the instant of autoreclosure. The span movements can be amplified if autoreclosure occurs during the swing out or limited if it appears after the swing out maximum. The worst case occurs when autoreclosure coincides with the maximum separation speed. Critical cases are then:

$$T_k + t_u < 0.25\ T \quad \text{and}$$

$$0.75\ T < T_k + t_u < 1.25\ T$$

(where t_u = dead time)

In general, the effects of autoreclosure are smaller for flexible bus than for rigid bus; tension and deflections are not usually amplified by a factor of 2.

4.6.3   Effects on Deflections

These effects are illustrated qualitatively in the curves given in Figs. 4.6.5 to 4.6.7. Increases in effective sag are the result of conductor heating, elasticity of the conductors and anchoring structure and changes in the span geometry. For case A, movement of the bus is strongly influenced by the presence of droppers (connections to apparatus). For case D, the initial static tension may be very low, and thus P_4 may be considered at the highest value. Clearance is simply given by:

$$a - 2\ Y_{in}$$

where Y_{in} is the inwards deflection of the span at midpoint. Recalling that b_c is the sag of the cable only (excluding the insulator string), real clearance will also be reduced by the movement of insulator strings.

In general the influence of P_1, P_2, P_3 on deflections is similar to that for the swing out maximum F_t. Figure 4.6.5 illustrates the significant influence that the duration of the short-circuit has on deflections; deflections can be amplified by a factor of 3 between a very short and a very long fault. A very long fault time could, for the purposes of parameter analysis, be equivalent to a normally cleared fault followed quickly by unsuccessful autoreclosure.

The hypothesis that maximum inward movement is limited to the initial sag ($Y_{in}/b_c < 1$) is not correct. As with mechanical tension, the structural factor P_4 relates to clearance effects; an increase of P_4 (i.e. a more rigid structure) will limit the displacement and increase the stress. But the benefit in clearance caused by an increase of P_4 is much lower than the increase in stress (fall of span) for the same modification of structural stiffnesses.

Autoreclosure effects can clearly amplify the displacement and critical cases are the same as for tension.
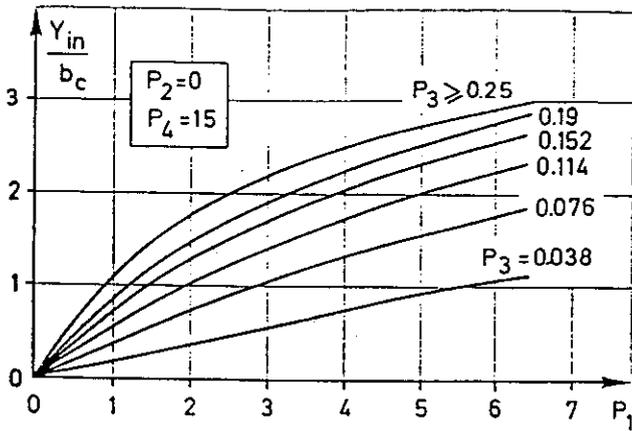
Fig. 4.6.5 Sensitivity of relative displacement to force factor (P_1) for several short-circuit duration factors (P_3)
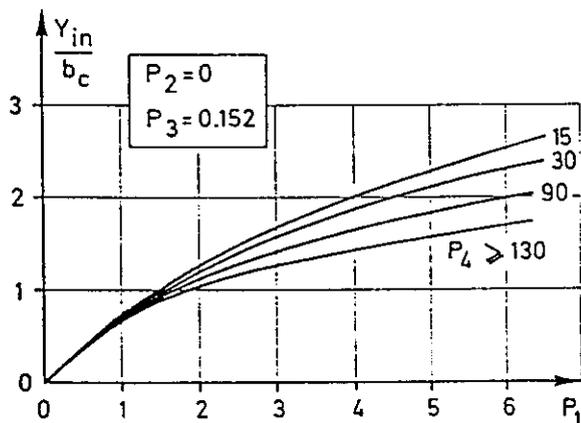

Fig. 4.6.6 Sensitivity of relative displacement to force factor (P_1) for several structural factors (P_4)
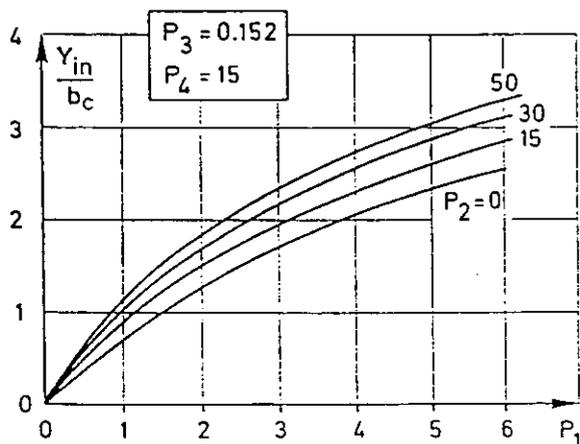
Fig. 4.6.7 Sensitivity of relative displacement to force factor (P_1) for several network factors (P_2)

4.6.4 Pinch Effects

Bundle pinch tension is clearly a separate problem from that of interphase effects. This fact is a result of the completely different mechanical time constants for the two phenomena. The bundle pinch phenomenon has been described in section 4.4. This section describes the parameter sensitivity aspects of bundle pinch.

Parameter sensitivity

This study is based on the sensitivity of the peak value of the bundle pinch tension, F_{pi}, as a function of the parameters which influence it (see Table 4.6.1). As discussed earlier, dimensionless parameters for bundle pinch effect are reduced to only three values: P_{1s} (short-circuit force factor), P_2 (time constant) and P_5 (structural factor). As far as a qualitative approach is concerned, the effect of P_2 can be included in P_{1s}, as in section 4.2.1, by the factor m.

Figures 4.6.8 and 4.6.9 illustrate influences on the design F_{pi} value in two sets of graphs which give the same information in two different ways. These figures have been obtained from tests and calculations based on four different conductors and four different subspans. Because of the close connections between tests and calculations [12,106], the parametrical approach can give good results. Figure 4.6.8 shows the linear relation between peak force and current. This is a justification a *posteriori* of the choice of P_5. Figure 4.6.9 gives the same information for a wider range of P_5, which also points out the non-contact zone. The dotted line is the border between subconductor contact and non-contact. For low P_{1s} (low short-circuit force) contact between subconductors does not occur. But this current level is more an overload than a short-circuit and for these cases designers should refer to [22]. For a given short-circuit force, the maximum peak will occur at the border line. This is logical because the border line corresponds to conditions for maximum force action (shortest contact length). On crossing the border into the contact zone, there is a rapid decrease of the peak force because the contact length increases very quickly and the effective length contributing electromagnetic force decreases proportionately.

Configurations in substations can typically fall in the dangerous zone of high peak tension. Jumpers, because of the very short subspan length, are generally designed in the non-contact zone. Overhead lines are typically designed with a very large P_5 and contact will always occur. Substation busbars (case A) or connections between apparatus (case C) are in between. Hence, this problem should be given careful consideration in design.

The optimal choice of subconductor separation and subspan length is not obvious. Some examples are given in section 4.6.5. As a first, very rough approach, the relative overstress $(F_{pi} - F_{st})$ increases with the ratio a_s/l_s. This ratio has a critical value corresponding to critical values of P_5. Limiting consideration to only a specific a_s or l_s is ineffective as only the ratio is important. In the example of section 4.6.5, the ratio a_s/l_s must be lower than 0.02.

An increase in the number of subconductors, all other data unchanged, increases the stress for the phase. Heating of the conductors resulting from the short-circuit current does not influence F_p because the temperature increase is usually negligible before the time of peak
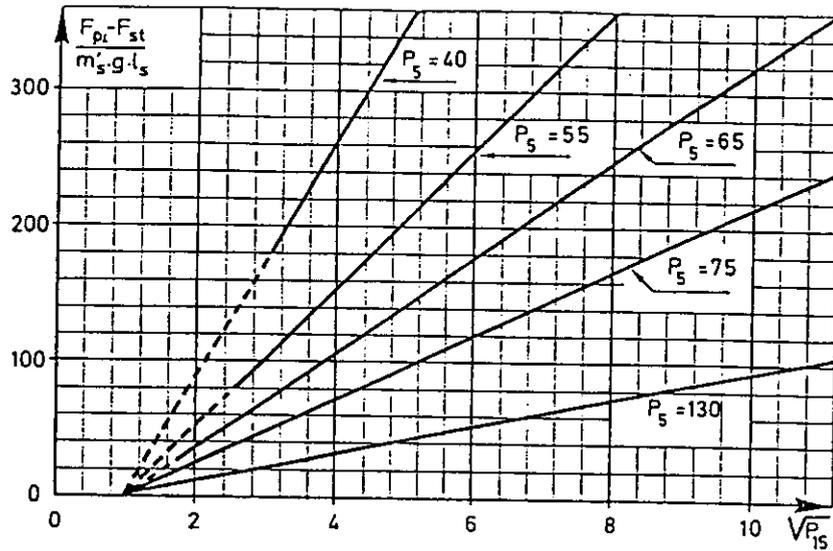
Fig. 4.6.8 Normalized pinch effect tension as a function of force factor (P_1) for several structural factors (P_5)

Fig. 4.6.9 Normalized pinch effect tension as a function of parameter sensitivity

tension. Short-circuit time duration (T_k) generally has no influence on bundle pinch because peak tension usually occurs before T_k. Autoreclosure causes the same effects as the first fault, but the autoreclosure pinch effect must be superimposed on the interphase effect to obtain the total phase tension. Thus, coincidence of unsuccessful autoreclosure with maximum swing out or fall of span time will cause a very significant increase of the stress as shown in Fig. 4.6.10.

Generally the analysis of one subspan will give the same results as for the complete span. Also as indicated above, this effect can be superimposed on the interphase effects. However, in some cases, unsymmetrical subspan lengths can cause additional effects. This is represented in P_5 by S_d the equivalent dynamic spring rate of end point of the subspan. Because of the high frequency of the phenomenon, this value is not the same as the static spring rate. It is always a larger value than the static spring rate and it is also indirectly a function of the current. S_d is also dependant on the inertial behaviour of end points of the subspan. For case C, it can be considered to be infinite; but for case A, S_d is a function of the inertial behaviour of the connecting hardware and insulator string. An estimate of the order of magnitude of S_d is 10^7 N/m.

4.6.5 Applications

The qualitative effects of variations of parameter values can be easily deduced from the grouped parameters described in the previous sections. Thus a good appreciation for the design sensitivity can be obtained. The following examples are based on the data given in section 4.6.1.

Interphase interaction

Figures 4.6.1 to 4.6.3 can be used as correcting factors. Referring to section 4.6.1 (example of calculation), the 245 kV substation busbar is characterized by:

$$P_1 = 3.0; P_2 = 18.8; P_3 = 0.144; P_4 = 31.8$$

Figure 4.6.1: $F_f/F_{st} = 2.4$ for $P_1 = 3.0$, $P_2 = 0$ and $P_4 = 15$.

Because the busbar has another P_2 and P_4, Figs. 4.6.2 and 4.6.3 can be used as correcting factors:

$$\text{Finally } F_f/F_{st} = 2.4 \cdot 1.2 \cdot 1.3 = 3.74$$

The factors 1.2 and 1.3 are the relative increase values of F_f/F_{st} according to Fig. 4.6.2 ($P_4=15$ to $P_4=31.8$) and Fig. 4.6.3 ($P_2=0$ to $P_2=18.8$).

66

F−F_st (daN)

Without reclosure ($T_k = 0.15$)

With reclosure
($T_k = 0.1$, $t_u = 0.3$, $T_k = 0.1$)
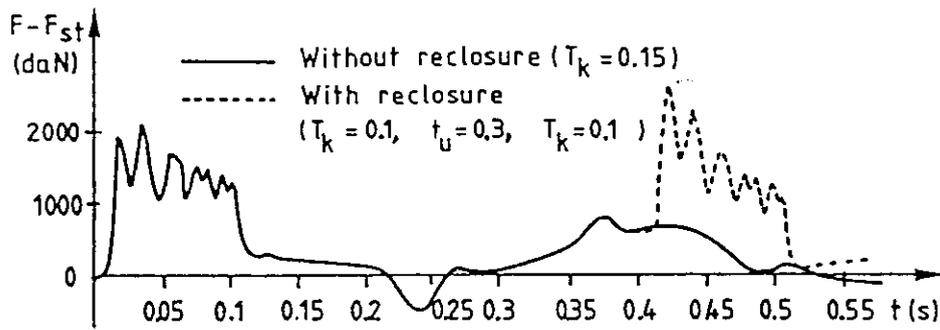
$I_k^{''} = 44$ kA $i_p = 100$ kA $a_s = 0.2$ m $\mathcal{l}_s = 18$ m
$m_s^{'} g_n = 20$ N/m $F_{st} = 7.5$ kN/conductor

Fig. 4.6.10   Tension in a twin bundle ACSR 2x587 mm²
($d_s = 0.0315$ m) according to the calcula-
tions by Mlodzianowski

Qualitative influences can then be deduced:

-   The influence of an increase of the mass by 20%,
    keeping the sag constant, resulting in a modified
    weight = 18 N/m (instead of 15) leads to: P_1 =
    3.0/1.2 = 2.5; P_2 = 18.8; P_3 = 0.144; P_4 = 31.8/1.2 =
    26.5 correcting factors are deduced from Fig. 4.6.1
    (0.9) and 4.6.2 (0.9). The corrected F_t/F_{st} =
    3.74x0.9x0.9 = 3, a decrease in relative stress by
    20%. Because F_{st} had been increased to keep sag
   constant, the final absolute stress is modified by
    3x1.2/3.74 = 1. *Thus, the increase of mass, keeping
    sag constant, makes no modification of the stress
    which has to be supported by the anchoring struc-
    ture.*

-   *The influence of an increase of the span length, by
    20%, keeping the ratio of sag to span ($b_c/\mathcal{l}$) constant,
    leads to:* a modified span length = 48 m (instead of
    40). P_1 = 3.0; P_2 = 18.8; P_3 = 0.144/√2 = 0.131; cor-
    rected P_4 = 25 (equ. 4.6.13). The correcting factors
    are negligible, thus F_t/F_{st} is not affected. Because
    F_{st} had to be increased by 1.2 to keep the ratio of
    sag to span ($b_c/\mathcal{l}$) constant, *the final absolute stress
    is increased by 20% in comparison with that of the
    initial structure.*

-   *The influence of an increase in initial static tension
    by 20% leads to:* a modified static tension = 12 kN
    (instead of 10 kN). P_1 = 3.0; P_2 = 18.8; P_3 =
    0.144x√1.2 = 0.158; P_4 = 31.8/1.2³ = 18. The cor-
    recting factor resulting from P_3 is negligible. The
    correcting factor resulting from P_4 = 2.5/3.0 = 0.83
    (Fig. 4.6.2) which means a decrease by about 20%
    in the relative stress (F_t/F_{st}), but the increase, by the
    same 20%, in initial static tension *gives no change in
    the final absolute stress F_t.*

-   The influence of anchoring stiffness: modified spring
    constant = 0.5 S = 500 kN/m. Only P_4 is modified:
    P_4 = 19. The correcting factor = 2.5/3.0 = 0.83. Be-
    cause nothing, other than S has been modified, this
    factor can be directly applied to the absolute stress.
    *Thus a reduction of 50% in anchoring stiffness gives
    about a 20% reduction in swing out maximum
    stress.* Fig. 4.6.2 also shows that the fall of span
    maximum tension increases very quickly with P_4,
    thus a flexible structure is favoured.

Bundle pinch effect

Case D corresponds with very short spans having very
low mechanical tension. In these cases (very low P_5),
there is generally no contact. Thus P_5 must be adjusted
to as low a value as possible by the correct choice of a_s
and $\mathcal{l}_s$. Figures 4.6.8 and 4.6.9 give F_{pi} (that is, for
$F_{st}=0$). For the same example as earlier but with $\mathcal{l}_s = 0.4$
m (jumper) and $a_s = 0.4$ m, the calculation of P_5 gives
6.6, from which $F_{pi} = 2$ kN/subconductor is obtained.

Cases A and C must be considered differently from that
of jumpers (case D). For cases A and C, contact is ad-
vantageous because it results in lower stresses. *Thus
P_5 must be chosen as high as possible.* This is based
on Fig. 4.6.9, which illustrates that values of P_5 in the
critical range between 20 and 50 should be avoided.

The same 245 kV substation as described in section
4.6.2 is used to provide an illustrative example for
bundle pinch parameter analysis. P_{1s} = 35.6, P_5 = 80,
asymmetry not taken into account. Figure 4.6.9 gives a
relative overstress: $(F_{pi}-F_{st})/(m_s^{'} g_n \mathcal{l}_s) = 75$, that is an ab-
solute maximum pinch (per subconductor), namely:

$$F_{pi} = 75 \times 15 \times 10 + 10,000/2 = 16250 \text{ N}$$

Modification of the structural data gives the following ef-
fects:

-   The influence of an increase in a_s of 100%:
    modified subconductor distance = 0.3 m (instead of
    0.15 m). P_{1s} = 35.6/2 = 17.8; P_5 = 47.
    modified normalized tension = $(F_{pi}-F_{st})/(m_s^{'} g_n \mathcal{l}_s)$ =
    170
    which results in an increase in the relative stress
    $(F_{pi}-F_{st})$ of 170/75 = 2.2.

-   The influence of a decrease in a_s by 100%:
    modified subconductor distance = 0.075 m
    $P_{1s} = 2 \times 35.6 = 71$; $P_5 = 154$
    modified normalized tension = $(F_{pi}-F_{st})/(m_s^{'} g_n \mathcal{l}_s)$ =
    40
    which results in a decrease by 40% of the relative
    stress.

- The influence of an increase in subspan length by 50%:
  modified subspan length = 15 m (instead of 10 m)
  $P_{1s} = 35.6$; $P_5 = 116$
  modified normalized tension = $(F_{pi}-F_{st})/(m'_s \, g_n \, \mathcal{L}_s) = 50$
  because $\mathcal{L}_s$ has been increased by 50%, the relative stress $(F_{pi}-F_{st})$ is unmodified (50x1.5 = 75).

- The influence of a decrease in subspan length by 50%:
  modified subspan length = 5 m
  $P_{1s} = 35.6$; $P_5 = 44$
  modified normalized tension = $(F_{pi}-F_{st})/(m'_s \, g_n \, \mathcal{L}_s) = 280$
  Which results in an increase in the relative stress by about (280x0.5)/75 = 1.87.

These examples illustrate that a decrease in subconductor separation is compensated by an increase of P_{1s} and P_5. The overall effect is a limited reduction in bundle pinch tension. Nevertheless, subconductor separation should be chosen as small as possible to maintain separation for ampacity considerations (minimization of mutual heating) and the subspan length should be chosen as long as possible. The combined selection of a_s and $\mathcal{L}_s$ must ensure bundle separation under normal maximum load conditions. In the example, the ratio $\mathcal{L}_s/a_s$ must be greater than 50 to avoid the critical range of P_5. For example, $a_s < 20$ cm and $\mathcal{L}_s > 10$ m. Acceptable design in this specific case might be $a_s = 20$ cm and $\mathcal{L}_s = 10$ m or $a_s = 40$ cm and $\mathcal{L}_s = 20$ m and so on. In practice $\mathcal{L}_s$ is sometimes constrained by dropper connections and a_s must be coordinated.

4.7   Conclusions

A brief summary of the calculation methods which have been described previously in this section is given in Table 4.7.1. The reader should refer to sections 4.2 to 4.6 for more detail.

4.7.1   Parametric Approach

The parametric approach can provide a very good qualitative understanding of the effects of data variations. This approach can illustrate how far a particular design is from the dangerous zones (e.g., high fall of span tension for phase-to-phase effects, and maximum pinch effect due to critical subspan length for bundles).

4.7.2   Recommendation for Use in Practical Design

Chapter 5 gives generalized guidelines for design. The following paragraphs describe practical procedures for the application of the methods of calculation detailed in this section.

Static analysis

Static analysis includes the calculation of stress levels and sags resulting from the tensioning of the flexible conductors. An advanced method for static analysis may be used to facilitate the analysis, giving tension and lengths of cables taking into account the deformation of the cable and of the supporting structures, and the influence of any other connecting hardware.

Evaluation of risks of resonance effects

Calculation of Eigenfrequencies of portal structures and apparatus along with calculation of Eigenfrequencies of cables and insulators and the comparison of these frequencies forms the basis for avoiding resonance problems. The estimation of the frequencies of the cable can be performed using formulae derived from medium methods (these formulae are given in Appendix 3) or from an advanced calculation. The Eigenfrequencies of the structures are more difficult to predict; but advanced methods offer the best chance of success. In this case the accuracy of prediction is strictly dependent on the accuracy of the data used for the calculation.

In both cases, it is necessary to take into account the lack of precision in Eigenfrequencies for a non-linear structure and that caused by uncertainties regarding variations in temperatures, ice loads and imprecise structure data. The reader is referred to [5] for a similar situation with respect to rigid conductors.

If no resonances are possible, the design can continue with simple, medium or advanced methods, depending on the desired level of the accuracy (simple or medium at the first stage, advanced if necessary the final stage). If resonances are possible, the structures may be modified to avoid resonances, and then new calculations are carried out (best solution). Alternatively, the design may be continued with advanced calculations methods. In this case, precautions must be taken to determine the existence of resonances. (Such resonances are clearly evident in time evolution plots.) The use of Simple, Medium, Advanced and Bundle Pinch calculation methods follow the sequences described below:

Simple calculation methods

1. Determine electrodynamic forces.

2. Use simple formulae to evaluate the stress levels in conductors.

3. Calculate the stress levels in structures, adding dynamic stresses to the already calculated static stresses.

4. If the stresses are above acceptable values, the design may be modified and a new calculation carried out or a more advanced calculation may be used to obtain more confidence and more detailed information.

5. A rough and pessimistic estimation of displacements must be done to check clearance.

6. For more detailed studies, such as the evaluation of stresses on apparatus, droppers, etc, use an advanced method.

Medium calculation methods

1. Use medium method calculations to obtain stress levels in conductors and conductor displacements and clearance.

2. Determine stress levels in structures, adding dynamic stresses to the previously calculated static stresses.

Table 4.7.1
Summary of Calculation Methods

Simple Methods	Time-Integrated Medium Methods	Time+Space Integrated Medium Methods	Advanced Methods	Bundle Pinch Effect (medium methods only, for advanced refer to column to the left)
Costs data set preparation is easy	data set preparation is easy	data set preparation is easy	data preparation can be extensive depending on the detail included in the model	data set preparation is easy, except for the above-mentioned problem (spring rate of connected apparatus)
no computer	computer time ±10 s cpu	computer time ±3 min cpu	computer time ±1 hour cpu	computer time 15 s cpu
engineering time: 1 hour	engineering time: 1 hour	engineering time: a few hours	engineering time: 1 week	engineering time: 1 hour
Results only maximum tensions	time-histories of tensions at midpoint of the cables	time-histories of tensions at several points in the cables	time-histories of tensions at each point in the cables, connected hardware and supporting structure	maximum values of pinch tension and compression forces on spacers in one phase
envelope of displacement	time-histories of displacement of midpoint of the cables	time-histories of displacement at several points in the cables	time-histories of displacements at each point in the cables and supporting structure	
Limitations case C, "pure case A" is possible but not recommended	cases C, D and "pure case A" (no droppers)	cases C, D and "pure case A" (no droppers)	cases A, A+B, B, C, D and other arrangements	for phase-to-phase behaviour, advanced method is required
supports are defined by stiffness (no mass)	supports are defined by stiffness (sometimes the first mode is also included)	supports are defined by stiffness and mass giving first mode of vibration	dynamic model of supports with mass, stiffness and accurate modelling	
rough precision, depending on the case, generally conservative	fair precision depending on the case	fair precision, depending on the case	good precision, if all mechanical data are precisely known and no resonance problem arises	fairly good precision (same comment as about data preparation)

3. Evaluate stress levels in conductors, insulators and structures and examine conductor motions.

4. If the stresses are above acceptable values, or if the displacements exceed maximum allowed values, the design may be modified and the calculations repeated. Alternatively, advanced calculations may be used, to obtain more confidence and more detailed information.

5. For more detailed studies, such as the evaluation of stress on apparatus, droppers, etc, use an advanced method.

Advanced calculation methods

1. Design an accurate model (e.g. finite element model) of the structure, including the conductors, insulators, connecting hardware and support structures. This latter component can often be reduced to a linear super-element to save computer time.

2. Calculate the static reference equilibrium position (before short-circuit).

3. Calculate the short-circuit response of the structure, obtaining stresses and displacements at each node in the model, including the cables, supporting structures, apparatus, etc.

4. If the stresses are above acceptable stress levels and/or the conductor displacements exceed maximum tolerated values, the design should be modified and the calculation repeated.

Bundle pinch effect calculation

1. If bundled conductors are used, determine peak tension in conductors due to pinch effect and compression forces in spacers.

2. If the stresses are above acceptable stress levels, the design should be modified and the calculations repeated.

4.7.3 General Remarks

Design of a new structure

Avoidance of resonance problems is desirable for new structure design. If resonances exist, simple and medium calculation methods may not give the correct results. The formulae given in Appendix 4 can be used in preliminary studies to detect resonance problems, and parameter analysis as given in Section 4.6 can facilitate the identification of suitable structural modifications. Parameter analysis given in section 4.6 can be of great help in determining how bus designs can be effectively modified.

Uprating of existing structure

In this case, the use of advanced methods to get less conservative and more accurate results may be justified in comparison with the costs of possible structural modifications.

In some cases, depending on technical requirements and cost/benefit considerations, uprating may be limited to avoid any modification, by accepting the evaluation of the existing structure and fully utilizing the revised rating.

Parametric approach

This qualitative approach can give information concerning the sensitivity of designs to data variations and to provide correcting factors to be applied to calculation results. In this way, the results of data modification can be quickly estimated from curves. Alternatively, the determination of the modification of parameters needed to obtain a desired modification of the structure response can be established. The use of dimensionless parameters facilitates direct interpretation of data interactions.

The choice of an advanced method

Of the computer design methods presently available, advanced analyses offer much more capability than any other calculation method. Droppers, structures, apparatus and so on can be included which, depending on specific circumstances, may be of great importance for the designer. However, in some cases there is considerable sensitivity of the final results to the data used in the calculations. These sensitivities are also apparent in experimental testing. Hence, advanced computer analyses can be applied to reveal these sensitivities and can thus be of assistance for experimental testing.

In future work, designers should obtain a better understanding of the structural details and their influence on the final results. With this experience, attention can be focused on the important details of the data needed for modeling and on the reduction of data requirements. An advantage of advanced methods is that results may be obtained for any member of the structure, for both stresses and displacements, as a function of time. If structural tests are to be carried out, these results can be used as a guide for the selection of locations to be considered for measurements during testing. Advanced methods are not simple, but several computer programs are presently available, which offer the technical capabilities required for analysis of structures with flexible conductors. The designer must be experienced in the use of advanced methods.

As far as bundled conductor systems are concerned, more applications of advanced analyses are needed to validate these methods. This may be a subject for future work.

The development of pre- and post-processors facilitates the application of the advanced analyses by reducing engineering time needed for data preparation and analysis of results which will be improved continually.

Finally it is emphasized that the accuracy of the calculated results should be confirmed for each individual case and that the responsibility for using the results remains with the user.

Thanks to the steady improvements in computer hardware and software, a shift to the more advanced methods has to be expected. For example, some years ago, computer time was considered to be relatively expensive. Today, for the same cost as that for an advanced calculation at that time, it is possible to buy a micro/mini computer capable of performing the calculation in a reasonable time. Moreover, in the near future, designers will have to consider coupling calculation methods and CAD (Computer Aid to Design) systems to reduce the amount of engineer time required to prepare advanced calculation data. Several such applications are currently being introduced.

5 GUIDELINES FOR DESIGN

5.1 Introduction

The mechanical phenomena, which are a consequence of short-circuit currents in substations as presented in Chapter 3 (for rigid conductors) and in Chapter 4 (for flexible conductors), must be considered in design. These phenomena influence the design arrangements and mechanical strength requirements of substation components. In particular, the mechanical strength of apparatus, insulators and conductors and of the supporting structures have to be considered. In addition, in substations with flexible conductors, conductor displacements and the resulting reductions in electrical clearances can be significant. This chapter of the Brochure provides guidelines for design with respect to arrangements, mechanical loads and electrical clearances.

5.2 Arrangements

Typical arrangements used for the physical design of outdoor substations are described in section 1.4. The design of open outdoor substations to withstand mechanical short-circuit effects, indicate the following general considerations.

- In the case of high short-circuit currents, rigid bus systems are relatively easy to design and result in effective substation designs including apparatus connections with lengths exceeding a few meters.

- All possible mechanisms for the initiation of secondary faults should be limited. Therefore, insulator-tube-clamp arrangements for busbars and rigid connections must be designed such that a "domino-effect" will be avoided in the case of a post insulator failure. The possible risk of secondary faults caused by reduced flexible conductor clearances are discussed in section 5.4.

- As far as possible, designs should be flexible, that is, some changes must be possible without greatly influencing the short-circuit design concept (e.g. avoiding resonance).

In the following sections some aspects of the most common arrangements are described.

5.2.1 Special Aspects of Strain Bus Arrangements

In this section, aspects related to increased tension in a bus configuration of type Case A (Fig 1.8) resulting from a short-circuit are discussed. However, for practical design, the final solution must also satisfy other requirements such as limitations caused by conductor displacements (section 5.4) and sag variations, corona and radio noise (RIV) requirements, component standards, requirements associated with other load combinations, control equipment principles and so on. Questions of special interest centre on swing-out tensions and bundle pinch forces.

Swing-out Tensions

Concerning swing-out tensions (F_t and F_f), the reader should note that in certain cases savings may be possible if the maximum short-circuit duration for design purposes is low (for example, 0.3 s). Such a value could be accepted if the appropriate local back-up and breaker failure protection exist. In addition, the static tension and the resulting sag are important design variables. If, for example, the sag is 3.5 m, then the period of the equivalent pendulum oscillation will be:

$$1.79 \cdot \sqrt{3.5} = 3.35 \text{ s (eq. 4.6.8 of section 4.6)}$$

and from the same section, P_3 is obtained:

$$P_3 = \frac{0.3}{3.35} = 0.090$$

From Fig. 4.6.4 the effect of these key design parameters on F_t is apparent. Also as a result of the specified conditions F_f is not expected to be a limiting consideration in this example.

Bundle Pinch Forces

Suitable spacings, between conductors and between bundle spacers, are important factors for the limitation of pinch tensions. Generally the distance between spacers should be as large as possible, while maintaining conductor separation under maximum operating current conditions [22,34,67]. The other possible solution for minimizing bundle pinch tensions, involves the use of a very large number of spacers to ensure that the design is not in the dangerous zone. This solution might be used in special cases for jumpers, connections between apparatus and loops; but is generally not recommended for the majority of applications.

The spacing between subconductors may be wide (for example, 450 mm at 420 kV) for short-circuit levels up to 40-50 kA rms as the resulting low number of spacers reduces costs and corona and RIV problems. However, for higher short-circuit currents, reduced spacing (with the centre-to-centre spacing between conductors ≥ twice the conductor diameter) is preferred.

The use of relatively heavy conductors in a bundle results in several advantages:

- Designs with reduced spacing are facilitated without corona or RIV problems.

- Heavy conductors result in lower pinch forces than a lighter conductors [12].

- Ampacity requirements can be satisfied with fewer subconductors of heavy size which is consistent with reducing pinch tension (section 4.6).

- Static load combinations, including wind, ice and so on, result in lower static tensions if fewer and heavier conductors are used compared with more numerous and weaker conductors.

- Labour costs are reduced and arrangements for terminations, T-connections, and so on, are simpler.

The static tension has very little influence on the pinch tension as indicated in reference [12] and section 4.6. Furthermore, increased static tension allows distances between bundle spacers to be increased, which reduces pinch tension. As a result, the relative increase of pinch tension becomes more significant as static tension is decreased.

In the normal design procedure, preliminary values for static tension are based on static load combinations and clearance requirements resulting from conductor swings. For example, the procedure outlined in [12] is to choose the initial tension such that the sag is in the range of 3% of the span length. Otherwise, if no other requirements exist, a static tension of 5-10 N/mm² is recommended as a first design value. The final and optimal sag is based on further calculations (according to Chapter 4 for the short-circuit load case).

5.2.2 Connections to Apparatus

The following aspects refer to both rigid and flexible connections. In switchgear bays a simple and inexpensive solution is to use the terminals of apparatus as supports. The problem with this is that acceptable dynamic loading limits on these terminals are not very well known. The allowable loading depends on terminal strength, clamp strength, the terminal-connection-clamp arrangement, the strength of supporting insulators, the design of isolator bearings, current paths in the apparatus, dynamic characteristics and so on. In most cases, often as a result of standards, the static withstand strength or the highest static loading, which will not cause maloperation, is given by the manufacturer as well as the safety factor. Higher acceptable loadings in the case of short-circuits can be estimated based on reduced safety factors. If no information is available concerning an acceptable dynamic peak loading, up to 3 kN at the outmost end of the apparatus terminal could be expected and accepted at the risk of the user for circuit-breakers, isolators and current transformer when $I_n \geq 1250$ A.

A safer way to design connections to apparatus for mechanical effects of short-circuits is to use information from tests on realistic apparatus-conductor configurations (for example, according to [38] for isolators). In this way, very difficult configurations, such as pantograph isolators connected to busbars, can also be carefully designed.

Some additional effects to be taken into account include:

- When slack bundled conductors are used as connections (case C, Fig. 1.8), it is very important that the subconductors be spaced closely in order that they can touch each other effectively in the case of a short-circuit [57,65].

- For case C arrangements, a sag of about 8% of the span length will usually lead to acceptable results [12].

- In the case of rigid conductors connected to apparatus with fast operating mechanisms, (for example, circuit-breakers) the influence of switching forces should also be considered because the short-circuit forces and switching forces might appear simultaneously.

- Depending on the apparatus-conductor configuration and phase-to-phase distances, the relative influence of angle forces may require consideration in calculating terminal loadings. The method described in Appendix 2 can be used to estimate angle forces associated with right angle bends.

5.2.3 Droppers to Apparatus

Droppers connecting a span to apparatus below (Case A + B illustrated in Fig. 1.8) is an important but difficult arrangement from the design point of view. Forces on the terminals of the connected apparatus, as well as the displacements of droppers must be considered for the range of temperatures appropriate for the span. The required position and length of the droppers to satisfy static and dynamic demands must be determined. As well, designers must recognize the increased tendency of droppers to swing if the droppers are connected to isolators having terminals which are journaled in bearings. Calculations for specific dropper connections are presently possible using advanced methods. Therefore, no parametric studies for the purpose of finding general or optimal solutions have been done.

One possible design concept is to limit the motions of the span by the use of V-string insulators and by choosing a suitable static tension. The droppers in such arrangements can be designed so that the risk of flashover, as well as of violent dropper stretching due to span motions, can be avoided [66]. In some countries, a minimum bending radius at the bottom of the dropper is recommended (10-50 cm, depending on the conductor). In other cases, the use of common sense or engineering judgement is the preferred approach (Fig. 5.2.1). When mutual influences of droppers may be significant, a specific check is necessary (Fig. 5.2.2). Figure 5.2.3 shows how a dropper connection to a span can function as a flexible spacer in the span.

5.2.4 Design of Jumpers

The relatively large sag of jumpers (Case D Fig. 1.8) and the proximity of earthed structures frequently necessitates the use of means for restricting jumper displacement to avoid secondary faults and conductor damage. Suitable means include additional weights, V-string insulators for the span, vertical insulators, pinch-limiting spacers or combinations of these solutions. Vertical insulators are effective, especially vertical V-string or post insulators. The disadvantage is that more insulators and their associated leakage paths are introduced, which increases the risk of insulator flashover especially in contaminated areas.

By using V-string insulators to support the span, the jumper terminations are nearly fixed and jumper movements can be easily calculated using a simple pendulum model.

Single insulator strings and additional jumper weights provide an effective and cheap design, which also minimizes the number of insulators (Fig. 5.2.4). The swing of the span insulator strings during short-circuits is an additional complicating influence which makes jumper movement difficult to predict.
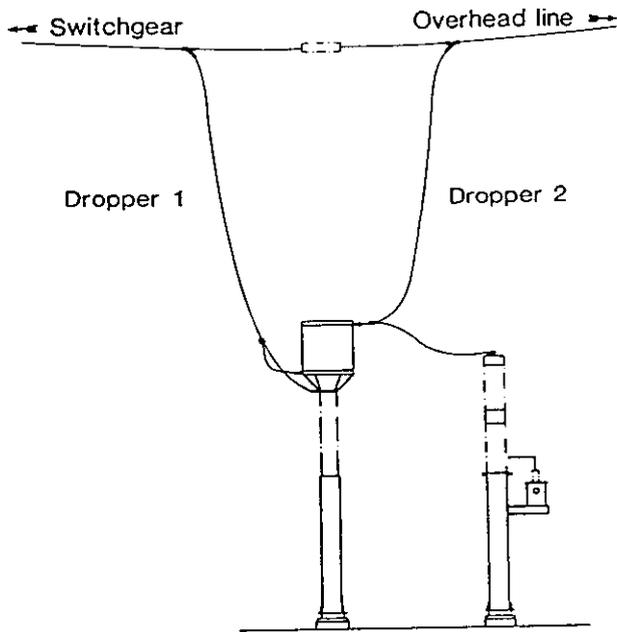
Fig. 5.2.1   Dropper 1 has the highest tension and is connected to the top of the post insulator supporting the line trap. In this way no terminals of the apparatus will be overstressed
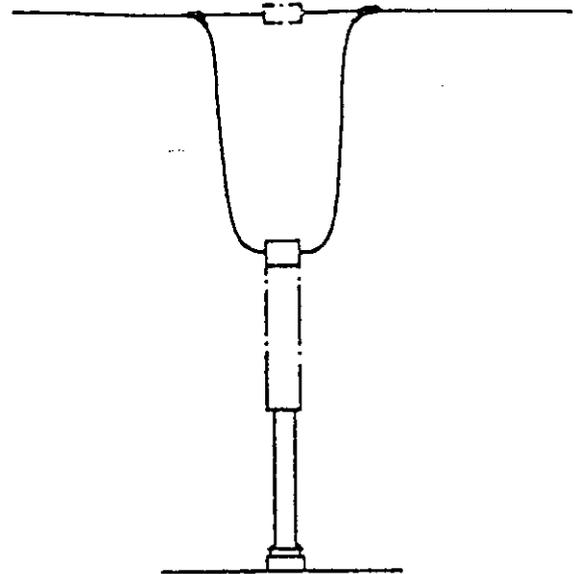
Fig. 5.2.2   Two parallel droppers with narrow spacing cause short-circuit load components which must be considered. This example refers to the connection of a current transformer
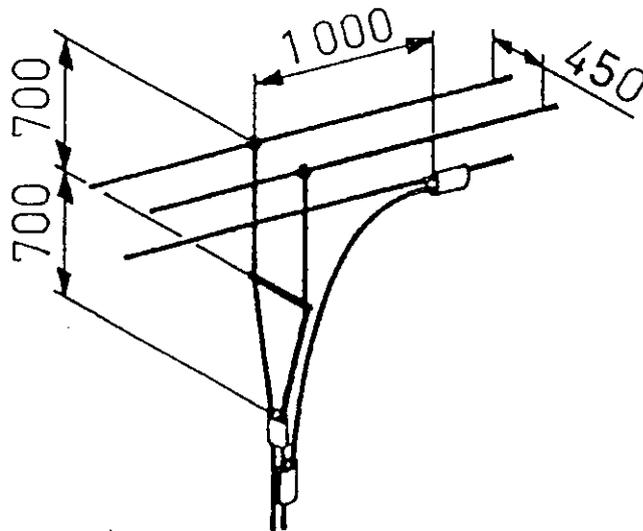
Fig. 5.2.3   The connection of a dropper to a span can be arranged such that it has the effect of a flexible spacer in the span

73
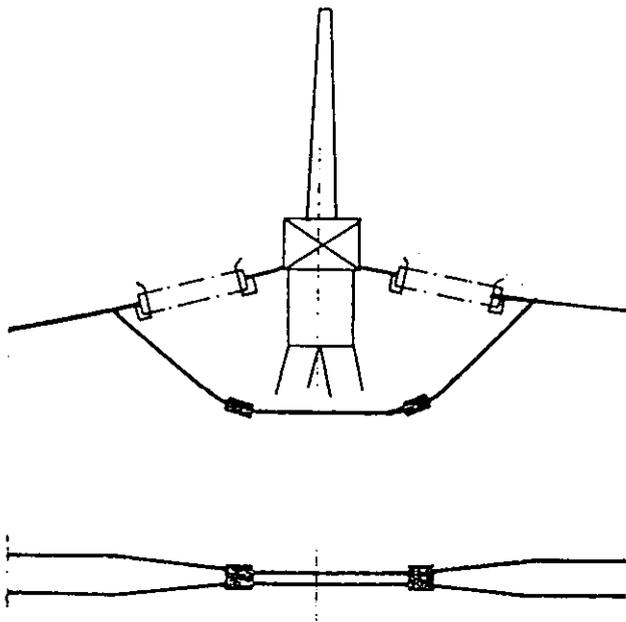
Fig. 5.2.4   Additional jumper weights introduced to limit conductor swing can be so arranged that the pinch effect can be reduced and some extra clearance obtained due to reduced conductor size. As an example 2x 40 kg has been used in many cases

5.3   Loads

Conductors in outdoor switchyards are not only influenced by short-circuit forces, they may also be affected by other external forces such as wind, ice and earthquakes. Mechanical design must be based on several loadcases which include the relevant load combinations. Some of these exclude short-circuit forces, and they must be based on local conditions, which will not be discussed here.

Regarding the combination of short-circuit forces with the environmental forces, there are differing opinions [18,21,28]. However, there are several indications that short-circuit forces need not be combined with wind and ice:

-    The probability that ice and snow coatings can withstand vibrations due to a short-circuit is very low. Furthermore, experience indicates that ice and heavy snow loads are much less frequent on substation conductors than in other applications.

-    Wind load and short-circuit load both vary in time, independently of each other. As well, the direction of wind varies. There are no mathematical procedures available for a true or reasonable combination of short-circuit and wind loads. (Although probabilistic methods may be possible.) Therefore, no equivalent static load-case can be formulated and short-circuit test results cannot be transferred to any other loading condition.

-    The short-circuit loading may depend on very special effects which cannot easily be combined with other loads. Examples include the consequences of unsuccessful autoreclosure which may be of considerable importance in the case of rigid conductors or in relation to pinch- and conductor-fall sequences in the case of flexible conductors.

-    The magnitudes of the conductor weight and wind load depend on rigid or flexible conductor characteristics but are roughly of the same order. The short-circuit load is the decisive factor for design in modern installations for $I_k \geq 31.5$ kA, $U_n \leq 420$ kV.

Based on these reasons, designers typically accept short-circuits as a separate load case (particularly if the short-circuit calculation gives results on the safe side) for the mechanical dimensioning of flexible as well as rigid busbars and connections.

5.3.1   Conductors and Insulators

Loads on Insulators

The calculated dynamic force acting perpendicular to the top of a post insulator, F_d for rigid conductors and F_t, F_f or F_{pi} for flexible conductors, must not exceed the minimum failing load. Limits on acceptable loading as low as 70% of the minimum failing load, (that is the loading used for routine tests of post insulators) are preferred by some users. If the force is acting at a point higher than at the top of the post insulator, (this is the situation for rigid buses and in some special applications) a force which gives an equivalent moment must be considered. The critical point is not necessarily the insulator base.

For insulator strings of the cap and pin type, allowance for 65% of the electromechanical failing load (porcelain) or mechanical failing load (glass) is reasonable. The basis for this is that insulator units are type tested with that load to verify the withstand mechanical strength in case of a disk crack.

Conductor Stress

As a consequence of the theory of plastic deformation, the calculated tubular-conductor stress must not exceed 1.35 - 1.50 times the yield point ($R_{p0.2}$) for bending depending on the ratio between conductor wall thickness and diameter [39].

Flexible conductors in strain bus systems are not expected to be significantly overstressed in the case of a short-circuit. However, in exceptional cases, a check to ensure that 70% of the breaking load will not be exceeded, is recommended. The reason for this recommendation is that some margin is necessary to take into account reduced conductor strength in the anchoring points. Some users prefer a lower allowable stress (~55% instead of 70%). Subconductors in slack bundle connections may be permanently deformed at the spacers in the case of a short-circuit if the design is unsuitable.

Loads on Conductor Hardware

Connectors, clamps, spacers and other arrangements for terminating conductors are directly exposed to the full force amplitudes generated by short-circuits. Therefore, their dynamic loading will not be reduced by the filtering

74

effects which reduce the effective loadings for supporting structures, rigid bus post insulators and so on (Fig. 5.3.1). For this reason, a factor of 1.5 is taken into account in the calculations, if the maximum tension in the conductor is determined according to formula 4.2.6. Also, the use of conductor hardware with a sufficient degree of toughness is recommended. For connection clamps manufactured from aluminum alloy, type test specification of the percentage elongation after fracture according to [44] is recommended, (for example, A_5 = min 2% for a separate cast-to-size piece). For a machined test piece manufactured from connector parts, a minimum of 1% seems reasonable for a cast piece and a minimum of 5% for a wrought piece. Other components such as tension clamps, spacers, and so on, should have a good toughness value down to the lowest temperature which may be experienced.
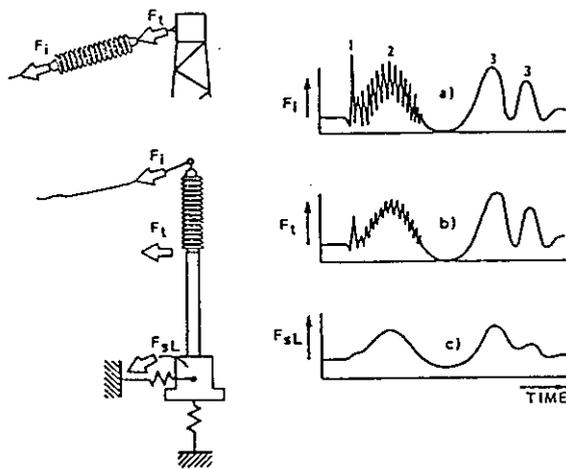

Fig. 5.3.1 Typical time histories of tensile forces caused by short-circuit loads on flexible conductors
  a) Tensile forces in the flexible conductors and insulator strings
    Peak 1 - bundle pinch effect
    Peak 2 - span motions within the short-circuit duration
    Peak 3 - span motions subsequent to the short-circuit
  b) Smoothed tensile forces applied to the structures
  c) Soil loading further reduced by foundation inertia

Short-circuit design recommendations for connection clamps include:

- The connectors must not apply excessive forces to apparatus terminals.

- Connection tongues of connectors should be so arranged that the effective section modulus for the case of a short-circuit loading is as large as possible.

- Short-circuits must not give rise to permanent deformation, cracks or failure of the connectors. However, permanent deformation of flexible parts can be accepted if such deformation does not affect the function of the connectors.

- Permanent deformation, cracks or failures must not occur in connectors for bundled stranded conductors as the result of conductor clash in the event of a short-circuit.

- Electric current must not be carried by the mechanical bearing parts of tube connectors, whether during normal operation or during short-circuits. Arcs must not be established during short-circuits.

- Tubes should be so supported that it is not possible for a direct impact to arise between a tube and terminal in the event of a short-circuit.

- Connectors should be so designed that tubes cannot fall out of them in case of a short-circuit.

The short-circuit withstand capability of conductor hardware, and especially of spacers and connection clamps, should be verified by tests under relevant conditions.

5.3.2 Supporting Structures

Introduction

There exist two main kinds of supporting structures in outdoor substation:

1. portal structures for strained conductors, typically consisting of two vertical towers and a horizontal beam, and

2. pillars supporting the post insulators for rigid bus or apparatus.

These structures are made usually from steel, latticed, bolted or welded or solid webbed, and erected on concrete foundations [15]. Their design is typically carried out by civil engineers.

Based on national or company standards, all substation supporting structures are designed for existing and/or probabilistic combinations of different loads: dead loads, conductor tensile loads, thermal loads, ice, wind, reaction forces from circuit breakers [28]. These loads appear during normal substation operation and therefore adequate factors of safety are usually available. However, the structures may also be subjected to the exceptional load caused by short-circuit current.

With regard to this relatively rare phenomenon, the dimensioning of pillar type structures for post insulators is usually based on the guaranteed breaking strength of the insulators, which is needed to meet the short-circuit current load. Reduced safety factors, approximately 1.00, are considered for supporting structures.

On the other hand, portal structures have generally not been designed to withstand the full dynamic forces caused by short-circuit currents. For example, the current German Standard [41] states that according to their experience, strength calculation of portal structure subjected to short-circuit forces is not necessary. This recommendation for design was justified by the following:

- there have been no recorded destructions of structures,
- short-circuit current levels have been moderate in the past,
- there was a lack of verified calculation methods.

75

However at the present time, the majority of companies which responded to the CIGRE SC23 inquiry [28] take into account short-circuit forces in structure design. This is justified by the increasing levels of short-circuit currents, substation security requirements and economic pressures. Thus, the following basic strategy seems to be reasonable at the present state-of-the-art:

"First design structures for standard loads, later verify the structures for short-circuit current loads."

In the calculation procedures described in Chapter 4, the problems of analysis of supporting structures are associated with:

- the selection of a general mechanical model for calculation of mechanical effects of short-circuit currents in the substation, and in

- the stress analysis which concludes all calculations.

The problem of stress analysis of foundations for substation supporting structures working under short-circuit conditions has not been considered by WG 23.02 to date. However, adequate engineering precision can be obtained using the general routine approach. That is, the foundations are subjected to loads transmitted through the supporting structure. These loads, which have been deprived of high frequency oscillations (Fig. 5.3.1c) due to the filtering influence of the insulators and supporting structures, are known from the global dynamic analysis described in Chapter 4.

Support structure modelling

The properties of the supporting structure have an essential influence on the short-circuit current mechanical effects in the system: conductors-insulators-structures (CIS). For example, stiff structures generally lead to higher forces and the more elastic structures result in reduced forces (section 4.6). Consider now the problem of modelling the supporting structures, (that is, how to formulate a calculation model which is adequate for the real structure). The modelling is oriented to two goals:

- calculation of short-circuit current forces in which the whole CIS model is considered,

- stress analysis in which the supporting structure alone is involved.

In the most advanced methods of analysis, these goals are achieved at the same time. A real HV or EHV substation usually presents a complex arrangement (Fig. 1.7). However, for the purpose of analysis, it is necessary to select an appropriately reduced, but representative structure, usually a single portal frame, considering also the influence of other connected structures. Furthermore, depending on the level of calculating method assumed (Chapter 4), such a reduced supporting structure may be represented by:

- a spring stiffness only
- spring stiffness and mass
- a representative structure (usually portal) composed of beam or truss elements

For advanced methods, the full and detailed model of such a structure is required. Such selected structures, are modelled according to the routine methods of the theory of structures. Structural data reduction is either embedded in the method used (SAMCEF, ADINA) or

should be done by separate programs (STANAN). In simple cases data preparation is done directly by design engineer.

In each case, the relevant stiffness K, damping C and mass M characteristics must be determined in order to use these data later (Chapter 4) in the matrix equation 4.5.1. This equation describes the dynamic behaviour of the supporting structure. Usually damping effects are neglected, that is, C = 0, and as a result of the small displacements K = constant, M = constant. The only non-linearity then is caused by the conductor forces R (u,t), which depend on displacement u and time t. In the simplest static case, equation 4.5.1 reduces to

$$k u = R_{max} \varphi \qquad (5.3.1)$$

where φ is an assumed dynamic factor, k, u and R, are scalar values.

Short-circuit loads

The well known typical time history of the tensile forces in flexible conductors, caused by short-circuit loads is presented in Fig. 5.3.1a [70]. From the point of view of the civil design engineer, two characteristic types of forces are noted (Fig. 5.3.1):

- the bundle pinch maximum (1), acting as a short but high impulse force (representative frequency: 100 Hz)

- the motion maxima during (2) and subsequently (3) to the short-circuit duration with relatively slow variation in time (representative frequencies from about 0.5 to 3 Hz).

The force acting on the structure is presented in Fig. 5.3.1b and on the foundation in Fig. 5.3.1c. The filtering effect of insulators and of the supporting structure is indicated. The bundle pinch forces appear during all types of short-circuits (one, two- or three-phase) at almost the same time. For practical calculations, a simultaneous and equal pinch force in all phases can be assumed for three-phase faults which is usually the worst case.

The swing and fall forces are different in the case of two- or three-phase faults. In the first case, large forces appear only in the two faulted phases. The force in the third unfaulted phase, caused by structure deflection, is of a much lower value. In the case of a three-phase fault, the large forces appear in the outer phases, which experience significant displacement; the middle phase experiences only restricted movement and therefore the force in this phase is much smaller. Thus, considering the stress in the beam of the portal, the case of a two-phase short-circuit (one outer phase and the middle phase) is taken as the worst case, (that is, the largest bending moments will be produced).

In the case of a substation of lower voltage level (for example, 123 kV) the forces caused by phase-to-phase influences may be predominant; but for higher voltages (for example, 420 kV) usually the bundle pinch forces prevail.

The short-circuit current forces always act together with the dead loads. However, in some countries additional preliminary loads are added, (for example, wind load or ice load (section 5.3)). The selection of load combinations depends on the local climate conditions [28].

76

As presented in Chapter 4, short-circuit current forces may be calculated using a range of different methods (simple, medium, advanced) and also some combinations of these methods, if their accuracy is reasonable. In the most advanced methods a whole system is analyzed at the same time. Thus short-circuit current forces and stress analysis in a structure are obtained together. However, in other cases the output of short-circuit current force calculations for insulators serves as an input to the stress analysis of a supporting structure. The following forms for that input may be used:

- the complete time history of a variable force
- the peak value and the duration of a representative impulse
- a single value force, (usually the maximum force)

In the third case, no time characteristic of forces acting on the structure is available, so dynamic analysis is not possible and static analysis should be used as an approximation.

As discussed in earlier sections, there exists the danger of resonance between the supporting structure vibrations and the excitation force originating from the conductors. Therefore, the frequency of conductor movement should be checked to ensure that it is sufficiently different from the Eigenfrequency of the structure. Thus, a detailed or simplified analysis of the modes of vibration of the supporting structure (portal) is suggested. Usually only the structural vibrations of the first mode need be considered. The Eigenfrequency of portal structures is in the range of 1 to 15 Hz. (Lower values for EHV substations, higher values for HV substations.) Pillar Eigenfrequencies are usually of the order of several Hz to tens of Hz. The stiffness of portal structures is in the range from 10^5 N/m (for flexible structures) to 10^7 N/m (for very stiff structures). The pillar support structures have stiffness from 10^5 N/m to 10^7 N/m, which will be affected by foundations, such that the average may be 10^5 N/m (section 4.2).

Stress evaluation

Stress analysis is performed using routine methods for the full representative structure. In the case of the most advanced methods of analysis, the steel structure is fully represented (see Chapter 4). As a result, the full time history of stresses, $\sigma = \sigma(t)$, in the required elements of the structure is obtained. However, such direct dynamic analysis is relatively time consuming, expensive and usually not necessary.

Alternatively, stress analysis is obtained indirectly if the structure is considered to be loaded by short-circuit forces obtained from a preliminary conductor, insulator, structure model. For advanced methods the results may be almost as good as those obtained from the direct approach.

Stresses σ_i in an element i of cross-sectional area A_i are evaluated according to

$$A_i \, \sigma_i = K_i \, u_i + M_i \, \ddot{u}_i \qquad (5.3.2)$$

where i numerates stress components. ·

The first term represents the "static" and the second, the "dynamic" components of σ_i. Except for the very rapidly changing loads (for example, large pinch forces), the last term is much smaller than the first one and is often neglected.

If the analysis of the conductor, insulator, structure system has been performed using a medium method, rather simplified methods of dynamic stress analysis are used. The stresses caused by phase-to-phase forces and those caused by pinch effect may be treated separately because they are usually assumed to be independent of each other as they generally occur at significantly different times (reclosure excluding).

The common design practice in the case of phase-to-phase forces is to assume that they are static forces and consequently to consider portal structures to be subjected to two equal static forces (corresponding to the two phases having significant displacement) applied on the crossarm.

The dynamic character of pinch forces is taken into account in particular countries using various approaches. In principle it may be done by addition of appropriate inertia forces. In the Canadian design practice, the pinch forces are treated as impulsive load represented by an equivalent static load [69]. In Swedish practice, design factors, defined as the relation between experimentally measured maximum stress in the structure members due to pinch force and the stress obtained from a static solution under this force taken as the static load, are introduced. Typically, the value of this design factor is in the range of 0.7 - 1.1, but it does not exceed 1.4. This procedure is recommended for well-known structure types.

The admissible stress for short-circuit load must satisfy general regulations and usually is assumed to be higher than ordinary loads. Therefore, the effective safety factor is lower. In common engineering practice for short-circuit loading (in exceptional cases), the safety factor is typically about 1.3, while for normal loads, the safety factor is about 1.5.

In the case of short impulsive loads, for which large stress rates occur, structural steels experience a delayed plastic flow phenomenon which results in a temporary increase of strength (yield point) [87]. For example, in the case of load changing with a frequency of 100 Hz, steel strength increases by about twice. This phenomenon provides an additional justification for assuming allowable stresses higher than for static loads.

Recommendations

Obviously the more advanced methods of analysis have the potential to produce the most detailed and accurate results; but the results obtained are more expensive. The basic practical question for the design engineer is, "Is it necessary to apply advanced methods or are the simple methods adequate?".

The answer depends on many factors, such as designer experience, access to appropriate computer software and hardware, availability of detailed structural data and so on. Overall experience with stress analysis of supporting structures working under short-circuit current conditions is relatively limited. Consequently, no detailed recommendations can be given here. However, the following general pattern may be suggested:

- Simple methods may be applied either for structures and current levels for which design practice and service conditions and experience have proven to be sufficient or for those cases that have been verified against confirmed advanced methods and models.

- In the case of significant change in the type of structures, their parameters or short-circuit current level, and where the cost of failures or overly conservative design is significantly greater than the cost of detailed design methods, the advanced methods are strongly recommended.

5.4 Conductor Displacement and Temporary Air Clearances

5.4.1 Introduction

Multiphase short-circuit currents generate interphase forces which result in phase conductor displacements. In rigid bus systems, the resulting displacements are relatively minor and do not significantly reduce the phase-to-phase clearance. However, for flexible bus systems the phase displacements can be very significant depending on the bus configuration, the short-circuit current magnitude and duration. The mechanics of the phenomenon are described in Chapter 4 of this brochure. This section is concerned primarily with means to design for temporarily reduced clearances and with the consequences of the temporarily reduced clearances in terms of the capability of buses to withstand the applied voltage stresses following short-circuits. The ability of buses to operate successfully following short-circuits is an important factor for substation and system reliability. Secondary bus faults can also have a severe effect on power system operations and stability. For line entrance buses the impact of secondary faults may be relatively small; however, for main bus sections the impact would likely be severe.

5.4.2 Conductor Displacement

In substations with low tensioned spans without droppers or other restricting arrangements, conductor displacements are usually a more serious problem than other short-circuit effects, especially if the short-circuit power is not high. Figure 5.4.1 illustrates the movements of a typical 130 kV, 36 m strain bus in the cases of normal fault tripping (duration 0.1 s) and back-up tripping (duration 0.5 s). The conductor movements are complicated in general, but they are particularly complicated for the case of back-up clearing. Conductor behaviour varies significantly depending on physical and short-circuit parameters. For normal fault clearing, or for configurations or short-circuit levels resulting in relatively modest displacements, pendulum models may be used to represent the conductor movements. Representation of the more violent motions obtained for back-up clearing or in situations involving relatively light conductors and high fault currents, more elaborate modelling is required. Figure 5.4.2 presents, in a simplified way, the conductor movements in two typical cases: namely two and three-phase faults.

The three-phase fault causes the outer phase conductors (phases L1 and L3) to swing outwards from their normal position, whereas the middle phase (phase L2) experiences a very restricted motion. After interruption of the fault, phases L1 and L3 swing back. During the two phase fault, for example between phases L1 and L2, both conductors swing initially outwards then inwards in synchronism. For relatively short duration faults, the maximum swingout angle for the outer phases is nearly the same for two or three-phase faults, as the forces at the rest position are nearly the same. Therefore, the affected phase conductors approach one another more
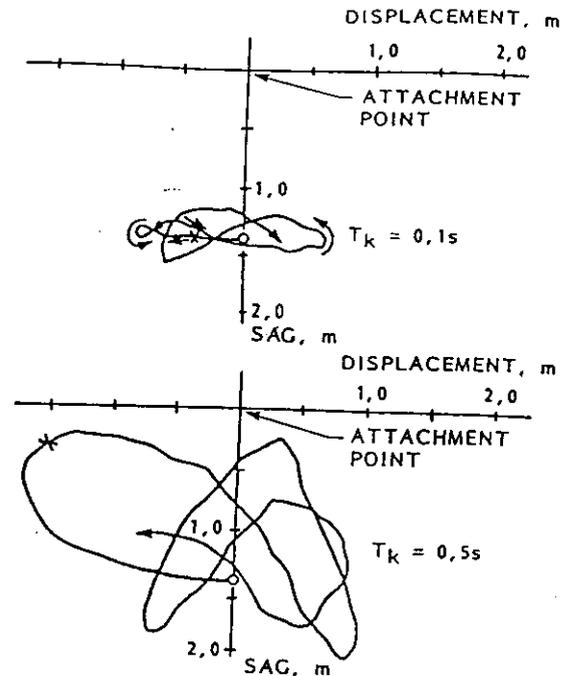

Fig. 5.4.1 Movements of the mid-point of a span resulting from a two-phase short-circuit test (36 m span, 130 kV, single insulator strings, phase separation 4.0 m, sag of insulators and conductor 1.45 m, conductors 2×910 mm^2 Aℓ, I$_k'$ = 40 kA, X = short-circuit interruption)
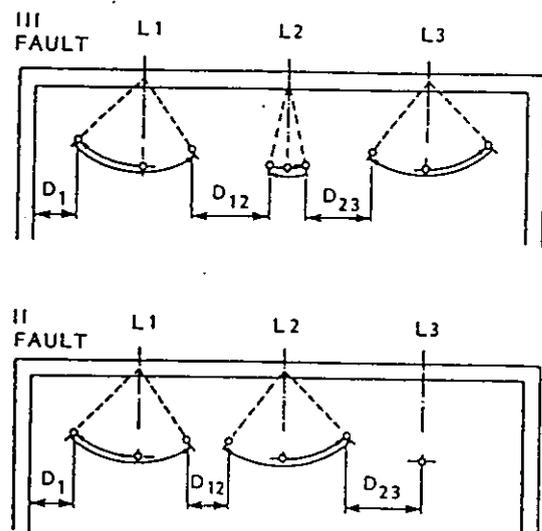

Fig. 5.4.2 Simplified phase conductor motions caused by multiphase faults

78

closely in the case of the two phase fault. Hence, designers should consider the two phase fault as the decisive case for clearance calculations.

Referring to Fig. 1.8, the displacements of span A and also of jumper D are of interest. Concerning the jumper D, the approach of the outer conductor (phase L1) to the structure is also important. In the case of bundled conductors, the effective swingout angles may also be affected by subconductor swings within the bundle configuration. Also, under certain circumstances, jumpers consisting of multiple conductors can be thrown vertically against the girder due to pinch forces. Although clearance problems for jumpers are potentially more severe than span clearance because of the proximity of the jumpers to the grounded structures, the presence of the support structures provides relatively straightforward means to limit jumper displacement. In this regard, the use of rigid post insulators and jumper connections, the provision of stabilizing weights, the use of V-string insulator arrangements and the application of inter-phase insulating links provide effective means for limiting jumper displacement and thereby circumventing clearance problems.

Three minimum distances D_1, D_{12} and D_{23} are important for air insulation considerations as illustrated in Fig. 5.4.2. If a typical swing frequency of approximately 0.5 Hz. is assumed, it is clear that the air distances D_1 and D_{23} appear in the first second of conductor swing and the distance D_{12} usually not earlier than one second after fault initiation. The minimum distance D_{23} for two-phase faults (mutual deflection of only one phase conductor), which appears also in the first half of the conductors swing cycle, is considerably greater than the distance D_{12} and is not decisive.

The philosophy of avoiding secondary faults must be based on control equipment principles and substation design. For example, consider the one line diagrams shown in Fig. 5.4.3 and assume an overhead line fault at L just outside the substation. The overhead line circuit breaker CBL has high speed autoreclosure capability as presented in Fig. 5.4.4 (discussions concerning autoreclosure are valid only as far as three-phase, high-speed autoreclosure is concerned). Also assume that there is no delay between the two relay systems in the case of local back-up and that the high speed autoreclosure is blocked if normal fault clearing does not occur.

Possible sequences regarding the affected conductor movements are shown in Fig. 5.4.5. Figure 5.4.5 I, illustrates the behaviour of the conductors outside CBL for normal fault clearing. Figure 5.4.5 II, illustrates the motion of bus spans for normal clearing and Fig. 5.4.5 III, illustrates the conductor motion when the failure is cleared by breaker failure protection or by remote back-up protection. In this example, unsuccessful high-speed autoreclosure is not expected to be the decisive dimensioning factor for the displacement of energized bus spans because of the common relations between swing frequency and dead time interval. Of greatest interest are movements of the spans affected by the short-circuit current when the circuit breaker operates normally (Fig. 5.4.5 I and II). The primary fault just outside the substation, might cause a secondary fault after the reclosure at point 1 (Fig. 5.4.3) at the bus (point 2b) as well, if the conductor swing out at these locations is big enough. A secondary fault could also appear at 3 resulting in the loss of a main feeding transformer.
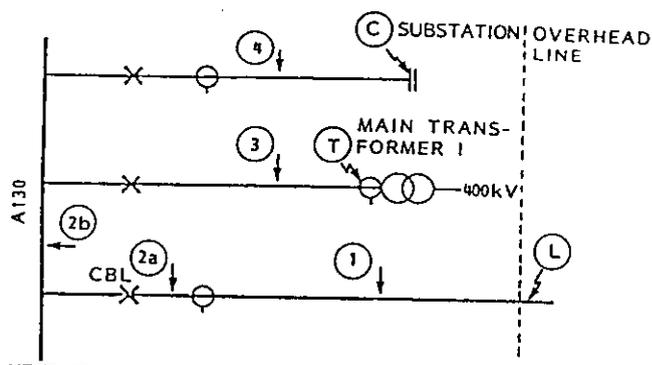

Fig. 5.4.3 Possible secondary fault locations (1, 2a, 2b and 3) in a substation in the case of a primary overhead line fault at L. Primary faults at C and T are also discussed.
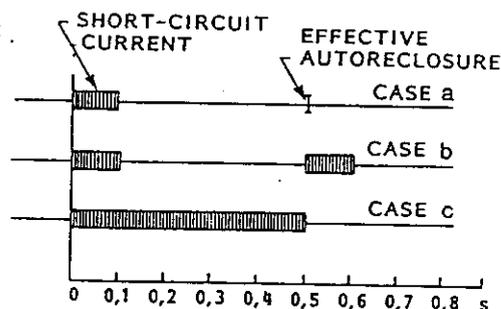
Fig. 5.4.4 Examples of time sequences of fault current for line faults.
a: fast clearing and subsequent successful reclosure
b: fast clearing, unsuccessful reclosure and ultimate clearing
c: failure to clear by relevant circuit breaker or protection and subsequent clearing by relay or breaker back-up protection
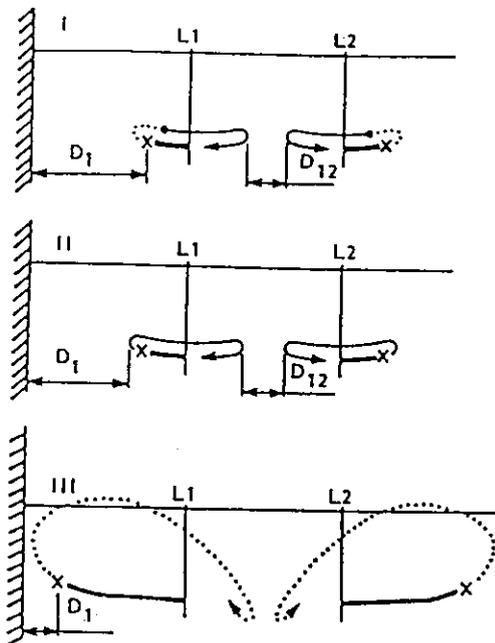
LEGEND:

——— SHORT-CIRCUIT LOADED
········· DISCONNECTED
——— ENERGIZED

X CURRENT INTERRUPTION
• HIGH SPEED RECLOSURE

Fig. 5.4.5 Movements of conductors at possible
secondary fault locations in the case of a pri-
mary line fault at L (Fig. 5.4.3).
I: refers to locations 1 and 2a (Fig. 5.4.3) and
to Fig. 5.4.4 case a
II: refers to locations 2b and 3 and to case a
III: refers to case c and to locations 1, 2a and
2b

A secondary fault in a substation constitutes a very
serious disturbance from the operational point of view
because it causes an enlargement of the de-energized
network area. In particular, it is very disturbing for the
operation of the network if a secondary flashover results
in a main bus fault. A secondary fault (unsuccessful
autoreclosure) outside the current transformer (for exam-
ple point 1) is not particularly disturbing because it will
affect only one outgoing overhead line. From an opera-
tional point of view, the case of fault tripping via breaker
failure or remote backup protection (Fig. 5.4.5 III) is
equivalent to a bus fault, as the fault is connected to the
bus via the nonoperative circuit-breaker until the bus is
disconnected from the network. Following clearing,
clashing of non-energized conductors or contact be-
tween a jumper and a steel structure is harmless. How-
ever, risk of flashover between affected conductors and
any other circuit (for example, conductors in a neigh-
bouring bay or at another level) cannot be accepted. In
the case of faults initiated at C or T in Fig. 5.4.3, the
situation will not be significantly worse as a result of ex-
cessive displacements of connecting spans (possible
secondary fault locations 3 and 4). In considering
secondary fault risk as a whole, knowledge of deflec-

tions, possible overvoltages and consequences of
flashovers is necessary. The overvoltages which might
appear must be considered consistent with the
autoreclosure sequence (high speed as described
above or delayed as is also common). Concerning the
possible consequences of flashovers, in addition to the
system effects described above, possible conductor
damage should be considered. Under many situations,
the electromagnetic and thermal forces acting on flash-
over arcs cause the arc to move rapidly along the bus
resulting in relatively minor damage. However, in some
configurations and particularly for high current arcs, it is
possible that an arc will establish a stable root point, in
which case, significant conductor damage can result. To
avoid fully the risk of flashover and subsequent conduc-
tor damage in all situations may not be possible.

Several approaches have been established to calculate
clearances between phases of bus systems under short-
circuit conditions. These include several models, of
varying sophistication, based on the pendulum and finite
element analysis. All of these techniques are similar or
identical to the methods used to calculate swing ten-
sions, with the provision built into the programs to calcu-
late the bus clearances from the geometrical relation-
ships between adjacent phases under multiphase fault
conditions.

5.4.3 Temporary Air Clearance Evaluation

Electrical clearance in substations, under normal condi-
tions, has been well treated in the insulation coordination
literature and by standards [16,23,37,92]. Both
deterministic and probabilistic methods have been
recommended depending on specific circumstances and
specific minimum clearances are given for the various
operating voltage levels. Unfortunately the use the
recommended procedures for the temporarily reduced
clearances in substations following short-circuits typical-
ly causes problems for substation design. For many ex-
isting substations the recommended clearances have
not been provided for several reasons, not the least of
which is the fact that methods to calculate minimum
clearances under short-circuit conditions have only
recently been available. For new substation designs,
provision of the general recommended electrical
clearances for short-circuit conditions would lead to ex-
cessively large phase spacings and significantly in-
creased substation costs. The reluctance of substation
designers to design for standard clearances under short-
circuit conditions is supported by the typically excellent
performance of existing substations which have not
been designed on this basis. The reasons for this have
not been quantified; but the generally conservative na-
ture of the standard clearances, the relatively infrequent
occurrence of high-current multiphase short-circuits and
the extremely low probability of lightning or switching
overvoltages during the period when the buses are
swinging are contributing factors.

Deterministic Methods

A number of deterministic and empirical approaches to
deal with this problem have been suggested. One ap-
proach is to base temporary air clearances on the mini-
mum permissible regulating gap between protective ar-
restors, as a function of the insulation level chosen for
the insulators [1,92]. For example on a 230 kV system,
a regulating gap of 900 mm, transformed to phase-to-
phase with about a 10% margin gives a minimum phase-
to-phase clearance of 1750 mm. Although this is sig-
nificantly less than the standard clearances it is consid-
ered conservative for temporary air clearance purposes.

For the purpose of illustration, Table 5.4.1 gives examples of temporary air clearances for various system voltage levels. Although the values indicated in this table are typical of those reported in the literature, the reader should note that specific geometrical factors and system conditions (switching surge and impulse levels) can require significant modification of these values. An approach, based on IEC Standard 71 [37] recommended minimum clearances, is described in the following paragraphs.

TABLE 5.4.1
Proposed Temporary Air Clearances

Highest System Voltage U_m (kV)	Clearance D_1 (mm)	Clearance D_{12} (mm)
123	450	390
145	522	458
245	850	824
420	1550	1558

The withstand capability of air insulation is determined by physical processes and cannot be controlled by substation designers. The withstand capability, as a function of phase-to-phase clearance, is illustrated in Fig. 5.4.6. This curve is based on Table VI of IEC 71-3 for the range 2.4 m to 7.9 m, and the well known Gallet expression [94] for the lower portion of the graph. If the designer uses the peak system switching overvoltage with this relationship, a minimum clearance, typical of static phase-to-phase clearance, will be obtained. An alternative approach, which is appropriate for short-circuit conditions, is to estimate only the specific switching surges generated by the switching sequence followed under short-circuit conditions. The switching sequence will vary somewhat depending on utility practice; however, a typical, normal switching sequence (with bus clearance implications) is given below.


○ DATA FROM IEC 71-3   —— GALLET FORMULA
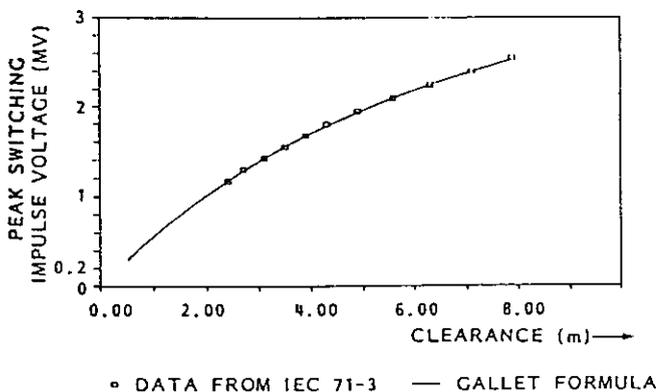
Fig. 5.4.6 Minimum phase-to-phase clearance based on IEC 71-3 Table VI and extrapolated to lower voltages and clearances using the Gallet formula [94]

1. A multiphase fault occurs on one of the lines terminating at the substation of interest

2. The fault is cleared in less than 0.1 s by the primary protection. The risk of secondary faults on the line entrance bus (up to the clearing breakers) is very low because these buses are de-energized before significant phase motion or reduction in phase-to-phase clearance occurs. Main bus sections, which remain energized throughout the disturbance, must sustain normal maximum line potential and are subjected to surges produced by reclosing as discussed in the next paragraph.

3. After some time, a single circuit breaker is closed to re-energize the line. The timing of the reclose is an important factor. Although the risk of secondary flashover is relatively low immediately after the initiating fault because phase displacements are relatively small at that time, the risk obviously increases if reclosing occurs during the bus swinging period when phase-to-phase clearance may be significantly reduced. Because of the typical mechanical swing frequencies of bus systems, and the fact that the initial movements of the faulted phases increases clearances, relatively high-speed reclosing (before 1 s approximately) will typically result in satisfactory operation. Similarly, slow reclosing (later than 10 s) will likely be satisfactory because phase displacements will have attenuated before reclosing occurs. Based on mechanical swing frequencies of typical bus systems, reclosing in the 1.5 s to 2 s interval would result in the greatest risk of coinciding with the bus phases being in the minimum clearance position.

The switching surge associated with reclosing varies depending on system and equipment related aspects including: the possible use of closing resistors, the direction of energization, the number of lines terminating at the associated substation and so on. If the line is energized from the substation in question, the surge will be applied to the whole substation and its magnitude will depend on the system configuration at the substation. Such surges are typically a small fraction (n/(n-1) where n is the number of lines terminating at the substation) greater than the normal maximum system voltage at the substation. If the line is energized from the remote end, the surge will be applied to a limited portion of the substation in question (line entrance up to open circuit breakers). The surge may be of greater magnitude in view of the impedance discontinuity at the open end of the line. The consequences of secondary faults also depend on the direction of energization; but fault levels will generally be lower because only one end of the line is energized.

Under abnormal conditions the switching sequence is as follows:

1. A multiphase fault occurs on one of the lines terminating at the substation of interest.

2. The fault is not cleared by the primary protection but is cleared in the interval 0.1 s to 0.5 s. by back up protection.

81

3. Because of bus inertia and the fact that initial displacement of the faulted phases is such that clearance is increased, the impact of delayed clearing on line entrance bus is minimal. After the line is cleared by back up protection, automatic reclosing is generally blocked. In this case the bus will remain de-energized and phase-to-phase clearance is not a problem. Although reclosing and associated surges will eventually occur, by that time the bus will be in its static position.

For main bus or bus sections which remain energized throughout the disturbance, withstand of normal maximum system voltage is required, but switching will typically not occur during the bus swing period.

Through a careful analysis of the switching sequence as outlined above the designer can estimate the specific switching surge level for the substation in question under fault conditions. This will likely result in reduced surge levels and from Fig. 5.4.6, lower clearance requirements.

Probabilistic Methods

As suggested in [37], deterministic methods may be suitable for the lower voltage classes where the cost of the excessive conservatism inherent with these methods is not significant. However, for high-voltage and extra high-voltage substations, a probabilistic procedure adapted for short-circuit conditions is recommended [64]. This procedure is described in the following paragraphs.

The IEC Standard 71-2 "Insulation Coordination Part 2 Application Guide" [37] provides a good description of the use of probabilistic techniques for the design of air clearances under normal conditions. This procedure is illustrated in Fig. 5.4.7. Rather than establishing a maximum surge magnitude and minimum air gap withstand strength and separating these with a suitable safety factor, the method includes the specific statistical variability of these parameters in the analysis. On the left of the figure, the probability density distribution of surge magnitudes is sketched. This curve illustrates the probability of specific surge magnitudes. In practice, this curve is obtained from switching surge analysis programs, such as the Electromagnetics Transients Program (EMTP) for switching surge distributions, or from lightning discharge current data (modified by the surge impedance of the system being designed) for lightning surge distributions. The curve on the right is the cumulative distribution of air gap strength. This is a plot of the probability of breakdown of the gap as a function of surge magnitude. This curve is obtained by measurement for specific air gap distances and specific electrode configurations. Considerable data are available for standard electrode configurations and these have been used as a basis for recommended clearances in the IEC Standard.

The region where these two distributions overlap is the range of surge magnitudes for which failure is possible. In this region surge magnitudes can exceed the air gap withstand in which case air gap breakdown occurs. If the distribution of surge magnitudes is statistically independent of the distribution of air gap strength, the probability of breakdown can be calculated by the convolution integral shown in the figure. If the distributions are

Normal, the probability of breakdown is Normally distributed and can be obtained from standard Normal probability tables (F(z) giving the cumulative probability x≤z) using the formula:

$$z = \frac{X_S - X_s}{\sqrt{s_S^2 + s_s^2}}$$

Where:

X_S = the mean of the strength distribution
X_s = the mean of the stress distribution
s_S = the standard deviation of the strength distribution
s_s = the standard deviation of the stress distribution

Uncertainty regarding the specific shapes of the distributions, particularly in the tail regions, can be a cause of concern. Two approaches are possible. The first is to attempt to obtain by analysis and/or testing sufficient statistically significant data to provide reliable representation of the distributions in the low probability regions. The second is to assume somewhat conservative distribution functions (for example the Normal distribution function) with conservative statistical parameters for these functions. Although the latter approach is not as desirable as the former, it is preferred over the deterministic approach. If the distributions are not Normal, alternative fairly straightforward methods are available to perform the convolution integral. Working the process in reverse, given an acceptable probability of breakdown or risk level, it is possible to calculate standard clearances for specific electrode configurations and voltage levels. This is the basis for the recommendations provided by the IEC Standard on insulation coordination [37].
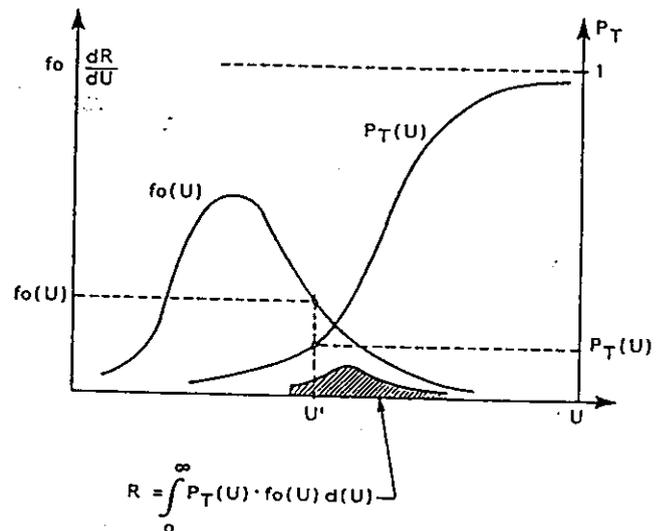

Fig. 5.4.7 IEC 71 Probabilistic insulation co-ordination method

The same approach, as recommended by the IEC Standard, can be used for the problem of temporary clearances following short-circuits in substations with flexible conductors. As described under deterministic methods, during the period of swinging motion following multiphase faults, the electric stress on the temporarily reduced air gaps can vary considerably. For example, switching surges produced by system operations following a fault, may be applied to the bus system. For main bus sections, which remain energized throughout the disturbance, these surges must be considered and factors such as the number of lines connected to the substation and the direction of energization of lines are significant factors. Line entrance bus sections (related to the faulted line) are de-energized during most of the swinging motion until re-energization is attempted. In this case, the timing and the direction (that is if the line is energized from the remote end or from the end terminating in the substation in question) are critical factors, not only in regard to the magnitude of the stress applied, but also to the magnitude of fault current should a secondary fault occur. The probabilistic formulation of this problem must therefore deal with both the variability of the physical clearance produced by faults of variable magnitude and duration, and the variability of the electric stress imposed on the air gaps. Figure 5.4.8 illustrates in general the steps required for this calculation.

The probability of breakdown as a function of clearance calculation is illustrated in the upper left of the figure. This calculation is identical to that recommended by the IEC Standard [37] as described in the previous paragraphs. In this case the switching surge distribution is shown. As described, this distribution is determined by calculation for the specific substation in question. For the problem of temporary air clearances under short-circuit conditions, the probability of lightning being coincident with the disturbance and specifically with the occurrence of the bus conductors being in the minimum clearance position, is extremely low. (Based on 6 faults per year and a significant bus swinging duration of 30 seconds per fault, the probability of lightning during the swinging period is approximately 2×10^{-6}. This is based on statistical independence between multiphase faults and lightning occurrences and the very conservative assumption that the bus is in the minimum clearance position throughout the swing period.) Therefore, lightning impulse conditions need not be included. On the right of this illustration are some typical air gap strength distributions for a range of air gap distances. As before, these distributions are obtained by measurement for air gap electrode geometries representative, as close as possible, of the bus configuration in the substation of question. Standard data are available for this purpose [42].

PROBABILITY OF BREAK-
DOWN FOR A SPECIFIC
SWITCHING SURGE DIS-
TRIBUTION AND GAP

PROBABILITY DENSITY
DISTRIBUTION OF
CLEARANCES GIVEN BY:

$p(c)\ dc = p(l)\ dl$

$p(c) = \dfrac{p(l)}{\left|\dfrac{dc}{dl}\right|}$

PROBABILITY OF BREAK-
DOWN FOR THE SPECIFIC
SWITCHING SURGE DIS-
TRIBUTION AS A FUNC-
TION OF CLEARANCE

CONVOLUTION GIVES THE
PROBABILITY OF FAILURE

INCREASING
FAULT DURATION
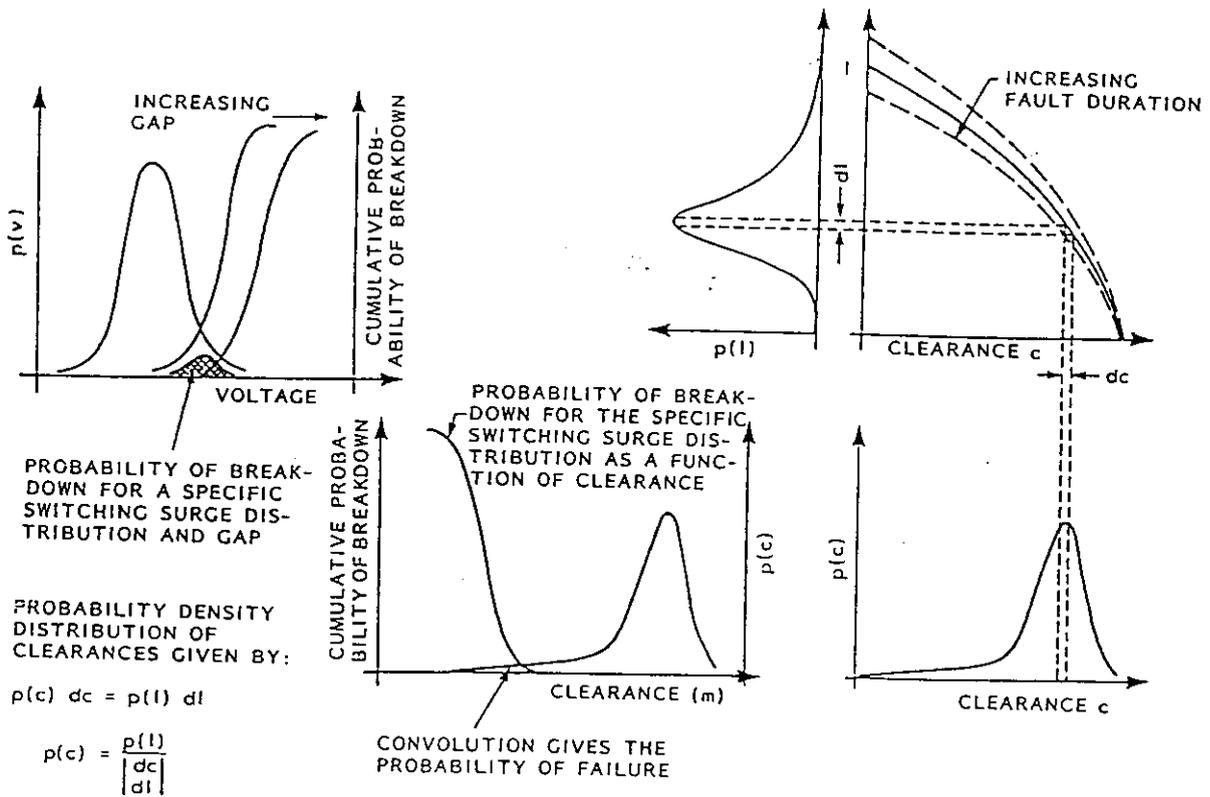
Fig. 5.4.8 Probabilistic formulation of the flexible conductor bus clearance problem

As with the IEC procedure, the probability of breakdown for any specific gap distance is calculated by convolving the stress and strength distributions. When this is done for a range of gap spacings, a plot of the probability of breakdown for the specific switching surge distribution of the substation in question as a function of clearance is obtained. This curve is shown on the left of the illustration at the bottom center of the figure. The curve on the right of that illustration is the probability density distribution of specific clearances under short-circuit conditions. This curve is obtained by the following the procedure illustrated on the right of the figure.

Starting in the upper centre of the figure the illustration plotted on its side is the probability density distribution of short-circuit current magnitudes. This curve is obtained by methods analogous to those used to calculate the switching surge distribution described previously. As with the switching surge distribution, this curve is obtained specifically for the substation in question. The curve illustrates the typical expectation that high magnitude short-circuit currents have relatively low probabilities. Methods to calculate this distribution for specific systems have been developed and have been described in the literature [29,73,76]. Monte-Carlo based methods offer the capability to handle highly complex systems and the best accuracy, but at some cost in terms of computational effort. Simplified analytical methods offer ease of use but at the expense of accuracy for complex systems. The selection of methods depends on the specific application, its complexity, computational effort permitted, and the accuracy required.

The short-circuit current magnitude probability density distribution is transformed into the probability density distribution of clearances using the relationships between short-circuit current and clearance. These relationships, which are shown in the illustration in the upper right corner of the figure, are based on calculations of flexible bus displacements described in Chapter 4. The simple transformation relationship for a given fault duration is shown in the figure. The fault duration is an important parameter as illustrated in the figure. The distribution of short-circuit durations is generally somewhat system dependent; but data are available from power system operations records. Inclusion of this parameter, complicates the calculation only slightly in practice since the transformation of p(I) into p(c) is accomplished with simple numerical methods which can easily accommodate the additional clearing time distribution. The result is the clearance probability density distribution shown in the lower right of the figure and replotted on the right of the illustration in the middle of the bottom of the figure. The convolution of this function with the previously described probability of breakdown as a function of clearance curve gives the overall probability of breakdown under short-circuit conditions. The calculation, as described, makes the conservative assumption that the electric surge stress occurs at the instant at which the conductors are at their minimum clearance position. Although analysis of the probability of coincidence of the mechanical swing with the application of surges is theoretically possible, it adds a degree of complexity which is probably not required for most applications.

5.4.4 Conclusions

The process described above provides a means to calculate the probability of bus failure under short-circuit conditions which is identical in principle and result to the recommendations of the IEC Standard. Thus this technique can be used to design bus systems having the same risk of failure under short-circuit conditions as under the normal static clearance conditions. In the case of normal static conditions, all types of electric stresses and surge conditions must be considered, and as well, all of these stresses are applied to all parts of the substation insulation. In the case of temporarily reduced clearances under short-circuit conditions, the types of surges which must be considered are reduced in view of the low probability of lightning surges coincident with the bus being at its minimum clearance position, and as well, the number of air gaps affected by temporary reduced clearances and exposed to stress is greatly reduced in comparison with the normal case. Thus, although the normal clearances as recommended by the IEC Standard 71 are not accepted, the risk of flashover and the method for its calculation are consistent with IEC Standard 71 [37].

The generalized procedure described above is complex and detailed application requires considerable effort and expense. Therefore, the use of the detailed procedure is only justified in those cases where the cost savings in terms of substation design, operational and construction costs exceed the cost of carrying out the detailed studies. In many practical situations, the process may require simplifications. Simplification is best carried out in the context of the process as described. In this case, consideration of the probability distributions for specific cases may reveal that they can be reduced, with little effect on the accuracy of the overall result, to deterministic quantities. For example the switching surge stress distribution can typically be considered as a deterministic value corresponding to the maximum steady state ac voltage on the substation bus system if the number of lines terminating at the substation bus is relatively large and the lines are energized from the substation in question. Similarly, the fault current magnitude probability density distribution may be considered to be a deterministic value equal to some fraction of the maximum fault current available at the substation bus [43]. In this case, the fraction should be selected carefully taking into account the location of the substation in question with respect to major generating stations. Simplified analytical methods are useful for this purpose. Simplifications such as these can have a significant effect on the convolution calculations and result in much reduced calculation effort. Care must be taken to ensure that when simplifying assumptions are made, that they are conservative. The more conservative simplifying assumptions are made, the closer the result will approximate the normal static clearances recommended by the IEC Standard and the less likely an economically acceptable design will be obtained.

6 GENERAL CONCLUSIONS

Based on international experience, failures of substations, caused by the mechanical effects of short-circuit currents, have been extremely rare. However, design engineers must ensure that substation designs meet the extreme requirements associated with short-circuit conditions. This can be achieved through the use of the calculation methods and criteria provided in the previous sections, and in exceptionally complicated cases through laboratory testing.

The authors hope that this Brochure will help engineers ensure safe and economical design. The Brochure cannot serve as an exhaustive engineer's handbook; but it should help in developing better understanding of the phenomena and in finding proper design solutions.

In general, rigid bus designs may be preferred for substations exposed to high short-circuit currents because their design methods are simpler and more reliable. However, flexible designs may be preferred in many cases, in spite of the difficulty and uncertainty in calculation methods, for their relatively low cost and their ability to withstand earthquakes.

The problems of short-circuit current effects in open air substations have been described in the brochure as completely as possible. However, not all of the problems presented here are at the same level of development. Some problems have already been formulated as IEC recommendations, others are fully understood but not developed to standardization stage, while others have not yet been definitely solved. In the latter case, simply defined design guidelines cannot be provided. These problems may be the subjects of further study work and this brochure may serve as the starting point.

L'expérience internationale montre que les défaillances de postes à haute tension aux effets mécaniques de court-circuits sont extrêmement rares. Néanmoins, l'ingénieur concepteur doit s'assurer que le poste peut supporter les sollicitations maximales dues au court-circuit. Cet objectif peut être atteint par l'utilisation des méthodes de calcul et des critères décrits dans les chapitres précédents ou par des tests de laboratoire, dans des cas particulièrement compliqués.

Les auteurs espèrent que cette brochure apportera un soutien précieux à l'ingénieur soucieux d'une conception fiable et économique. La brochure ne doit pas être considérée comme un manuel d'ingénierie complet, mais comme une aide pour acquérir une meilleure compréhension des phénomènes et effectuer des choix judicieux lors de la recherche d'une solution adéquate.

On préfèrera en général utiliser des jeux de barres rigides pour les postes potentiellement exposés à des courants de court-circuit élevés, du fait de méthodes de conception plus simples et plus fiables. Néanmoins, l'emploi de connexions souples pourra s'avérer intéressant dans de nombreux cas, en dépit du degré plus élevé de complexité et d'imprécision des méthodes de calcul, vu le prix de revient relativement faible de ce type de connexions et leur aptitude à supporter les sollicitations sismiques.

Les auteurs se sont efforcés de décrire dans cette brochure les problèmes relatifs aux sollicitations mécaniques de court-circuit d'une façon aussi complète que possible. Cependant, tous les problèmes ne sont pas au même niveau de développement. Certains ont déjà fait l'objet de recommandations CEI, d'autres ont été analysés et compris sans atteindre le stade de la standardisation, enfin, quelques-uns restent actuellement partiellement posés. Dans ce dernier cas, il est difficile de donner une ligne de conduite simple, et il y a lieu de poursuivre l'analyse. Cette brochure pourra alors servir de point de départ.

7 REFERENCES

CIGRE Working Group 23.02 Publications

1. Palante, G. "Study and Conclusions from the Results of the Enquiry on the Thermal and Dynamic Effects of Heavy Short-circuit Currents in High Voltage Substations. Appendix III: Cakebread, R.J. Electrodynamic stress in the design of rigid conductor arrangements. Appendix IV: Hosemann, G., Deter, O. Methods of calculating the forces to which support insulators are subjected during short-circuits." *Electra*, No. 12, 1970, pp 51-89.

2. Deter, O., Gibbon, R.R., Hosemann, G., Stein, N. "Measurement of Short-circuit Stresses on Rigid Conductor Busbar Systems and Comparison of Test Results." *Electra*, No. 30, 1973, pp 35-54.

3. Palante, G. "Behaviour of Rigid Conductors and Their Supports Under Short-circuit Conditions. Comparison of Calculated and Measured Values." CIGRE 1976, Report 23-10.

4. Hosemann, G., Tsanakas, D. "Calculated and Measured Values of Dynamic Short-circuit Stresses in a High-Voltage Test Structure with and without Reclosure." *Electra*, No. 63, March 1979, pp. 147-161.

5. Hosemann, G., Tsanakas, D. "Dynamic Short-circuit Stress of Busbar Structures with Stiff Conductors. Parameter Studies and Conclusions for Simplified Calculation Methods." *Electra*, No. 68, January 1980, pp. 34-64.

6. Adami, H., Batch, B.A. "Aeolian Vibrations of Tubular Busbars in Outdoor Substations." *Electra*, No. 75, 1981, pp. 99-120.

7. Lehmann, W., Lilien, J.L., Orkisz, J. "The Mechanical Effects of Short-circuit Currents in Substations with Flexible Conductors. Numerical Methods - Computer Approach." CIGRE 1982, Report 23-08.

8. Matagne, E., Orkisz, J. "Computer Aided Approaches to Evaluate the Mechanical Effects of Short-circuit Currents in Substations with Stiff Busbars." *Electra*, No. 88, 1983, pp. 115-130.

9. Gauffin, L., Lilien, J.L. "Mechanical Effects of Short-circuits in Substations with Strain Bus Systems - Medium Complexity Calculation Methods." CIGRE Symposium Brussels, 1985, Report 330-01.

10. Fraikin, R. "Mechanical Effects of Short-circuit Currents in Substations with Strain Bus Systems - Comparison Between Calculation Results." CIGRE Symposium Brussels, 1985, Report 330-05.

11. Landin, I., Gauffin, L., Fraikin, R., Ford, G.L. "Mechanical Effects of Short-circuit Currents in Substations with Strain Bus Systems - A General Description." CIGRE Symposium Brussels, 1985, Report 330-06.

12. Dalle, B., Ford, G.L. "Behaviour of Bundled Conductors in Substations Under High Short-circuit Currents." CIGRE Symposium Brussels, 1985, Report 330-08.

13. Lilien, J.L., Brokamp, L. "Mechanical Effects of Short-circuit Currents in Substations with a Strain Bus System - Parameter Analysis and Simple Method of Calculation." CIGRE Symposium Brussels, 1985, Report 330-07.

Other CIGRE Publications

14. Buter, J., Markworth, E., Richter, F. "Field Tests in a 220 kV Network of High Short-circuit Power." CIGRE 1968, Report 13-09.

15. Nartowski, Z. "Foundations, Supporting Structures of Steel and Prefabricated Concrete." *Electra*, No. 34, 1974, pp. 75-100.

16. Parizy, M.J., Muller, M.H.G., "Insulation Characteristics of Substations with a Nominal Voltage up to 765 kV." *Electra*, No. 39, March 1975, pp. 31-46.

17. Ford, G.L., Cenanovic, M., Craig, D.B., Huestis, H.W., Short, T.A. "Studies Leading to Increased Current Ratings for Substation Buses." CIGRE 1976, Report 23-04.

18. Deter, O., Lehmann, W., Rameil, W., Stein, N., Terhorst, A. "Influence of the Very High Load and Short-circuit Currents on Outdoor Substation Design for the Highest system Voltages of the German Interconnected Grid." CIGRE 1976, Report 23-05.

19. Thomas, Y., Pigoet, P., Benistan, G., Kupiec, M. Casale, J.P., Roussel, P., Coullot, J. "Influence of an Increase in Short-circuit Currents on the Design of 400 kV Installations of the Electricité de France." CIGRE 1976, Report 23-06.

20. Hosemann, G., Tsanakas, D. "Dynamic Stress in Substations Taking into Account the Short-circuit Currents and Electromagnetic Forces due to Non-simultaneous Faults." CIGRE 1978, Report 23-04.

21. Cakebread, R.J., Brown, H.J. "Integrated Mechanical Design Loading for Open Type EHV Substation Structures and Equipment." *Electra*, No. 60, October 1978, pp. 31-55.

22. Adami, H., Leppers, P.H., Lilien, J.L. "The Behaviour of Spacerless Bundles due to High Load Current. Experimental Results and Theoretical Calculations." *Electra*, No. 90, 1983, pp. 23-43.

23. Thione L. "Evaluation of the Switching Impulse Strength of External Insulation" *Electra* No. 94 May 1984 pp77-95.

24. Ketola, A., Maaskola, J., Hiironniemi, E., Komulainen, R., Uusipaikka, U. "Disconnector Dimensioning and Comprehension of Tests." CIGRE 1984, Report 13-05.

25. Neumann, C., Suiter, H., Kugler, R., Rees, V., Voss, V. "Design and Testing of 420 kV Pantograph Disconnector for Rated Withstand Current of 80 kA/200 kA." CIGRE 1984, Report 13-11.

26. Stein, N., Bauer, E., Brandt, E., Dannheim, H., Lehmann, W., Meyer, W., Pietsch, K. "Dynamic Behaviour and Strength of High Voltage Substation Post Insulators Under Short-circuit Loads." CIGRE 1984, Report 23-12.

27. Stein, N. "Strain/Stress Concentrations In Insulators due to Sheds." CIGRE Proceedings 1984, Vol. 1, Group 23, pp. 45-46.

28. Arhomaa, A. "Mechanical Design Criteria of Outdoor Substations." CIGRE Symposium Brussels, 1985, Report 310-01.

29. Stegemann G. and F. Berger "Stochastic Determination and Evaluation Concerning Loads of Short-Circuit Current in Electric Energy Transmission Installations" CIGRE Symposium Brussels 1985, paper No. 310-02

30. Adami, H., Vos, C.W.M. "Short-circuit Tests and Measurements of Mechanical Stress on Full-scale Sections of 420 kV Outdoor Substations." CIGRE Symposium Brussels, 1985, Report 330-03.

31. Kind, R., Neumann, C. "Dynamic Short-circuit Stress of 380 kV Busbar Arrangement with Flexible and Stiff Conductors." CIGRE Symposium Brussels, 1985, Report 330-09.

32. Tsanakas, D. "Dynamic Stress in High-Voltage Structures by Short-circuits of Short Duration." CIGRE Symposium Brussels, 1985, Report 500-01.

33. Hosemann, G., Lehmann, W., Landin, I. "Calculation of Short-circuit Currents and Their Mechanical and Thermal Effects - State of International Standardization." CIGRE Symposium Brussels, 1985, Report 500-02.

34. Leppers, P.H., Lilien, J.L. "The Behaviour of Spacerless Bundles. Attraction and Release Values Arising from High Load Currents." *Electra,* No. 81, 1982, pp. 91-116.

International and National Standards

35. IEC Publication 168. Tests on Indoor and Outdoor Post Insulators of Ceramic Material or Glass for Systems with Nominal Voltages Greater than 1000 V, 1979.

36. IEC Publication 38. IEC Standard Voltages. Geneva, 1983.

37. IEC Publication 71 "Insulation Co-ordination Part 1 Terms, Definitions, Principles and Rules, Part 2 Application Guide, Part 3 Phase-to-Phase insulation Co-ordination Principles, Rules and Application Guide", 1976 & 1982.

38. IEC Publication 129. Alternating Current Disconnectors and Earthing Switches. 1984.

39. IEC Publication 865. Calculation of the Effects of Short-Circuit Currents. Geneva, 1986.

40. IEC Publication 909. Short-circuit Current Calculation in Three-Phase AC-Systems, Geneva, 1987.

41. DIN 57103/VDE 0103. Feb 1982. Mechanical and Thermal Short-circuit Strength of Electrical Power Installations. German Standard/VDE Specification. Beuth Verlag, Berlin VDE Verlag, Berlin.

42. Canadian Standards Association "Electric Strength of Insulation" CSA Standard CAN3-C308-M80 Section 4.4.2, 1980.

43. VDE-Standard 0141/7.76. VDE Specification for earthing in installations for rated voltages above 1 kV ac.

44. ISO-6892: Metallic Materials Tensile Testing, 1984.

Other Publications

45. Lehmann, W. "Elektrodynamische Beauspruchung Paralleler Leiter." *ETZ-A,* 1955, Vol. 76, pp. 481-488.

46. Atwood, A.W. *et al* "Dynamic Behaviour of a 220 kV Dead-end Suspension Bus During Short-circuit." Transactions of AIEE, Vol. 81, Pt III, June 1962, pp. 153-169.

47. Lehmann, W., Sieber, D. "Mechanische Kurzschlussbeanspruchungen durch Leitungsseile in Schaltanlagen." VDE-Fachberichte 24, 1966, VDE-Verlag Berlin, pp. 149-153.

48. Manuzio, C. "An Investigation of Forces on Bundle Conductor Spacers under Fault Conditions." IEEE Transactions on PAS, Vol. 86, No. 2, 1967, pp. 166-184.

49. Attri, N.S., Edgar, J.N. "Response of Busbars on Elastic Supports Subjected to a Suddenly Applied Force." *IEEE Transactions on Power Apparatus and Systems,* PAS-86, 1967, pp. 636-650.

50. Serizawa, Y. "Behaviour of Dead-end Suspension Double-conductor Bus During Short-Circuit." *The Journal of the Institute of Electrical Engineers of Japan,* Vol. 87, No. 11, November 1967, pp. 100-111.

51. Schäffer G. "Kurzschlusskräfte von Zweierbündelleitern in Schaltanlagen" Elektrotechnik und Maschinenbau Vol. 86 1969, pp. 357-361

52. Borhaug, J.E., Cambias, S.M., Devey, J., Thompson, H.A. "The Response of Substation Bus Systems to Short-circuit Condition. Part I: A comparison of design methods. Part II: Measurements on the transverse vibration of selected station post and pin-cap insulators." *IEEE Transactions on Power Apparatus and Systems,* PAS-90, 1971, pp. 1698-1718.

53. Logunov, L.P. "On the Impact Strength of Porcelain Support Pin Insulators." *Soviet Power Engineering,* No. 12, 1974, pp. 729-734.

54. Deter, O. "Calculation of the Dynamic Short-circuit Stress in Substations with Stiff Conductors and Elastic Supports." *Brown Boveri Review*, 62, 1975, pp. 99-104.

55. Adami, H., Ykema, Th. "Aeolian Vibration of Tubular Busbars in Outdoor Substations and Its Damping." *Journal of Applied Science and Engineering*, A,1 (1975/76), pp. 259-280.

56. Hosemann, G., Tsanakas, D. "Beitrag zur analytischen Berechnung der dynamischen Kurzschlussbeanspruchung von Schaltanlagen." *ETZ-A*, 97, 1976, pp. 493-498.

57. Mathejczyk, M. and Stein, N. "Kurzschlussseilzüge enggebündelter Doppelseile in Schaltanlagen." *ETZ-A*, Bd 97, 1976, pp. 323-328.

58. Gröber, R. and Stein, N. "Beitrag zur dynamischen Kurzschlussbeanspruchung in Schaltanlagen. *ETZ-A*, 1976, Vol. 97, pp. 293-298.

59. Landin, J.I., Lindquvist, C.J., Bergström, L.R., Cullen, G.R. "Mechanical Effects of Short-Circuit Currents in Substations." *IEEE Transactions on Power Apparatus and Systems*, Vol. PAS-94, No. 5, September/October 1975, pp. 1657-1665.

60. Olszowski, B., Orkisz, J., Waszczyszyn, Z. "Calculation of Mechanical Effects in EHV Outdoor Substations at Short-circuit Currents." *Revue Electrotechnique*, 12, 1977, pp. 275-285.

61. Tsanakas, D. "Dynamische Kurzschlussbeanspruchung von Hochspannungsschaltanlagen mit biegesteifen Leitern." *ETZ-A*, Bd. 98, 1977, pp. 399-403.

62. Stefanik, W., Votta, G.A., Stipcevich, J.M. "Short-circuit Tests on a 3-Phase, 230 kV Rigid Bus Assembly." IEEE Summer Meeting, Mexico, July 1977.

63. Tsanakas D. "Erhöhung der dynamischen Kurzschlussbeanspruchung infolge erfolgloser Kurzunterbrechung." *ETZ-A*, 99, 1978, pp. 86-88.

64. Ford G.L. and Srivastava K.D. "Probabilistic Short-Circuit Design of Substation Bus Systems" IEEE Winter Power meeting New York 1978 Paper No. A 78 211-5.

65. Stein, N., Hermann, B. "Kurzschluss-Seilzüge in Schaltanlagen." *Elektrizitätswirtschaft*, 78, 1979, pp. 179-186.

66. Engel, B. "Mechanische Beanspruchung von Teilleiterseilen in Anlagen nach einem Kurzschluss." Elektrizitätswirtschaft 78, 1979, pp. 186-189.

67. Awad, M.B., Huestis, H.W. "Influence of Short-circuit Currents on HV and EHV Strain Bus Design." *IEEE Transactions on Power Apparatus and Systems*, PAS-99, 1980, pp. 480-487.

68. Hosemann, G. "Stand der Ermittlung von Kurzschlussbeanspruchungen elektrischer Anlagen mit baudynamischen Methoden." Elektrotechnik und Maschinenbau Vol. 97, 1980, pp. 248-252.

69. Craig, D.B., Ford, G.L. "The Response of Strain Bus to Short-circuit Currents." *IEEE Transactions on Power Apparatus and Systems*, Vol. PAS-99, 1980, pp. 422-434.

70. Lehmann, W. "Kurzchlussbeanspruchungen in Anlagen mit Leiterseilen." Symposium der Forschungsgemeinschaft für Hochspannungs und Hochstromtechnik e.v., Report 1-248/12, 1981, pp. 347-356.

71. Oeding, D., Scheifele, J., Komurka, J. "Calculation of Short-circuit Currents in High Voltage System." 7th Power Systems Computation Conference, Lausanne, 1981.

72. Tavano, F., Tomassi, A. "Sbarre di Stazione a 420 kV: Comportamento Meccanico in Corto Circuito. Analisi Teorica e Risultati Sperimentali." *L'Energia Elettrica*, No. 10, 1981, pp. 421-432.

73. Ford G.L. and S. Sengupta "Analytical Methods For Probabilistic Short-Circuit Studies" Electric Power Systems Research, Vol. 5, 1982, pp13-20.

74. Tsanakas, D. "Einfluss der Zeitverläufe der elektromagnetischen Kurzschlusskräfte auf die dynamische Beanspruchung." *ETZ-A*, Bd. 4, 1982, pp. 365-368.

75. Stauch, G., Bohme, H. "Schwingungsverhalten von Stromleitanordnungen in Mittelspannungsanlagen bei Kurzschluss. Beinflussung der Grundfrequenz." *Elektrie Berlin 37*, 1983, 12, pp. 651-655.

76. El-Kady M.A. and G.L. Ford "An Advanced Probabilistic Short-Circuit Program" IEEE Transactions on Power Apparatus and Systems Vol. PAS-102 1983, pp. 1240-1248.

77. Tsanakas, D., Papadias, B. "Influence of Short-circuit Duration on Dynamic Stresses in Substations." *IEEE Transactions on Power Apparatus and Systems*, PAS-102, 1983, pp. 492-501.

78. Waeber, M. "Bestimmung der Ausschwingbewegung von schwach gespannten Leiterseilen und des Fallseilzugs in Schaltanlagen bei Kurzschlüssen." *ETZ-A*, 5, 1983, pp. 103-107.

79. Lilien, J.L. "Contraintes et Conséquences Electromécaniques liées au passage d'une intensité de courant dans les structures en câbles." Université de Liège, Collection des Publications de la Faculté des Sciences Appliquées, No. 87, April 1983.

80. Miri A.M. and Heinrich C. "Berechnung des Bewegungsablaufs und des dynamischen Zugkraftverlaufs von gebundelten Seilsammelschienen im Kurzschlussfall" Elektrizitätswirtschaft Vol. 82, No. 9, 1983, pp. 318-325.

81. Brandt, E., Kuhnel, G., Terhorst, A., DeWendt, G. "Dynamisches Verhalten von Abspanngerusten in Hochspannungsanlagen bei Kurzschluss." *Elektrizitätswirtschaft*, 83, 1984, Heft 16, pp. 711-716.

82. Tsanakas, D. "Dynamische Beanspruchung von Hochspannungsanlagen bei kleiner Kurzschlussdauer." *ETZ-A*, Bd. 6, 1984, pp. 387-392.

83. Kugler, R. "Thermische und dynamische Kurz-schlussbeanspruchung bei Hochspanungs-leistungsschaltern." *Elektrotechnik und Maschinenbau*, 102, 1985, Heft 7/8, pp. 298-304.

84. Stauch, G. "Mechanische Grundfrequenz von kompakten Schaltanlagen." *Elektrie* Berlin 39, 1985, 10, pp. 381-383.

85. Orkisz, J. and Tomana, A. "A Discrete Dynamical Model of Duplex Conductors at Short-circuit Currents." Polish Academy of Science, Cracow, Mechanics 10, 1979, pp. 53-78.

86. Havard D.G. et al. Probabilistic Short-circuit Uprating of Strain Bus System - Mechanical Aspects" *IEEE Transactions on Power Delivery*, Vol. PWRD-1, July 1986, pp104-110.

87. Campbell, J.D. "Dynamic Yielding of Mild Steel." Acta Mat. 6, 1, 1953, pp. 706.

88. Newmark, N.M. "A Method of Computation for Structural Dynamics." *ASCE Journal*, Eng. Mech. Division, 85, 1959, pp. 65-94.

89. IEEE Working Group 59.1, "Minimum Line-to-Ground Electrical Clearances For EHV Substations Based on Switching Surge Requirements" IEEE Transactions on Power Apparatus and Systems Vol PAS91 No. 5 Sept/Oct 1972 pp1924-1930

90. Bathe, K.J., Wilson, E., Peterson, E. "SAP IV: A Structural Analysis Program for Static and Dynamic Response of Linear Systems." University of California, College of Engineering, Report No. EERC 73-11, June 1973.

91. IEEE Surge Protective Devices Committee "Sparkover Characteristics of High Voltage Protective Gaps" IEEE Transactions on Power Apparatus and Systems Vol PAS93 No. 1 Jan/Feb 1974, pp. 196-205

92. Diesendorf W. "Insulation Co-ordination in High Voltage Electric Power Systems" Butterworths & Co. 1974.

93. Bathe, K.J., Wilson, E.L, Iding, R.M. "NONSAP: A Structural Analysis Program for Static and Dynamic Response of Non-Linear Analysis." University of California, Engineering Laboratory, Report No. US-CESM 74-3.

94. Gallet G. et al "General Expression for Positive Switching Impulse Strength Valid up to Extra Long Air Gaps" *IEEE Transactions on Power Apparatus and Systems*, Vol PAS-94 No. 6 Nov/Dec 1975 pp 1989-1993

95. Bathe, K.J., Wilson, E.L. "Numerical Methods in Finite Element Analysis." Prentice-Hall Inc., 1976.

96. Roussel, P. "Numerical Solution of Static and Dynamic Equations of Cables." Comp. Meths. in Appl. Mech. and Engng., 9, 1976, pp. 65-74.

97. Bathe, K.J. "ADINA: A Finite Element Program for Automatic Dynamic Incremental Nonlinear Analysis." Massachusetts Institute of Technology, 1978, Report 82448-1.

98. Sander, G., Gerardin, M., Nyssen, G., Hogge, M. "Accuracy versus Computational Efficiency in Nonlinear Dynamics." Congress FENOMECH'78. North-Holland Publication, II, 1979, pp. 315-340.

99. Dannheim, H., Oel, H.J. "Einfluss von Oberflächendefekten auf die mechanische Festigkeit bei keramischen Wekstoffen für Hochspannungs-isolatoren." Berichte der Deutschen Keramischen Gesellschaft, 56, 1979, pp. 323-327.

100. Universite de Liège. SAMCEF Manuels théorique et d'utilisation. Laboratoire de technique aérospatiales, 1981.

101. Dannheim, H., Oel, H.J. "Festigkeit von keramischem Porzellan für Hochspannungsisolatoren bei dynamischer und zyklischer Belastung." Ceramic Forum International, 61, 1984.

102. Ballus, H. "Ein Beitrag zur Berechnung elektromagnetischer Krafte zwischen stromführenden Leitern." *ETZ-A*, 90, 1969, pp. 539-544.

103. Schwab, A.J. "High-voltage Measuring Techniques," The M.I.T. Press, Cambridge, Mass, 1972.

104. Kiessling, G. "Das Seilspannfeld als physikalisches Pendel, eine analytische Losung der Kurzschlussvorgange." A für Elektrotechnik 70 (1987), pp 273-281.

105. Lilien, J.L., Pirotte, P. "The Behaviour of H.V. Strained Cables due to Short-Circuit Currents." First Symposium on Electric Power Systems in Fast Developing Countries, Riyadh, March 1987, pp. 577-583.

106. Lilien, J.L., El Adnani, M. "Faisceaux de conducteurs et efforts électrodynamiques. Vers une approche numérique fiable." IEEE - Montech 86, Conference on AC Power Systems, Montreal, October 1986, pp. 79-84.

8 SYMBOLS

This section provides a list of the most important symbols used throughout the brochure which are primarily based on the standardized symbols given by IEC according to IEC Standard 865: "Calculation of the effects of short-circuit currents." However, as the scope of this Brochure concerns only open switchgear for higher voltages, some symbols are left out and others, based on the IEC directives, are introduced. As well, some symbols are defined in the specific chapters and sections.

To obtain the necessary degree of flexibility, this symbols list is divided into two parts, one dealing with quantities and one containing subscripts. An attempt has been made to adopt, as much as possible, the IEC symbols. Therefore, quantity symbols, such as A (cross-section), f (network frequency), f_c (mechanical frequency), l (length), m' (mass per unit length), and so on, are used without special subscript in accordance with the IEC Standard 865. However, they are also considered as general units. With the relevant subscript they then could be used for any purpose, (for example, f_{ci} natural frequency of insulator string). In the symbols list, these general definitions are given within brackets. Note, however, that in contrast to IEC 865, all units are consistent with SI practices.

When multiple subscripts are necessary, the part indicating geometrical conditions is placed last, e.g. S_{dg} for dynamic spring constant of girders. Only quantities with subscripts which are used frequently are listed separately.

Symbol	Definition	Units
A	conductor cross-section [cross-section]	m^2
a	center line distance between phase conductors	m
a_s	center line distance between subconductors	m
b_c	sag of cable, insulator strings excluded	m
b_i	sag of insulator string at cable connection	m
C	finite element damping matrix	kg/s
C'	reference force per unit length	N/m
c	conductor specific heat capacity	Ws/kg°C
D	distance	m
d	diameter	m
d_o	outside diameter of tube conductor	m
d_i	inside diameter of tube conductor	m
E	Young's modulus	N/m^2
$e_g(t)$	exponential term of e(t), decaying with time constant $\tau/2$	
e_o	constant term of e(t)	
e(t)	time function of electromagnetic force F'(t) related to C'	
e_ω	oscillation with electrical frequency, decaying with τ	
$e_{2\omega}(t)$	undamped oscillation at double the electrical frequency, term of e(t)	
F	Force/tension	N
F_d	force on support of rigid conductors during a short-circuit (peak value)	N
F_f	tension in a flexible conductor caused by a fall-of-span sequence	N

Symbol	Definition	Units
F_o'	force per unit length on an outer phase flexible conductor caused by a balanced three-phase short-circuit (rms)	N/m
F_p'	short-circuit peak force per unit length	N/m
F_{pi}	tension in a multiple flexible conductor caused by the pinch effect	N
F_s	force between subconductors (peak value)	N
F_{st}	static tension in a flexible conductor, static force on rigid conductor	N
F_t	tension in a flexible conductor during the swing out sequence	N
$F'(t)$	time function of electromagnetic force per unit length	N/m
f	system frequency (electrical)	Hz
f_c	mechanical frequency	Hz
g_n	standard value of acceleration of gravity = 9.81	m/s^2
h	height	m
i	instantaneous value of conductor current	A
I_k	steady state short-circuit current (rms)	A
I_k''	initial symmetrical short-circuit current (rms)	A
I_{k2}'', I_{k3}''	Two of three-phase short-circuit current (initial symmetrical, rms)	A
i_p	peak short-circuit current	A
I_{th}	thermal equivalent short-circuit current (rms)	A
J	second moment of relevant area	m^4
k	number of spacers	
K	finite element stiffness matrix	N/m
l	conductor length between supports or string insulators [length]	m
l_i	length of one insulator string or supporting insulator	m
l_o	unstrained span length of cable bus bar	m
l_s	subconductor length between spacers	m
M	mass	kg
M	finite element mass matrix	kg
m	factor for the heat effect of the DC component	
m'	main conductor mass per unit length [mass per unit length]	kg/m
m_i	mass of insulator (string)	kg/m
m_s	mass of subconductor per unit length	kg/m
m_t	equivalent mass of tower or supporting structure	kg
m_z	mass of one spacer	kg/m
n_s	number of subconductors	

Symbol	Definition	Units
p	specific mass	kg/m³
$P_1, P_{1s}, P_2,$ P_3, P_4, P_5	dimensionless parameters defined in section 4.6	
q	factor of plasticity	
R	resistance	Ω
R	finite element force vector	N
$R_{p0.2}$	yield point	N/m²
r	short-circuit load/dead load	
$\bar{r}$	mean short-circuit load/dead load	
S	resultant spring constant of conductor dead end [spring constant]	N/m
S_d	dynamic spring constant	N/m
T	time of one cycle or pendulum oscillation period	s
T_k	short-circuit duration	s
t_u	dead-time of autoreclosure	s
t	time	s
u	transverse displacement	m
u	finite element displacement vector	m
V_F	ratio between dynamic and static force on support	
V_r	ratio between stress with and without unsuccessful three-phase autoreclosure	
V_σ	ratio between dynamic and static conductor stress	
W	section modulus	m³
X	reactance	Ω
x	coordinate along the bar axis	m
$X_{in}\ X_{out}$	upward (downward) deflection of span midpoint	m
$Y_{in}\ Y_{out}$	inwards (outwards) deflection of span midpoint	m
y_{st}	static deflection	m
α	factor for force on support	
$\alpha(\lambda)$	conductor linear expansion coefficient	1/°C
α_{20}	conductor thermal resistivity coefficient at 20°	1/°C
β	factor for conductor stress	

Symbol	Definition	Units
γ	Eigenvalue	
γ'	factor for natural frequency estimation	
γ_z	impedance angle	rad
δ	conductor + insulation string swing out angle	rad
δ_1	insulator string swing out angle	rad
δ_2	flexible conductor swing out angle	rad
θ_b	conductor temperature at the beginning of a short-circuit	°C
θ_e	conductor temperature at the end of a short-circuit	°C
κ	factor for peak short-circuit current	
Λ	logarithmic damping decrement	
μ_o	magnetic permeability = $4\pi \cdot 10^{-7}$	Vs/Am
ρ	conductor resistivity	Ωm
σ	stress	N/m^2
τ	time constant of network [time constant]	s
ω	angular frequency	rad/s

Subscripts and Abbreviations

c	cable (flexible conductor)
CIS	Cable + Insulator string + Structure
cl	clearing, clearance
d	dynamic
g	girder (cross-arm)
i	insulator, insulator string
k2	line-to-line short-circuit without earth connection
k3	three-phase short-circuit
L1-L2-L3	phase symbols
max	maximum
min	minimum
n	nominal (harmonic) number
rsl	resulting
s	subconductor
S	structures
sl	soil
st	static
t	tower, supporting structure
tot	total
z	spacer

DATA REQUIRED AND EXAMPLE OF
RESULTS FOR RIGID BUS ARRANGEMENTS

The complete data for a structure with 245 kV insulators are given in Table A1. This structure is fully described in [4] and is shown in Fig. A1.1. Data or data-groups characterized by * are not required for calculations according to IEC 865/86 [39].

Table A1: Example Data

Electrical Data

Characteristic Values	First short circuit duration	Interval without short-circuit	Second short-circuit duration
System frequency	50 Hz	---	50 Hz
Short-circuit	line-to-line	---	line-to line
Time interval*	0<t<0.135s	0.135 s<t <0.580 s	0.580 s<t <0.885 s
Max. asymm. short-circuit current i_p (peak value)	41.0 kA	0	40.8 kA
Short-circuit current I''_{k2} (rms value) phase-to-phase	15.6 kA	0	15.6 kA
Time constant $\tau = L/R$	0.066 s	---	0.062 s

Mechanical Data

General	
number of spans	$n = 2$
span-length	$\mathcal{l} = 11.5$ m
distance between conductor centers	$a = 1$ m
boundary conditions	continuous conductor, supported at clamps A, B and C
Conductors	
mass	$m' = 6.04$ kg/m
Young's modulus	$E = 7.0 \cdot 10^4$ N/mm^2
outside diameter	$d_o = 121.1$ mm
inside diameter	$d_i = 108.7$ mm
log. damping decrement	$\Lambda = 0.05$ *
Insulators	
natural frequency	$f_i = 21.5$ Hz *
spring rate - insulator 1	$c_i = 730$ N/mm *
spring rate - insulator 2	$c_i = 757$ N/mm *
spring rate - insulator 3	$c_i = 777$ N/mm *
height	$h_i = 2100$ mm
mass	$m_i = 180$ kg *
core diameter (porcelain)	
- at the base	$D_i = 155$ mm *
- at the top	$d_i = 131$ mm *
Understructures (steel pillars)	
natural frequency	$f_S = 27.2$ Hz *
spring rate - steel pillar 1	$c_S = 1460$ N/mm *
spring rate - steel pillar 2	$c_S = 1770$ N/mm *
spring rate - steel pillar 3	$c_S = 1880$ N/mm *
height (without plates)	$h_S = 2055$ mm
mass (without plates)	$m_S' = 36.8$ kg/m *
moment of inertia	$J = 0.335 \cdot 10^{-4}$ m^4 *
concentrated masses e.g. plate 440·340·30 mm^3	$m = 35$ kg *
Conductor clamps	
mass of clamp A	$m_A = 13.8$ kg *
mass of clamp B	$m_B = 18.2$ kg *
mass of clamp C	$m_C = 13.8$ kg *
distance between top of insulator and conductor axis	$h = 160$ mm

Results

With reference to the structure and the relevant data given above, Fig. A1.2 shows the time functions of the bending moment at the bottom of the middle insulator during a short-circuit. The experimental values are compared with the calculated results [4].
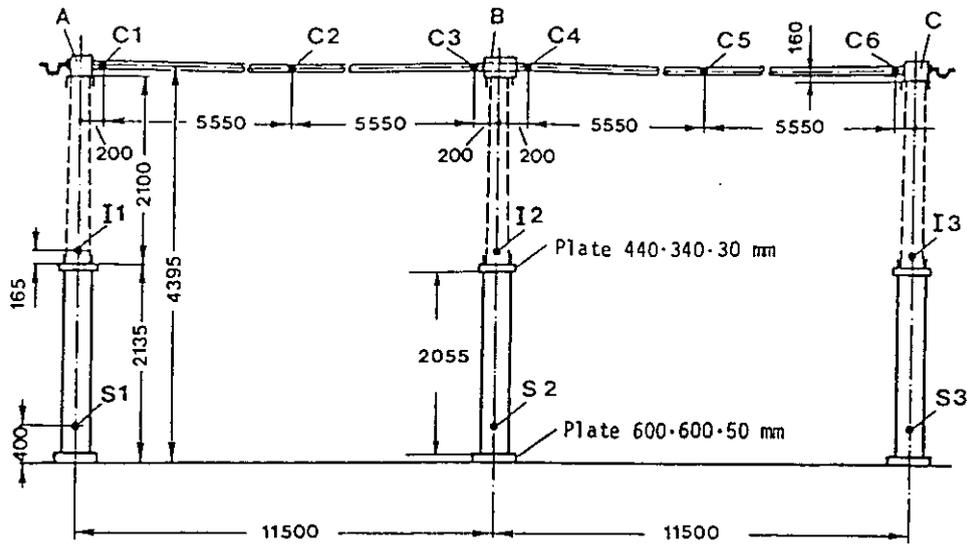
Fig. A1.1 Test Structure by FGH (DE)
I1,I2,I3,S1,S2,S3: Measuring and calculating
points for the bending moment in the insulators
and steel pillars
C1,C2,C3,C4,C5,C6: Measuring and calculat-
ing points for the bending stress in the conductor
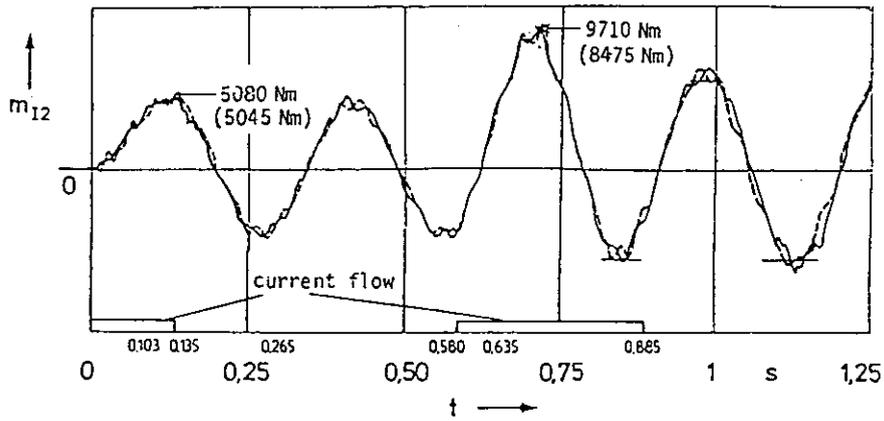
Fig. A1.2 Bending moment at the bottom of the middle insulator (measuring point I2)
[4]
─────── Calculated by one of the advanced methods
- - - - - - Measured
Measured maximum value prior to reclosure, 5080 Nm
Measured maximum value after reclosure, 9710 Nm
(5045 Nm and 8475 Nm respecitvely, calculated by IEC Publication 865 [39])

95

APPENDIX 2

CALCULATION OF FORCES IN A RIGHT ANGLE BEND

(Special Application to Terminals of Apparatus)

The conductors are assumed to be in the same plane and forming a right angle. The influences of neighbouring phases are also neglected. The method is described with reference to a practical example (Fig. A2.1) which could be a rigid or a flexible conductor connected at a right angle to a cable box or to a transformer bushing. Another practical application would be a horizontal connection to a pantograph isolator.

In Fig. A2.2, the distributed force acting on such a conductor with the length $\mathcal{l}_t$ between supports is illustrated. To simplify the procedure, the distributed force is replaced by the concentrated force F_y acting at the distance $\mathcal{l}_{Fy}$ from the terminal of the apparatus. Δs and Δt are assumed equal and are introduced to make it possible to use the centre line of a conductor as a fictitious current path. Newly introduced symbols are explained in figures and diagrams.

Basis for calculation

The method is partly based on work by Ballus [102], who has carefully studied the current paths in a corner and has also presented an analytical method for general use. The numerical method used for the presentation of diagrams, etc, can be understood by considering the following two formulas:

$$F_y = \frac{\mu_0}{4\pi} \cdot i_p^2 \cdot \int_{y=s2}^{y=s4} \int_{x=t1}^{x=t3} x/(x^2 + y^2)^{1.5} \cdot dx \cdot dy$$

$$F_y \cdot \mathcal{l}_{Fy} = \int_{x=t1}^{x=t3} (F'_y \cdot x) \cdot dx$$

($\mathcal{l}_{Fy}$ = the distance to the "gravity centre" of the distributed force).

For the design of open air substations, use of such a simplified procedure for the estimation of angle forces is reasonable because:

- the ratio conductor diameter to conductor length of interest is small

- variability in the design and influence of connectors makes it difficult and uncertain to foresee and to analyse the real current paths very near the corner

- a concentrated force is easier than varying distributed forces to analyze, especially in combination with simplified calculation methods.

Calculation procedure

Δs and Δt are both assumed equal to

$$\Delta s = \Delta t = \frac{r_s + r_t}{2} \quad \text{(Fig. A2.1, A2.2)}$$

then form the ratios

$$\frac{\mathcal{l}_s}{\mathcal{l}_t} \text{ and } \frac{\Delta t}{\mathcal{l}_t}$$

F_y using Fig. A2.3
$\mathcal{l}_{Fy}$ using Fig. A2.4

Superimpose angle forces with other short-circuit forces.

Example

$$\mathcal{l}_s = 5 \text{ m} \quad \mathcal{l}_t = 10 \text{ m} \quad r_s = 0.03 \text{ m} \quad r_t = 0.04 \text{ m}$$

then,

$$\frac{\mathcal{l}_s}{\mathcal{l}_t} = 0.5; \frac{\Delta t}{\mathcal{l}_t} = \frac{r_s + r_t}{2 \cdot \mathcal{l}_t} = \frac{0.03 + 0.04}{2 \cdot 10} = 0.0035$$

From Fig. A2.3: $F_y = 0.45 \text{ N/(kA)}^2$

From Fig. A2.4: $\mathcal{l}_{Fy} = 0.17 \cdot 10 = 1.7 \text{ m}$
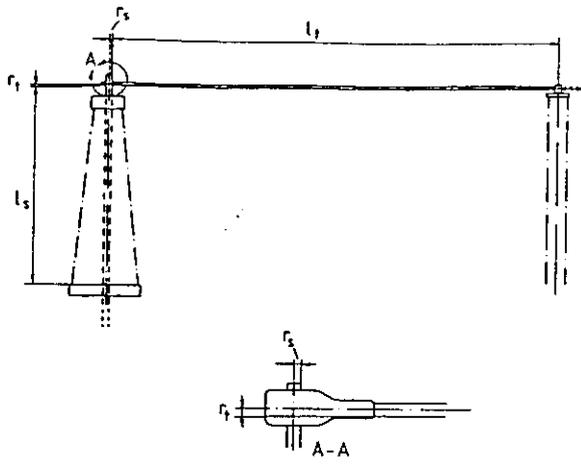
Fig. A2.1 Connection of a rigid or flexible conductor to a cable box or bushing in a right angle
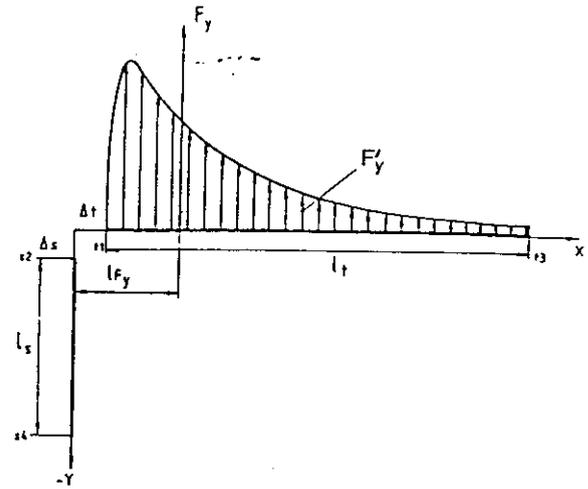

Fig. A2.2 Distributed force F'y on the conductor according to Fig. A2.1
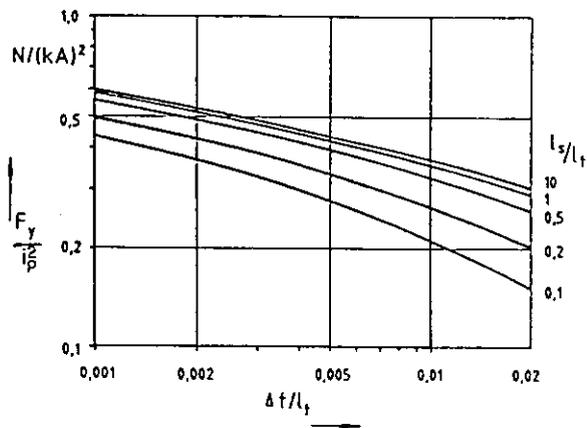
Fig. A2.3 Equivalent concentrated force F_y/i_p^2 in relation to l_s/l_t and $\Delta t/l_t$
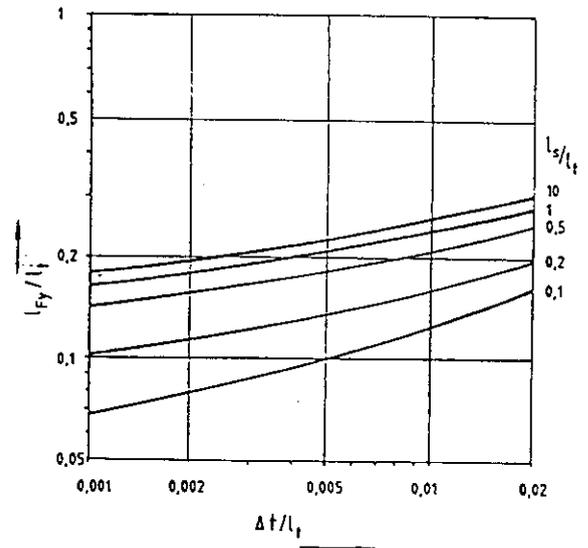

Fig. A2.4 Acting relative distance l_{Fy}/l_t in relation to l_s/l_t and $\Delta t/l_t$

APPENDIX 3

DATA REQUIRED AND RESULTS FOR FLEXIBLE CONDUCTOR ARRANGEMENTS

This appendix provides an example of data (Table A3.1) and results for a structure that has been used in Belgium by Laborelec [7] to perform full scale tests of phase-to-phase short-circuits with single conductors (Fig. A3.1). Extensive measurements have been made for the supporting structures, allowing for a verification of several advanced methods. Good accuracy was obtained.

A second data set (Table A3.2) provides data for a structure which has been tested in France by EDF [10]. This structure is more complicated than the preceding one because of resonance problems between cables and supports.

Table A3.1: Data Requirement Laborelec Test

Application Code	Description	Typical Data	Units
SMAR	Span	40	m
SMA	Distance between phases	2.5	m
AR	Complete geometry description		draft
SMAR	Youngs modulus of the cable	$12 \cdot 10^{10}$	N/m²
SMAR	Cross-section of the cable	$324 \cdot 10^{-6}$	m²
SMAR	Weight of the cable	28.35	N/m
MA	Dilatation coeffecient	$16.8 \cdot 10^{-6}$	1/°C
MA	Heat capacity	389	J/kg·°C
MA	Resistivity at 20°C	$1.72 \cdot 10^{-8}$	Ω·m
MA	Temperature coefficient of resistivity	0.00393	1/°C
A	Convection coefficient	35	W/m²·°C
AR	Length of droppers:		
	phase West	4	m
	phase East	6.5	m
AR	Concentrated masses and their location	draft	
MAR	Insulator string length		1.54 m
MAR	Insulator string mass		52.3 kg
A	Insulator stiffness force		$30 \cdot 10^6$ N
A	All data for portal structures or supports	draft	
SMAR	Stiffness of supports	$\pm 3 \cdot 10^5$	N/m
MR	First Eigenfrequency of the supports	± 5	Hz
MA	Initial temperature	15.8	°C
A	Ambient temperature	14	°C
SMAR	Initial pulling force:		
	phase West	7.65	kN
	phase East	7.85	kN
SMAR	Initial sag: phase West	0.97	m
SMA	Short-circuit current	29.4	kA(rms)
SMA	First peak current	72.7	kA
SMA	Short-circuit duration	0.8	s
MA	Equivalent time of aperiodic component of the current	0.033	s
MA	Network frequency	50	Hz

Application Code:
S = required for simple methods
M = required for medium methods
A = required for advanced methods
R = required for a precheck of the structure against resonances

CALCULATION RESULTS FOR LABORELEC TEST ARRANGEMENT

SIMPLE METHOD RESULTS

Preliminary Remark

The Laborelec data (Table A3.1) are adjusted for a line-to-line test arrangement. Using the simple method, the data "short-circuit current 29.4 kA" and "stiffness of the supports $3 \cdot 10^5$ N/m" are transformed into

$$I'_{k3} = 29.4/0.866 = 33.95 \text{ kA} \quad (I'_{k3} = 2I'_{k2}/\sqrt{3})$$

$S = 3 \cdot 10^5/4 = 0.75 \cdot 10^5$ N/m
(Resultant stiffness for one span, when two phases are acting on two supports)

Calculation Steps

Evaluation of r

Using Eqs. (4.2.1), (4.2.2) and Fig. 4.2.2

$$r_0 = \frac{0.15 \times 33.95^2/2.5}{28.35} = 2.439 \quad (4.2.1)$$

$$T_r = 1.79 \sqrt{0.97} (1+2.439^2)^{-0.25} = 1.086 \text{ s} \quad (4.2.2)$$

$T_{k1} = 0.8 \text{ s} > T_r/4$

so that

$$\left. \begin{array}{l} T' = T_r/4 = 0.271 \text{ s} \\ \kappa = 72.7/(29.4 \sqrt{2}) = 1.75 \end{array} \right\} \quad m = 0.127 \quad \text{Fig. 4.2.2}$$

$r = 2.439 (1+0.127) = 2.75$

Evaluation of $\bar{r}$, δ_k

Using Eqs. (4.2.3), (4.2.4) and Fig. 4.2.6

$$T = 1.79 \sqrt{0.97} = 1.763 \text{ s} \quad (4.2.3)$$

$T_{k1}/T = 0.8/1.763 = 0.454$ for Fig. 4.2.5 (and Fig. 4.2.7)

$b_c/a = 0.97/2.5 = 0.388$ for Fig. 4.2.6

First loop: $r = 2.75$ gives $\delta_k = 140°$ and $k_d = 0.70$
and $\bar{r} = 1.93$ \quad (4.2.4)

Second loop: $\bar{r} = 1.93$ gives $\delta_k = 125°$ and $k_d = 0.70$
and $\bar{r} = 1.93$

$\bar{r}$(begin) equal to $\bar{r}$(end), so that second loop = last loop
and $\bar{r}=1.93$ $\delta_k=125°$

Evaluation of δ_m, δ_1

Using Figs. 4.2.7 and 4.2.8

with $T_{k1}/T = 0.454$ and $\bar{r} = 1.93$ is $\delta_m = 136°$ \quad Fig. 4.2.7

$\delta_1 = $ arc tan $\bar{r} = $ arc tan $1.93 = 62.6°$ \quad Fig. 4.2.8

Evaluation of the maximum tensile force during the short-circuit F_t

Using Eqs. (4.2.5), (4.2.6), (4.2.7) and Fig. 4.2.9

$$\varphi = 3 (\sqrt{1+2.75^2}-1) = 5.78 \quad (4.2.5b)$$

$$\zeta = \frac{(28.35 \times 40)^2}{24 \times 7650^3} \times \frac{1}{1/(7.5 \cdot 10^4 \times 40)+1/(12 \cdot 10^{10} \times 324.10^{-6})}$$
$$= 0.33 \quad (4.2.7)$$

From Fig. 4.2.9 $\zeta = 0.33$ and $\varphi = 5.78$ give $\psi = 0.297$

$$F_t = 1.0 \times 7.65(1+5.78 \times 0.297) = 20.8 \text{ kN} \quad (4.2.6)$$

Evaluation of the maximum sag during the short-circuit b_{ct}

Using Eqs. (4.2.8) to (4.2.12)

$$C_F = 1.15 \quad (4.2.9)$$

$$\varepsilon_{\sigma} = (20800-7650) \times \left(\frac{1}{324 \cdot 10^{-6} \times 12 \cdot 10^{-10}} + \frac{1}{40 \times 75 \cdot 10^3} \right)$$
$$= 0.00472 \quad (4.2.11)$$

$$\varepsilon_{\theta} = \left(\frac{33.95}{324 \cdot 10^{-6}} \right)^2 \times 0.271 \times 0.88 \cdot 10^{-13} = 0.00026 \quad (4.2.12)$$

$$C_D = \sqrt{1 + \frac{3}{8} \cdot \left(\frac{40}{0.97} \right)^2 \times 0.00498} = 2.04 \quad (4.2.10)$$

$b_{ct} = 1.15 \times 2.04 \times 0.97 = 2.28$ m \quad (4.2.8)

Evaluation of the maximum tensile force after the short-circuit F_f

Using Eq. (4.2.13)

$$F_f = 1.2 \times 7.65 \times \sqrt{1+8 \times 0.33 \times \sin^3(0.7 \times 136°-36°)} = 15 \text{ kN} \quad (4.2.13)$$

Compilation of Results

First peak maximum of tension (F_t) = 20.8 kN
Falling down maximum of tension (F_f) = 15 kN
Maximum tension to be taken
for dimensioning = 20.8 kN
Maximum displacement outside
(from A) $\approx$ 2.28 sin 62.6° = 2.02 m
Maximum displacement inside
(from A) $\approx$ 1.625 sin 62.6° = 1.44 m
Maximum displacement up
(from A) $\approx$ 0.97 (1-cos136°) = 1.67 m
Maximum displacement down
(from A) = 2.28 - 0.97 = 1.31 m

A = normal midspan position

See also Fig. 4.2.8b in which:

|	
b_c	= 0.97 m
b_{ct}	= 2.28 m
$(b_{ct} + b_{ct})/2$	= 1.625 m
δ_1	= 62.6°
δ_m	= 136°
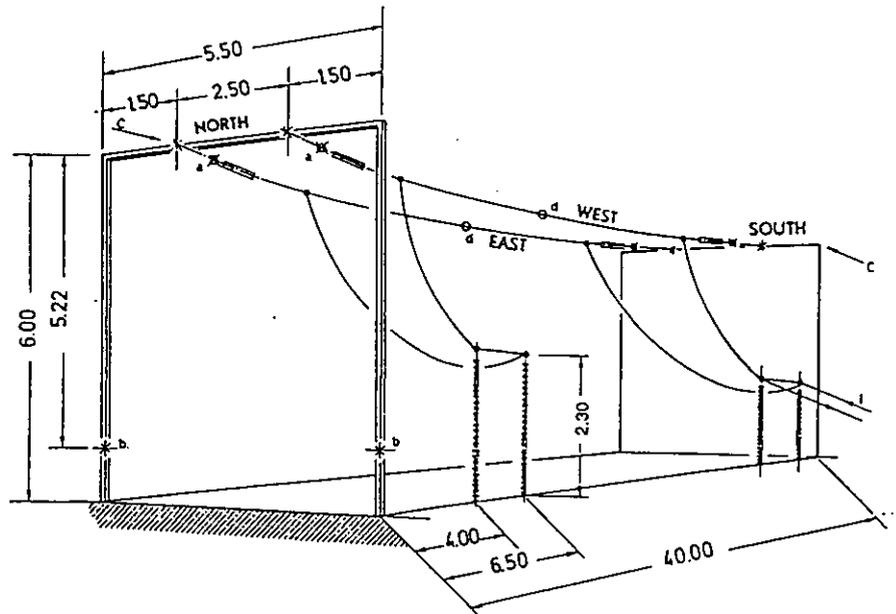
Fig. A3.1   Laborelec Test Structure

MEDIUM METHOD RESULTS

Time-history of tensions in middle point of each cable, giving for phase East:

- First peak maximum of tension   19.10 kN
- Falling down maximum of tension   19.74 kN
- Absolute maximum of tension   19.74 kN

- Plot of evolution of tension during and after short-circuit (e.g. Fig. A3.2)

Time history of displacements of middle point of each cable, giving:

- Maximum displacement outside   1.407 m
- Maximum displacement inside   0.860 m
- Maximum displacement up   0.990 m
- Maximum displacement down   0.655 m
- Minimum clearance between cables   0.645 m

- Plot of evolution of positions of middle point of each cable during and after short-circuit (e.g. Fig. A3.3)

ADVANCED METHOD RESULTS

Time-history of tensions in each point of each cable, giving for phase East:

- First peak maximum of tension   16.9 kN
- Falling down maximum of tension   23.5 kN
- Absolute maximum of tension   23.5 kN

- Plot of evolution of tension during and after short-circuit (e.g. Fig. 4.5.3)

Time history of displacements of middle point of each cable, giving:

- Maximum displacement outside   1.37 m
- Maximum displacement inside   0.7 m
- Maximum displacement up   1.1 m
- Maximum displacement down   0.6 m
- Minimum clearance between cables   1.5 m

- Plot of evolution of positions of middle point of each cable during and after short-circuit (e.g. Fig. 4.5.2)

Time history of tensions and displacements of each point of the structure (supports, cables, droppers, insulators, anchoring point on apparatus, etc.) giving:

- Clearances between cables and supports, apparatus, ...
- Stresses in insulator chains, on apparatus
- Displacements of supporting structures
- Plot of evolution of positions of each point of the structure during and after short-circuit
- Plot of the situation of the whole structure at a given time, allowing for generation of movies, giving a good knowledge of what exactly happens in the station during and after a short-circuit

TEST RESULTS

For phase East, measurements give:

- First peak maximum of tension   16.1 kN
- Falling down maximum of tension   22.4 kN
- Absolute maximum of tension   22.4 kN

- Maximum displacement outside   1.33 m
- Maximum displacement inside   0.75 m
- Maximum displacement up   1.10 m
- Maximum displacement down   0.66 m
- Minimum clearance between cables   1.45 m

100
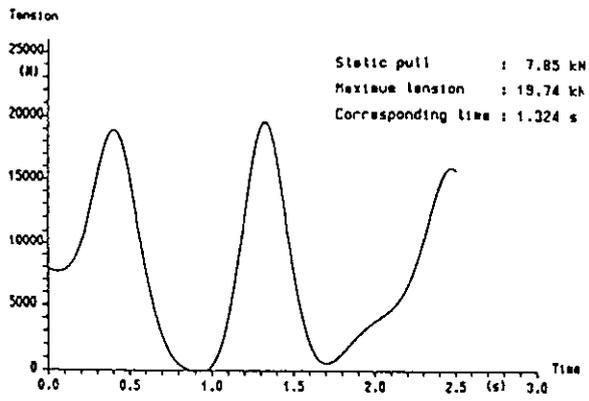
Fig. A3.2 Tension in dc cable according to Fig. A3.1 calculated by PENDBL
I_{k2} = 29.4 kA during 0.8 s
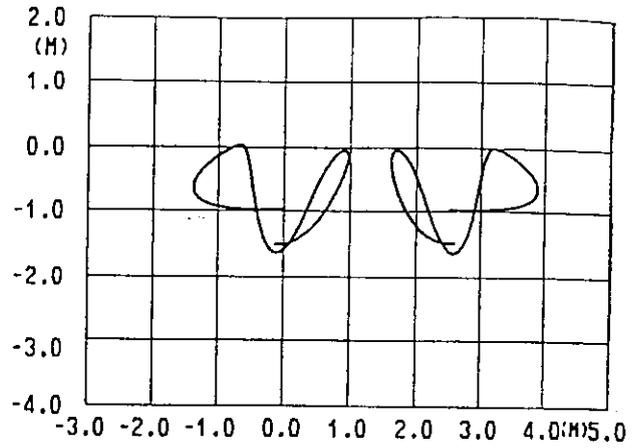
Fig. A3.3 Displacement (middle point of phases, Fig. A3.1) calculated by PENDBL
I_{k2} = 29.4 kA during 0.8 s
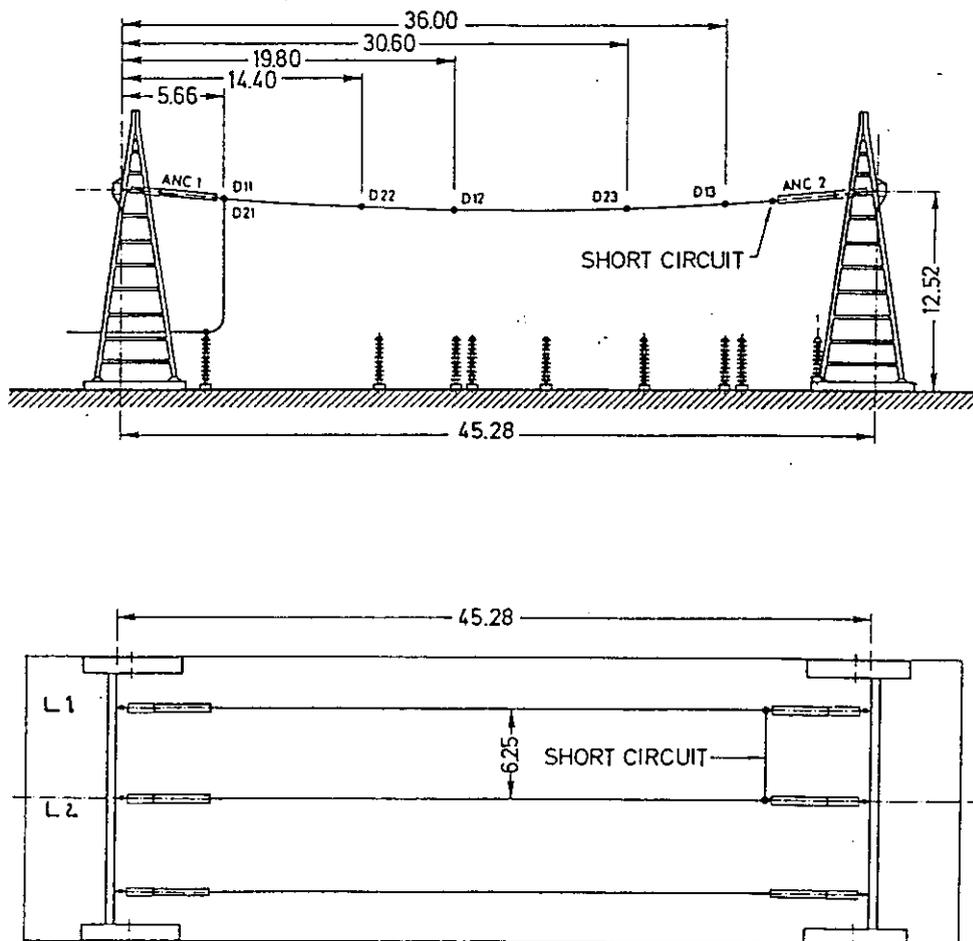
Fig. A3.4 EDF Test Structure

DATA FOR EDF TEST ARRANGEMENT

The calculation results using advanced methods for the EDF test arrangement are discussed in section 4.5.7 and presented in Figs. 4.5.4 and 4.5.5.

Table A3.2: Data Requirement EDF Test

Application Code	Description	Typical Data	Units
SMAR	Span	45.28	m
SMA	Distance between phases	6.25	m
AR	Complete geometry description		draft
SMAR	Young's modulus of the cable	$5.25 \cdot 10^{10}$	N/m^2
SMAR	Cross-section of the cable	$1144 \cdot 10^{-6}$	m^2
SMAR	Weight of the cable	31.04	N/m
MA	Dilatation coeffecient	$23 \cdot 10^{-6}$	$1/°C$
MA	Heat capacity	890	J/kg·°C
MA	Resistivity at 20°C	$3.25 \cdot 10^{-8}$	$\Omega \cdot m$
MA	Temperature coefficient of resistivity	$3.6 \cdot 10^{-3}$	$1/°C$
A	Convection coefficient	not available	$W/m^2 \cdot °C$
A	Length of droppers	8.6	m
A	Length of SCC connection	7.5	m
MAR	Insulator string length anc-1; anc-2	5.80; 4.85	m
MAR	Insulator string mass anc-1; anc-2	324; 325	kg
A	Insulator stiffness force	25.10^6	N
A	All data for portal structures or supports	draft	
SMAR	Stiffness of supports:		
	phase L1	$1.6 \cdot 10^6$	N/m
	phase L2	$1.9 \cdot 10^6$	N/m
MR	First Eigenfrequency of the supports		
	phase L1	2.47	Hz
	phase L2	2.57	Hz
MA	Initial temperature		°C
A	Ambient temperature		°C
SMAR	Initial pulling force:		
	phase L1	8.6	kN
	phase L2	6.5	kN
SMAR	Initial sag for 9.53 kN pulling force	1.98	m
SMA	Short-circuit current	63.7	kA(rms)
SMA	First peak current	148.3	kA
SMA	Short-circuit duration	0.242	s
MA	Equivalent time of aperiodic component of the current	0.022	s
MA	Network frequency	50	Hz

Application Code:

S = required for simple methods
M = required for medium methods
A = required for advanced methods
R = required for a precheck of the structure against resonance

APPENDIX 4

SIMPLE FORMULA FOR CALCULATION
OF RESONANCES IN FLEXIBLE BUS SYSTEMS

From the PENDBL model described in section 4.3.2, it is possible to obtain the pseudo-Eigenfrequencies of the cable, obtained assuming that:

- the two degrees of freedom of each cable are independent,
- the variations of the degrees of freedom may be linearized.

For each cable,

Horizontal pendulum oscillation:

$$f_{ch} = \frac{1}{2\pi}\sqrt{\frac{5}{4} \cdot \frac{g_n}{b_{co}}}$$

Oscillation of the cable in its plane:

$$f_{cv} = \frac{1}{2\cdot\pi}\sqrt{\frac{8.E.A.g_n.b_{co}}{F_{st}\cdot \mathcal{L}\cdot \mathcal{L}_0\cdot\left(1 + \frac{E.A}{S_1\cdot \mathcal{L}_0}\right)}}$$

For a quick resonance check, one may compare these two frequencies with the first Eigenfrequencies of the supporting structure. A problem of resonance can occur if a separation between these frequencies of less than 10% exists. It is then necessary to carry out a more detailed investigation, e.g. using an advanced method.

103